MOLECULAR IONS FOR THE ISOTOPE RATIO MEASUREMENT OF LITHIUM AND BORON BY THERMAL IONIZATION MASS SPECTROMETRY

By

K. SASI BHUSHAN

CHEM01201404010

Bhabha Atomic Research Centre, Mumbai

A thesis submitted to the

Board of Studies in Chemical Sciences

In partial fulfillment of requirements

for the Degree of

DOCTOR OF PHILOSOPHY

of

HOMI BHABHA NATIONAL INSTITUTE

December, 2021

Homi Bhabha National Institute

Recommendations of the Viva Voce Committee

As members of the Viva Voce Committee, we certify that we have read the dissertation prepared by **K. Sasi Bhushan** entitled, "**Molecular ions for the isotope ratio measurement of Lithium and Boron by Thermal Ionization Mass Spectrometry**" and recommend that it may be accepted as fulfilling the thesis requirement for the award of Degree of Doctor of Philosophy.

Chairman – Prof. Smruti Dash	Smruti	Date: 7/12/21
Guide / Convener – Prof. S. Kannan	S Kannan	Date: 7/12/2021
Examiner - Prof. Sandeep Singh	Sandeep Sir	Date: 7th Dec 2021
Member 1- Prof. Pramod Sharma	Pramod	Date: 07-12-2021.
Member 2- Prof. Sanjukta A. Kumar	Sjakk	Date: 07/12/2021
Member 3- Prof. S.C. Parida		Date: 07/12/2021
Technology Adviser- Dr. Radhika M. Rao	R. Rao	Date: 07/12/2021

Final approval and acceptance of this thesis is contingent upon the candidate's submission of the final copies of the thesis to HBNI.

I/We hereby certify that I/we have read this thesis prepared under my/our direction and recommend that it may be accepted as fulfilling the thesis requirement.

Date: 7/12/21

Place: Mumbai

Signature
Co-guide (if any)

Signature 7/12/2021
Guide

STATEMENT BY AUTHOR

This dissertation has been submitted in partial fulfillment of requirements for an advanced degree at Homi Bhabha National Institute (HBNI) and is deposited in the Library to be made available to borrowers under rules of the HBNI.

Brief quotations from this dissertation are allowable without special permission, provided that accurate acknowledgement of source is made. Requests for permission for extended quotation from or reproduction of this manuscript in whole or in part may be granted by the Competent Authority of HBNI when in his or her judgment the proposed use of the material is in the interests of scholarship. In all other instances, however, permission must be obtained from the author.

22/12/2021

K. Sasi Bhushan

DECLARATION

I, hereby declare that the investigation presented in the thesis has been carried out by me. The work is original and has not been submitted earlier as a whole or in part for a degree/diploma at this or any other Institution / University.

22/12/2021

K. Sasi Bhushan

List of Publications arising from the Thesis:

a. Journals:

1. "Simultaneous determination of non-natural isotopic composition of Li and B employing $Li_2BO_2^+$ by Thermal Ionization Mass Spectrometry", K. Sasi Bhushan, R. M. Rao, D. Alamelu, S. Jagadish Kumar, Raju V. Shah, A. R. Parab, *Inter. J. Mass Spectrom.,* **2016**, 406, 20
2. "Precise and rapid isotopic analysis of lithium in refractory materials using $NaLiBO_2^+$ by Thermal Ionization Mass Spectrometry", Radhika M. Rao, K. Sasi Bhushan, S. Jagadish Kumar, Raju Shah, *Inter. J. Mass Spectrom.*, **2020**, 451, 116292
3. "Isotopic dilution Thermal Ionisation Mass Spectrometry (ID-TIMS) for determination of concentration of enriched lithium using $NaLiBO_2^+$ ions", K. Sasi Bhushan, Preeti G. Goswami and Radhika M. Rao, *J. Radioanal. Nucl. Chem.*, **2020**, 326, 1009
4. "Study on effect of sodium based buffers on the isotopic measurement of boron using $Na_2BO_2^+$ by thermal ionization mass spectrometry", K. Sasi Bhushan, Radhika M. Rao, Preeti G. Goswami and S. Kannan, *J. Radioanal. Nucl. Chem.,* **2019**, 323, 1367
5. "Fusion method for sample preparation for isotopic composition determination of boron in refractory materials by thermal ionization mass spectrometry with validation using dissolved and purified samples", K. Sasi Bhushan, Preeti G. Goswami and Radhika M. Rao, *Inter. J. Mass Spectrom.,* **2021**, 467, 116624
6. "Precise determination of $^6Li/^7Li$ isotopic ratio with $NaLiBO_2^+$ ion using total evaporation and ion integration by Thermal Ionization Mass Spectrometry (TIMS)", K. Sasi Bhushan, Preeti G. Goswami, R. M. Rao, *Int. J. Mass Spectr.*, **2021**, https://doi.org/10.1016/j.ijms.2021.116683

b. Conference / Symposia:

1. "Monitor Pair Selection for the Accurate Determination of Isotope Ratio of B and Li simultaneously Employing $Li_2BO_2^+$ by TIMS, 28th ISMAS-WS 2014", K. Sasi Bhushan, R.M. Rao, S. Jagadish Kumar, A. R. Parab, D. Alamelu and S. K. Aggarwal, Parwanoo, Himachal Pradesh, CP - 30, Page 230 - 233.
2. "Feasibility studies on mixed alkali borate ions for isotopic analysis of Li and B by TIMS using alkali salt mixtures, 28th ISMAS-WS 2014", R. M. Rao, K. Sasi Bhushan, S. Jagadish Kumar, A. R. Parab, D. Alamelu and S. K. Aggarwal Parwanoo, Himachal Pradesh, CP - 26, Page 216 - 219
3. "Isotopic analysis of Boron by Thermal Ionization Mass Spectrometry using sodium contained buffers, NUCAR-2019", K. Sasi Bhushan, Preeti G. Goswami and R. M. Rao, January 15 - 19, **2019**
4. "Determination of isotopic composition of Lithium in synthetic ground water samples as $NaLiBO_2^+$ using Thermal Ionization Mass Spectrometry", K. Sasi Bhushan, Vivek G. Mishra, Dipti J. Shah, Preeti G. Goswami and R. M. Rao, (NUCAR - 2019), January 15 - 19, **2019**
5. "Lithium analysis by Thermal Ionisation Mass Spectrometry in Methyl Sulphonic Acid, a medium of chromatographic separation", K. Sasi Bhushan, Preeti G. Goswami and R. M. Rao, 32nd ISMAS - **2019**, MPH, TSH, Mumbai CP - 43 Pg. 204
6. "Total flash evaporation of $NaLiBO_2^+$ for high sensitivity analysis of lithium by Thermal Ionisation Mass Spectrometry (TIMS)", K. Sasi Bhushan, Preeti G. Goswami and R. M. Rao, 32nd ISMAS - **2019**, MPH, TSH, Mumbai, RSP

7. “Validation of direct fusion method for isotopic analysis of Boron in refractory materials”, K. Sasi Bhushan, Preeti G. Goswami and R. M. Rao, 32nd ISMAS - **2019**, MPH, TSH, Mumbai CP - 46 Pg. 215

DEDICATED TO

Ammu Venkateswarlu, Ammu Srídeví

&

Late G. Srínívasa Rao

ACKNOWLEDGEMENTS

The best way to begin this report I feel would be acknowledging my gratitude towards all the individuals responsible for its successful completion because, "The satisfaction and euphoria that accompany the successful completion of any task would be incomplete without mention of the people who made it possible".

First and foremost, I am very happy to express my profound sense of gratitude and indebtedness to Prof. S. Kannan for his patient guidance, continuous support, encouragement and his exquisite attention throughout this work.

I feel short of words in expressing my gratitude and appreciation to my technical advisor, Dr. Mrs. Radhika M. Rao, for her timely advice, meticulous scrutiny and scientific approach which served as a beacon light throughout my journey of this research-age. Starting from the formative stages of this thesis to the final version, I owe an immense debt of gratitude to her.

I wish to express my gratitude to the doctoral committee; Prof. Smruti Dash, Prof. Sanjukta A. Kumar, Prof. S. C. Parida and Prof. Pramod Sharma, whose suggestions and critical comments helped me in carving this work into the present shape.

I am immensely thankful to Mrs. Preeti G. Goswami for her diligent and keen observing attitude towards the experimental studies and wholehearted co-operation during the entire course of the work.

I would also like to express my sincere gratitude towards former immediate superior Shri A. R. Parab, who has introduced me into this field. In an equal measure, it is a genuine pleasure to express my deep sense of thanks to Dr. P. G. Jaison, for his valuable insight and persistent support throughout this work.

I am thankful to my former supervisors Dr. S. K. Aggarwal, Dr. D. Alamelu and former Doctoral Committee team; Prof. S. Mukherjee (chairman) and Prof. R. K. Vatsa (member) for their encouragement, insightful comments helped in the progress of my work.

I would be remiss without mentioning Shri Raju V. Shah and Shri S. Jagadish Kumar for their kind cooperation and valuable suggestions. I take this opportunity to thank my colleagues Dr. Arnab Sarkar, Dr. Pranaw Kumar, Dr. Sumana Paul, Dr. Vijay Telmore, Shri Vijay Karki, Shri Manjeet Singh and Shri Manish Singh for support and help provided at all stages of work.

I am highly thankful to Electronics Section; Dr. Suparna Sodaye, Shri Meena Ghanasyam, Shri Sandeep Viswasarao, Shri Rajesh Jhadav, Shri Anant Deolekar, Shri Sibusoren and Shri Vishal Chowgule for providing instant break-down maintenance for the smooth operation of the instrument.

Special thanks to Dr. (Mrs.) Pappu Kousalya, my sister-in-law for making me expertise in error analysis in the field of data computing. My deepest gratitude is to my family members for their support in my life.

Some however, deserve special mention:

My Parents: for their unconditional love and care

Grandfather: for his blessings and always aspired me to have a great future

Brother: for his invaluable Love and Affection

Little Son: for being an Astute observer at my Power Point presentations & Pictures in the thesis

Words fail to express my appreciation to my wife Abburi Bhavani for her unconditional love.

Contents

Summary

Lithium can be analysed as atomic ion (Li^+) as well as molecular ion ($Li_2BO_2^+$) in positive ion mode of TIMS. Boron is usually measured as alkali metaborate ($M_2BO_2^+$, where M = Na, Rb or Cs) as the monitoring ion. Though the sensitivity of atomic ion is very good, measurement accuracy in the isotope ratio determination of lithium is largely affected by the mass dependent instrumental isotopic fractionation, which depends on several analytical parameters such as ion source loading material, amount of lithium loaded on the filament, temperature and time of analysis. Monitoring molecular ion $Li_2BO_2^+$, at a mass range of m/z 54 to 57 a.m.u., is a better alternative as the severity of isotopic fractionation is greatly reduced when compared to atomic ions. Using a numerical value of $^{10}B/^{11}B$ ratio (e.g. certified value for SRM-951 since $^{10}B/^{11}B$ ratio cannot be independently determined) for the calculation of elemental isotopic ratio of lithium is the main shortfall of this method. In order to circumvent this, instead of monitoring one polyatomic ion ratio, two polyatomic molecular ion ratios of $Li_2BO_2^+$ ions have been used in the present work for the simultaneous determination of isotope ratios of both lithium and boron. The $Li_2BO_2^+$ methodology involves rigorous mathematical calculations for the selection of the correct combination of molecular pair which will give good precision for $^6Li/^7Li$ ratio. The very low abundance of one of the polyatomic molecular ions for the combinations of highly enriched isotopes of either of the element (Li or B), results in poor measurement precision, making the judicious selection of molecular ion pair even more difficult.

So as an alternative to this, a new approach has been explored in the present study by mixing sodium borate to the lithium compound to form sodium lithium (mixed alkali) borate which would produce $NaLiBO_2^+$ molecular ions (mass range of major abundant species 71 - 73),

$Li_2BO_2^+$ (mass range 54 - 57) along with $Na_2BO_2^+$ (88 - 89) in the ion source. The advantage of this method is that $^{10}B/^{11}B$ ratio can be independently determined by monitoring $Na_2BO_2^+$ to measure $^{88}I/^{89}I$ ion intensity ratio simultaneously instead of directly using the constant / certified as in the previously developed $Li_2BO_2^+$ ion method. Though the accuracy of isotopic analysis was improved by using molecular ions instead of atomic ions, the sensitivity of the measurement is compromised. The application of Total Evaporation and Ion Integration (TE & II) method for improving both sensitivity and accuracy for lithium has also been explored in the present thesis. Precise isotopic measurement by a new analytical methodology restricted to particular isotopic composition cannot prove the reliability of the measurement. Reliability of isotope measurement of $NaLiBO_2^+$ method has to be validated by measuring the isotope ratios of $^6Li/^7Li$ in the prepared SLIMs. For that purpose, Synthetic Lithium Isotopic Mixtures (SLIMs) with varying isotopic abundances of ^6Li: 1%, 8%, 20%, 35%, 50% and 85% were prepared and analysed by conventional limited scan measurement as well as TE & II method under the optimized conditions using $NaLiBO_2^+$ ions. The constancy of fractionation factor obtained over a wide range of $^6Li/^7Li$, authenticated the application of $NaLiBO_2^+$ as monitoring ion for the accurate isotope ratio measurement of lithium.

Refractory powder samples of lithium such as Li_2TiO_3, $LiAlO_2$ and boron such as B_4C, TiB_2, Rare Earth metal borides (LaB_6, CeB_6, NdB_6, ZrB_2) are being widely used in the nuclear industry. Isotopic measurement of such samples requires dissolution of these materials. However, a simple and robust methodology has been developed by employing the polyatomic molecular ions where in the Li and B samples were directly fused with sodium borate or sodium carbonate respectively on the filament itself which avoided the elaborate dissolution and purification procedures.

List of Figures

Chapter - 4

Chapter - 5

Chapter - 6

Chapter 7

List of Tables

Chapter - 5

Chapter 6

Chapter 1

Introduction

1.1. Origin of elements

Origin of all naturally occurring elements present in the modern form of the periodic table can be explained based on the cosmic events that happened a few billion years ago in the universe. However, the routes of their formation are different for different elements. Back to the times, when there was no concept of "Time and Space", the whole universe was concentrated in an exceptionally dense, tiny point source which was incredibly hot with temperature over 10^{32} °K [1]. The entire universe was born in the most symmetric state and started to expand from this tiny point resulting in a massive explosion called "Big-Bang". Instantaneously after the big-bang moment, the temperatures fell considerably to about 10^{11} °K during the expansion. Formation of the first elements was not possible at this stage owing to the substantially high temperatures and high kinetic energy of the newly formed protons and neutrons which resulted in random movement of these particles at ultra-high speeds [1, 2]. However, due to the continuous expansion of universe there was a considerable fall in temperature, resulting in a favourable environment for the formation of first elements (Hydrogen and Helium) and subsequently from them, rest of the chemical elements were formed by various cosmological events. A brief discussion on the origin of various elements is given below.

1.1.1 Hydrogen and Helium

After a few minutes of Big-Bang event, the temperature fell down to a billion degrees kelvin (10^{9} °K), which was sufficient for fusion of neutrons and protons to form the first atomic nuclei, Deuterium [3, 4]. Further**,** two Deuterium atoms fused to form the Helium nuclei. In the early stages of the universe, due to the outnumbering of protons over neutrons by a ratio of 7:1, the entire universe was filled with hydrogen and helium with a very high cosmic abundance of

about 75 - 95% and 25 - 5% respectively and trace amounts of ^{7}Li, with an abundance ratio of Li/H ~ $5.61 \pm 0.26 \times 10^{-10}$ [1, 5].

1.1.2 Elements up to Iron

As the universe continued to expand and cool further, the entire matter spread into giant clouds of gas in space. Under the influence of its own gravity, contraction of this large gas clouds created enormous pressure at the centre which enormously increased the temperature of the system. This increase in temperature ($15 \text{ X } 10^{6}$ °K) at centre made hydrogen nuclei to fuse together to form helium which was responsible for the release of huge amount of thermal energy during nuclear fusion. This is how "the first star in the universe got its shine about 200 million years" after the big-bang event. The giant gas cloud system was shaped into a spherical ball due to the fusion energy being counter balanced by the inward gravitational pull. The process continued until there is no more hydrogen to fuse at the star's core. At this stage, the core of the star was filled with helium nuclei. As there was no release of fusion energy from the star's core, its gravity resulted in an inward pull and further contraction took place which led to increase in the pressure and temperature. This collapse made hydrogen to fuse in the middle layers. Now the fusion energy released at the middle layers made the star to expand further, beyond its previous size, called as "Red Giant". However, continuous contraction took place at the star's core which increased the pressure and temperature of the core enormously. At some point, the temperature of the star's core was hot enough for the fusion of helium to occur. This is how the formation of higher elements have taken place. The formation of higher elements depends on the mass of the giant molecular cloud, in case of small mass stars, carbon was the last heavy element that could be formed. As the inward pull by the gravity is not sufficient (due to low mass) to increase the temperature and pressure of the star's core to fuse the carbon nuclei, formation of higher elements could not take

place in low mass stars. In the case of large mass stars (larger than 8 times the mass of the SUN), formation of elements up to iron could take place by further fusion of carbon nuclei. Iron was the end of line for the formation of elements by fusion process [1, 2, 6].

1.1.3 Heavy elements

Occurrence of heavier elements happened by the supernova explosion of stars (small or large). During this explosion, the core material of the stars (elements up to carbon or iron) got heated to incredible temperatures and underwent capture of neutrons through various processes. This neutron capture is the reason behind the formation of all heavier elements [1, 2 - 7].

1.1.4 Lithium – Beryllium - Boron

Hydrogen fuses to form Helium. Three such Helium nuclei fuse to form Carbon. These are continuously undergoing processes in small stars (low mass stars). This leaves out the explanation for formation of 6-Lithium (the formation of ^{7}Li is explained later), Beryllium and Boron (elements in between Helium and Carbon) in the universe. Formation of 6-Lithium, Beryllium and Boron fall under a special category of cosmic events which does not fit in the above three processes. In fact, the formation of Li-Be-B is said to be a “Cosmic Mystery” and even now it is a hot-topic in the branch of cosmology. The explanation for possible formation is based on the Galactic Cosmic Ray (GCR) spallation. Cosmic rays are high energy particles travelling throughout the galaxy with relativistic speeds and can consist of anything from tiny electrons to nuclei of any element in the periodic table. As cosmic rays are travelling with very high speeds, when they hit atoms, part of the target nucleus can be “chipped off” forming two new particles. Lithium is expected to be formed along with helium, by the spallation reaction of carbon nucleus

with the hydrogen atom. Similar explanation could be given to the formation of beryllium and boron along with their isotopes [1 - 2, 8 - 12].

1.2. Discovery of isotopes

In the recent years, sophisticated instruments are available worldwide to determine physico-chemical properties of elements in different matrices required for diverse fields of interest. Due to the advancement in technology, it is now possible to determine the presence of a single molecule. But the discovery of isotopes occurred, back in the 19^{th} century, where most of the famous scientists were not aware of the existence of sub-atomic particles in an atom. A couple of decades after the discovery of isotopes, J. J. Thomson published an article in the year 1936 wherein he stated, ‘‘At first there were very few who believed in the existence of particles smaller than atoms. I was even told long afterwards by a distinguished physicist who had been present at my (1897) lecture at the Royal Institution that he thought I had been pulling their legs’’ [13]. The discovery of isotopes happened as follows:

In 1910, Frederick Soddy discovered that the element “Lead” differed in its mass depending on whether it had been formed from the decay of thorium or the decay of uranium. This was originally considered as a peculiarity of radioactive materials, which Soddy called ‘‘**isotopes**’’, from the Greek, words ‘‘iso’’ (same) and ‘‘topos’’ (place) as they can be found at the same position within the periodic table of the elements [14]. In the year 1912, Thomson and Aston could successfully collimate the ion beam through a magnetic and electric field during their experiments on positive rays. The electric and magnetic fields resulted in the deflection of charged particles according to their mass – to - charge ratio leading to the formation of a parabola on the photographic plates. The first mass spectrograph recorded was of the isotopes of Neon.

Isotopes of an element are the nuclides with same atomic number (Z) but different mass number (A) due to the variation in the number of neutrons (N) in the nucleus. For mono-isotopic elements with only one stable isotope whose abundance is 100%, the mass of the isotope is the atomic weight of the element. For di-isotopic or poly isotopic elements the atomic weight is the sum of the individual weight components of the different naturally occurring isotopes taking into account their individual abundances.

1.3. Significance of Isotope ratio measurements

Out of 1700 known isotopes in the periodic table, nearly 16% (264 isotopes) are stable. Isotopic measurement of these stable and unstable isotopes present in bulk, trace or ultra-trace concentration levels in different matrices are of special interest for characterizing samples [15 - 23].

1) It is very imperative to have the data on isotopic analysis for the precise determination of Atomic Weight of elements.

2) In general, the isotopic abundance of stable isotopes of an element are not constant. Variations in the isotopic abundance occurs in nature due to various possible reasons:

a) Natural isotope fractionation effects: Isotope exchange reactions, formation and transport of minerals due to weathering, geological and cosmogenic processes [24].

b) Anthropogenic contamination: Nuclear-fallout from the testing of nuclear weapons, discharge from the nuclear powerplants, discharge of detergent in sewage [25 - 26].

c) Radiogenic decay of unstable isotopes, e.g., the β^- decay of ^{87}Rb to ^{87}Sr, which in turn causes the changes in isotope abundances in nature.

Variation of an isotope ratio is usually presented as δ value of an isotope expressed as per mil (‰)

$$\delta = \left(\frac{R_{sample}}{R_{standard}} - 1\right) \times 10^3$$

The commercially available delta Delta (δ) isotope reference materials for various elements are listed in Table 1.1.

Table 1.1. List of commonly available Delta (δ) reference materials provided by various certified laboratories

S. No.	**Element**	**Symbol**	**Common Delta (δ) reference material**	**Description of Standard / Certified laboratory**
1	Hydrogen	H	VSMOW SLAP (later NIST – RM – 8537)	**V**ienna **S**tandard **M**ean **O**ceanic **W**ater **S**tandard **L**ight Antarctic **P**recipitation **N**ational **I**nstitute of **S**tandards and **T**echnology
2	Lithium	Li	L – SVEC (later NIST – RM – 8545) IRMM – 016	Li_2CO_3 **I**nstitute for **R**eference **M**aterials and **M**easurements
3	Boron	B	NIST - SRM - 951	H_3BO_3 powder
4	Carbon	C	L - SVEC, VPDB	Li_2CO_3

				Vienna **P**ee **D**ee **B**elemnite (fossilized shell of a Belemnite)
5	Nitrogen	N	USGS 34 (later NIST – RM – 8568)	KNO_3 **U**nited **S**tates **G**eological **S**urvey
6	Oxygen	O	VPDB, VSMOW, SLAP	
7	Magnesium	Mg	NIST – SRM - 980	Mg metal chips
8	Calcium	Ca	NIST - SRM - 915a / 915b	$CaCO_3$
9	Chromium	Cr	NIST – SRM - 979	$Cr(NO_3)_3$
10	Iron	Fe	IRMM – 014	Fe metal
11	Bromine	Br	SMOB	**S**tandard **M**ean **O**ceanic **B**romide
12	Rubidium	Rb	NIST - SRM – 984	RbCl powder
13	Strontium	Sr	NIST – SRM - 987	$SrCO_3$ powder
14	Thallium	Tl	NIST - SRM - 997	Tl metal
15	Lead	Pb	NIST – SRM - 981	Pb wire
16	Uranium	U	NIST – SRM – 950a	U_3O_8 powder

1.4. Importance of isotopic ratio measurement of lithium and boron

1.4.1 Cosmology

Along with mystery of the origin of Lithium and Boron in the universe, the cosmic story of ^{7}Li is puzzling to the cosmo-chemists and its formation is entirely different from that of the other isotope viz. ^{6}Li and the isotopes of boron (^{10}B &^{11}B) [2, 8 -12, 27]. ^{7}Li is a very important product in the Big-Bang nucleosynthesis and was possibly produced by two routes (i) ^{3}T (α, γ) ^{7}Li and (ii) ^{3}He (α, γ)^{7}Be (n, p) ^{7}Li [28]. The overall schematic of the production of ^{7}Li is given in Fig. 1.1.

Unlike ^{7}Li, the other isotope ^{6}Li along with boron was neither produced in the big-bang, nor in stars. They were formed in the Galactic Cosmic ray interactions. ^{6}Li is produced by spallation reactions of cosmic rays (protons) with the C, N and O present in the interstellar medium (p + O → ^{6}Li) and the fusion reaction of interstellar helium (α+α → ^{6}Li) [29].

In contrast to lithium isotopes, the formation of both the isotopes of boron are by the non-thermal nuclear reactions between high energy (GeV) particles such as protons and alpha particles in galactic cosmic ray with the C, N and O present in the interstellar medium as shown below.

^{12}C (p, x) $^{10, 11}$B

^{14}N (p, x) $^{10, 11}$B

^{16}O (p, x) $^{10, 11}$B

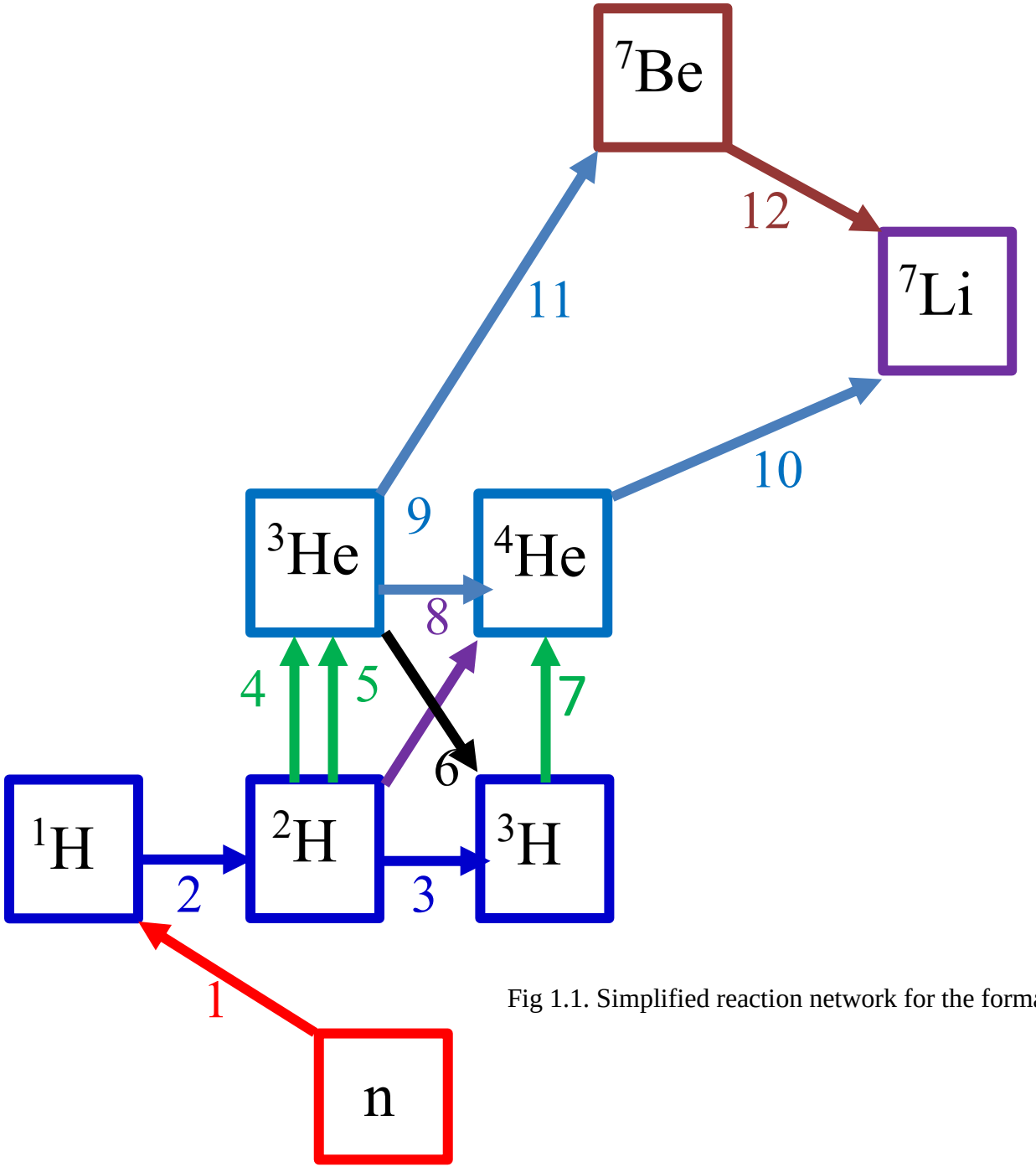

1. n to p
2. n (p, γ) d
3. d (d, p) t
4. d (p, γ) ^{3}He
5. d (d, n) ^{3}He
6. ^{3}He(n, p) t
7. t (d, n) ^{4}He
8. d (d, γ) ^{4}He
9. ^{3}He (d, p) ^{4}He
10. t (α, γ) ^{7}Li
11. ^{4}He (α, γ) ^{7}Be
12. ^{7}Be (n, p) ^{7}Li

Fig 1.1. Simplified reaction network for the formation of ^{7}Li during Big Bang Adapted from **[30]**

Even though the production route of ^{10}B and ^{11}B is same for the above reactions, the cross-sections of the reactions decided the fate of the isotopic abundance of the particular nuclei. Among the three reactions after a threshold energy, the cross-sections of ^{11}B formation are high and constant for increasing energy of the cosmic rays. Cross-sections for ^{10}B production with low proton energies are high and decreases exponentially with the increase in the energy of protons. It is also worth noting that the production of ^{11}B could also be produced by neutrino spallation reactions in carbon core collapse during supernovae explosion [31]. Though the explanations for the formation of these light elements were made through some experimental evidences, still some theories contradict the observations. So precise isotopic measurement of these elements can help in drawing some definite conclusions.

1.4.2 Geochemistry

It is the branch of science which not only explains the mechanisms of formation of Earth's crust and oceans but also deals with the distribution of chemical elements in the various layers of the earth. Lithium and Boron are considered to be the unique geological tracers because of their following physico-chemical characteristics: (i) moderate to high fluidic phase solubility [32, 33] (ii) large percentage mass difference between the isotopes (17% for lithium and 10% for boron), which leads to the large natural isotopic fractionation in different geologic reservoirs. Owing to these properties, at low temperatures (< 100ºC) the lighter isotopes (^{6}Li, ^{10}B) are preferentially retained in the condensed phase (rock, sediment etc) leaving the isotopically heavy isotopes (^{7}Li, ^{11}B) in the fluid [34, 35]. By measuring these small deviations in $\delta^{7}Li$ and $\delta^{11}B$ in these tracers, studies are being carried out on crustal assimilation, fluid tracking related processes in rocks and hydrothermal water-sediment-rock interaction [36 - 38].

1.4.3 Hydrology

Hydrology is the scientific study of flow path-ways of water, residence time of water in the catchment areas, source of water runoff and contaminant transport. Both lithium as lithium chloride and boron as sodium borate (borax) are selected as artificial tracers for the hydrological purposes [39]. One of the important applications employing these tracers is to find out the source of anthropogenic pollution caused by the sewage waters from households and effluents from various industries [40, 41]. The oxy compounds of boron are widely used in cosmetics, herbicides or fetilizers and household products. Manufacturing of the washing powders is one of the unavoidable and major source of boron content (in its perborate form) in the sewage from households. Usage of washing powders is the one of the main contributors of anthropogenic boron (about 60-70%) in the aquatic environment [42]. On the other hand Lithium is most widely used in the production of lithium battery materials, semiconductor detectors, in glass and ceramic industry [43]. It is also used in the clinical field as a therapeutic for mania, all of which require its accurate estimation. Apart from this, often distinctly low $^{6}Li/^{7}Li$ and $^{10}B/^{11}B$ isotopic signatures are observed in the sufrace waters nearer to the lithium and boron enrichment plants, where the tail product is disposed which is depleted in ^{6}Li and ^{10}B content. Lithium and Boron have a wide usage in nuclear industry. To figure out the source of anthropogenic contamination the measurement of isotopic ratios of lithium and boron is required for hydrological applications in addition to their quantitative determination.

1.4.4 Paleoceanography

It is “the study of the history of the oceans in the geologic past with regard to circulation, chemistry, biology, geology and patterns of sedimentation and biological

productivity". Deviations in the isotope ratios of Lithium and Boron from the isotopic standards (δ^7Li and δ^{11}B), in the oceanic marine organisms are considered as potential proxies for reconstruction of the changes in CO_2 and pH of oceans in the geological past. As residence times of lithium and boron are very large (~ 10 – 20 million years) when compared to oceanic mixing time of 1000 years, lithium and boron are considered to be the conservative elements with a mean oceanic concentration of 0.1 - 0.2 ppm and 4 - 5 ppm respectively [44, 45]. However, residence time of CO_2 in the earth's atmosphere is about 4 years; ocean is the best sink for this green-house gas [46]. Carbon dioxide dissolves in seawater to form carbonic acid, bicarbonate and carbonate ion by the following equilibrium.

$$CO_2 + H_2O \overset{K_1}{\Leftrightarrow} H^+ + HCO_3^- \overset{K_2}{\Leftrightarrow} 2H^+ + CO_3^{2-} \text{ ---------- Eqn. 1.1}$$

Sum of all the carbon containing molecules in the above equilibrium is known as total CO_2 or Dissolved Inorganic Carbon (DIC). This is how the acidification of an ocean takes place with the uptake of atmospheric CO_2. Reconstructions of pH of the ocean to the geological past can be made by measuring the isotope ratios of lithium and boron, which are also correlated with the amount ratios of Li/Ca or B/Ca of the oceanic marine organisms such as foraminiferal shells [47 - 49]. The routes of uptake of lithium and boron in these organisms are different and are still under debate.

1.4.4.1. Lithium incorporation

A recent study demonstrated that an increase in the amount ratio of $(Li/Ca)_{shell}$ and $(Li/Ca)_{seawater}$ was observed with the change in concentration of lithium in seawater. Whereas $(Li/Ca)_{shell}$ was found to be constant with the change in seawater Ca concentration. This suggests that, unlike divalent ions (such as Sr^{2+}), which compete for the binding sites of Ca^{2+} ion

transporters, monovalent lithium ions (Li^+) do not compete with Ca, rather they probably diffuse (through ion channels) to the lattice sites during the calcification of these marine organisms [50].

1.4.4.2. Boron uptake

Based on the laboratory culture experiments, it was suggested that foraminifera could store and concentrate Ca^{2+} and DIC internally by pumping Ca^{2+} and HCO_3^- in to a secondary reservoir. Further it was assumed that, similar to human Na^+- K^+ biological pump (for the energy production), a Ca^{2+} pump may be functioning from the secondary reservoir placed in the vacuoles of marine organisms. This pump is also responsible for this large discrimination in the accumulation of Ca^{2+} and other cations of similar size and charge in these shells. Similar to this mechanism, a transporter which is favorable to HCO_3^- might be allowing small quantities of the charged $B(OH)_4^-$ but not $B(OH)_3$ [51].

1.4.5 Nuclear Industry

Lithium, with its both the isotopes ^6Li and ^7Li has wide usage in the nuclear industry. Owing to its low thermal neutral absorption cross-section (0.045 barns), enriches ^7Li as LiOH is added to the coolant in PWR's to stabilize the pH for control of corrosion in the coolant channel, and also in the form of fluorides such as ^7LiF-BeF_2 and ^7LiF-NaF-KF are potential molten salt coolants and solvent to the fuel salts in High Temperature Reactor (HTR) [52, 53], ^6Li is used in blanket materials for breeding tritium for future fusion reactors. $LiAlO_2$ and Li_2TiO_3 enriched with ^6Li are among the proposed solid breeder materials for the International Thermonuclear Experimental Reactor (ITER) program [54].

Boron in various chemical compounds such as oxy-compounds, Boron carbide, refractory metal borides are required in nuclear industry, due to the high neutron absorption cross section of ^{10}B (3843 barns). Boron as Oxy compounds such as B_2O_3 and H_3BO_3 are used as liquid poison in heavy water moderator systems of PHWRs and in primary coolant circuit of PWRs respectively. Boron carbide (B_4C) is used in control rods due to its attractive features such as exceptional hardness, low density and excellent chemical and thermal stability. When used in FBRs, boron has to be enriched in ^{10}B (up to 65%) [55]. In view of better physical properties like high melting point (3200°C) which is superior to B_4C (2650°C), good thermal conductivity, low density and chemical inertness, boron in the form of titanium diboride TiB_2, is considered as an excellent candidate material for CHTRs [56]. In addition to this, various refractory and rare-earth metal borides like CrB_2, ZrB_2, HfB_2, EuB_6, LaB_6, CeB_6 and its composites have also been proposed for the development of an alternative material to titanium diboride [57 – 60].

1.5. Mass Spectrometer – A tool for isotope ratio measurements

Mass Spectrometers are "the analytical instruments that generates gas phase ions in the sample input systems, where ionization of the analyte may be carried out thermally by resistive heating or by bombarding with high energy electrons, ions or photons; the ions formed are separated according to their mass-to-charge ratios (*m/z*) using static or dynamic, electric or magnetic fields (or combination thereof) and their detection is carried out according to their respective mass to charge ratio (*m/z*) and abundance". Though the above definition dates back to 1968, when organic mass spectrometry was in its infancy [61], the broad definition is still valid for the present generation mass spectrometers with improved features such as.

Source of Ionization, not only affected by energetic electrons but also by

i) energetic neutral atoms (Fast Atom Bombardment – FAB)

ii) photons (Laser ablation - LA)

iii) (atomic) ions (Secondary ionization – SI)

iv) electro-statically charged micro-droplets (Electro Spray ionization – ESI)

v) heating by resistive means (Thermal Ionization – TI) or by plasma source (Inductively coupled – ICP, Glow discharge – GD)

Second, ion separation is not only affected by static or dynamic electric or magnetic fields but also in field-free regions, provided, ions are mono energetic and possess a well-defined kinetic energy at the entrance of the flight path (Time-Of- Flight – TOF).

Mass Spectrometers can be classified into various categories depending on the type of ionization sources, mass analyzers, species monitored and type of focusing. The broad classification of various mass spectrometers is given in Fig. 1.2. The required major components of any mass spectrometer can be represented in the form of the block diagram as shown in Fig. 1.3.

1.5.1 Ionization sources

Although different ionization techniques are being developed for different applications, the principle aim of the ionization source is to produce efficient ion beam. A large variety of ionization techniques based on different ionization processes are used for isotope ratio measurements, the principles and their key applications have been summarized in the Table 1.2.

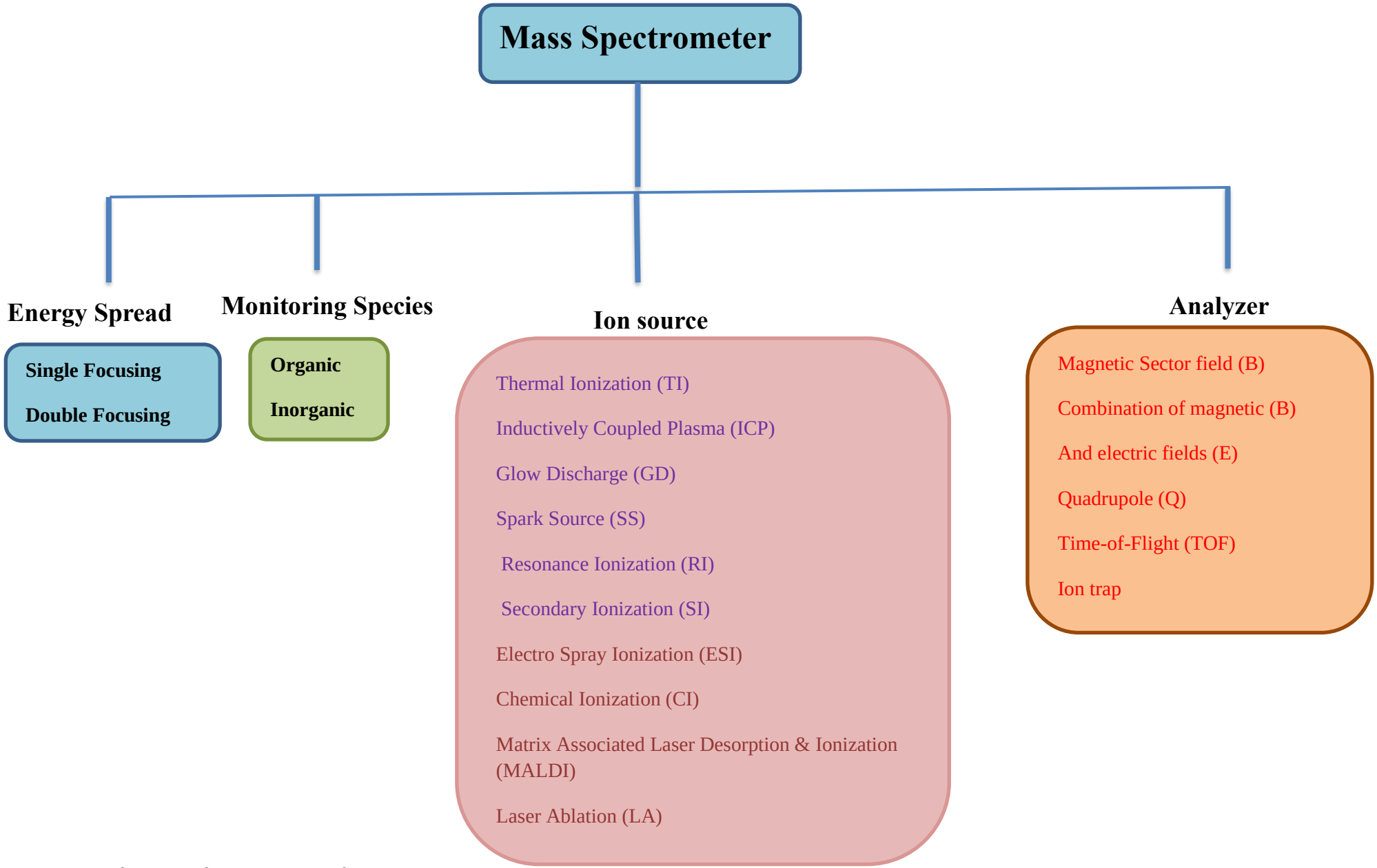

Fig. 1.2. Classification of various type of mass spectrometers

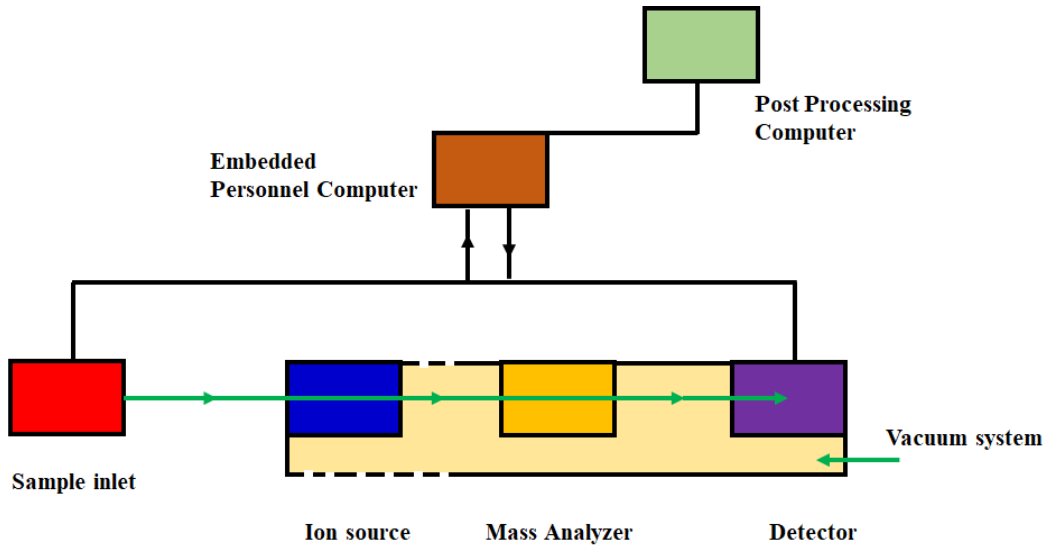

Fig. 1.3. Block Diagram of a Mass Spectrometer

1.5.2 Ion separators (analyzers)

An essential part of a mass spectrometer, the ion separation system has the task of separating the ions with respect to their mass to charge (*m/z)* ratios. The separated ion beams are then supplied to the ion detection system. Ion separation systems can be classified as

i) Static ion separation systems

Magnetic fields, electric fields and a combination of the two (double – focusing) are considered as static ion separation systems in a mass spectrometer

ii) Dynamic ion separation systems

These use different flight time of ions with different masses and different velocities. In addition to the flight time, separation of isotopes occurs due to the change in the strength of electric and / or magnetic fields. Time-Of-Flight, Quadrupole, Ion trap, Ion Cyclotron Resonance Mass analyzers are a few examples for dynamic mass separation systems.

Table 1.2 List of commonly used ionization methods for the isotope ratio measurements and their applications

S. No.	Method of Ionization	Principle	Conditions	Applications
1	Spark Source	Sample is vaporized & ionized by a high-voltage radiofrequency spark between two electrodes	Solid sample coated on cathode; ionization under vacuum	Multi-elemental technique for trace analysis
2	Glow Discharge	Ionization occurs in the discharge of Ar gas, called Plasma, developed between two electrodes	Solid sample coated on cathode; Ionization under Ar atmosphere	Multi-elemental technique for trace analysis & depth-profiling
3	Thermal Ionization	Ionization due to the resistive heating of the filament material	Sample solution loaded on the filament, ionization under vacuum	Isotope ratio analysis, quantification using Isotope dilution method
4	Inductively Coupled Plasma	Vaporization & Ionization in a radiofrequency argon plasma- torch	Aspiration of sample solution into Ar plasma-torch; Ionization under Ar atmosphere	Isotope ratio, Multi-element at trace levels
5	Secondary Ionization	Secondary ions (analyte ions) are produced by the bombardment of accelerated primary ions	Solid sample, ionization under vacuum	Surface characterization, depth profiling, imaging
6	Accelerator Mass Spectrometry	Secondary negative ions (analyte ions) are accelerated with low energies (10-100keV) to mega-electron Volt (MeV) energies in tandem accelerator. Positive ions are produced after stripping of electrons from negative ions and analyte positive ions are analyzed	Sample is converted to solid cathode; instrumentation is a coupling of MS-MS (Tandem Mass spectrometry)	Very low abundant isotope ratio measurement ($^{14}C/^{12}C$, $^{10}Be/^{9}Be$, $^{41}Ca/^{40}Ca$, etc.) at very low detection limits ~ 10^{-16}g

The classification and the general principles of all these static and dynamic ion separation systems have been tabulated in Table 1.3.

Table 1.3. List of various types of mass analyzers and their principles of operation

S. No.	Type	Acronym	Principle
1	Magnetic Sector	B	Deflection of a continuous ion beam; separation by momentum in magnetic field
2	Quadrupole	Q	Continuous ion beam in RF quadrupole field; separation due to instability of ion trajectories
3	Time-of-Flight	TOF	Time dispersion of a pulsed beam; separation by the flight time of the ions
4	Quadrupole Ion trap	QIT	Trapped ions; separation in three-dimensional RF quadrupole field by resonant excitation
5	Fourier transformation cyclotron resonance	FT-ICR	Trapped ions in magnetic field; separation by cyclotron frequency, image current detection and Fourier transformation of transient signal
6	Orbitrap	Orbitrap	Axial oscillation in inhomogeneous electric field; detection of frequency after Fourier transformation of transient signal

1.5.3 Detectors

The back-end portion of the mass spectrometry instrumentation is dedicated to a detection system, which generates the signal either by charge or current produced by the ions that passes or are incident on a detector surface. The characteristics of an ideal MS detector are shown in Fig. 1.4. None of the available detectors possesses all the said characteristics. Depending on the application there are various detectors employed for mass spectrometers which are listed in Table 1.4.

1.6. Isotope Ratio Measurements of Lithium and Boron

Minor differences in isotopic ratios of lithium and boron have to be detected as part of investigations in various fields of research as mentioned in the section 1.4, for which high precision and accuracy is required during their isotopic analysis. The nature of the sample of interest can be different for different fields of research. For example, chondrites, meteorites and star dust are used in cosmology; sediments, granites and basalt rocks are usually of interest in geology; geothermal, shallow, fresh and surface-waters are analyzed for hydrology; oxy compounds and certain refractory materials of lithium and boron with superior characteristics are being developed for advanced nuclear reactors.

A tabular representation of various type of samples of lithium and boron and the analytical techniques used for the determination of the natural variations in the isotopic ratios of lithium and boron reported in different review articles has been presented in Table 1.5 & 1.6.

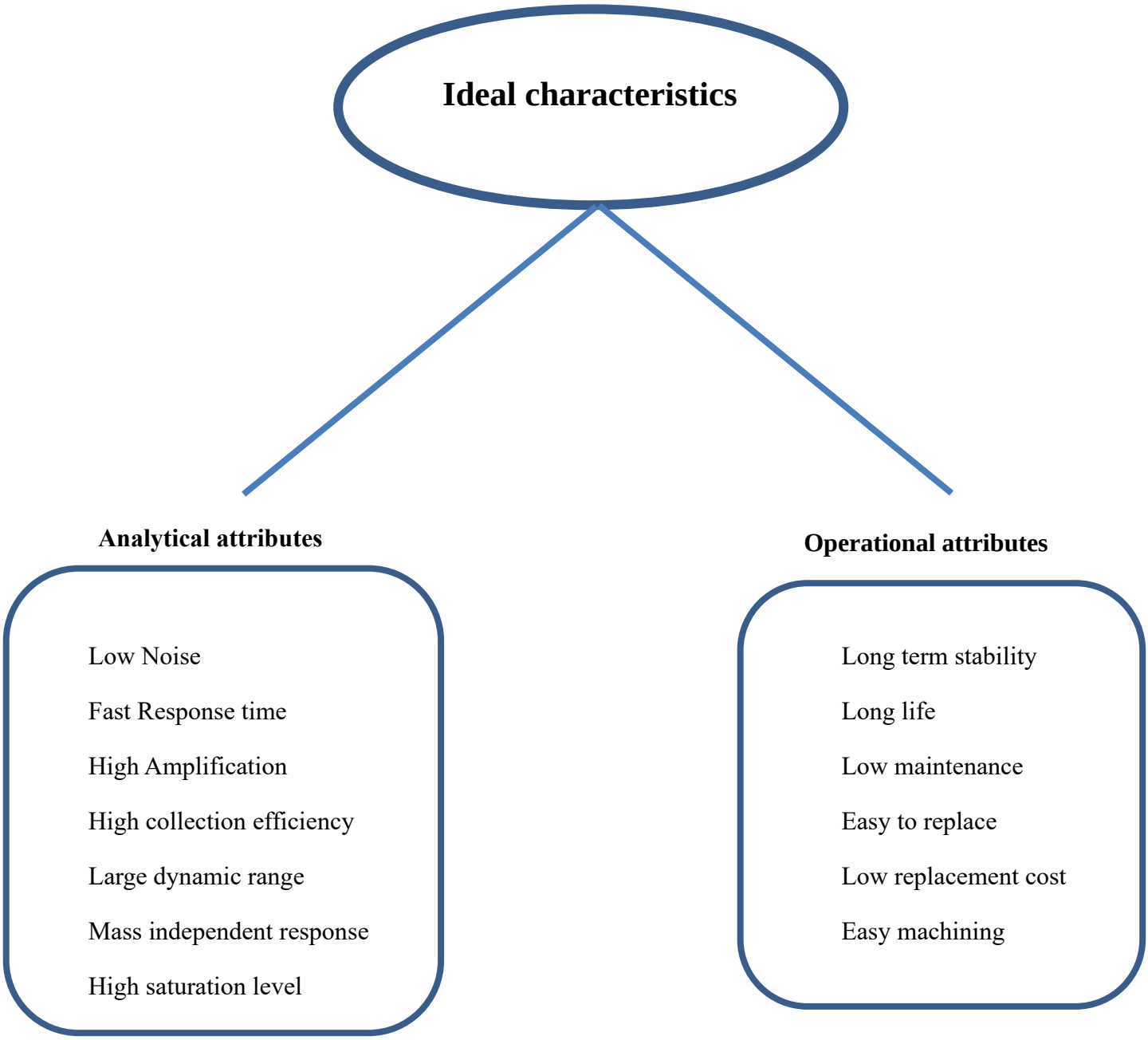

Fig. 1.4. Characteristics of an ideal detector

S. No.	Type of Detector	Principle		Application
1	Photographic plates	Dark tracks are produced upon ion impinging on the plate. Intensity of dark tracks is proportional to the number of ions striking the plate		Used for all most all the earlier generation mass spectrometry Still being used for simultaneous collection in focal plane detection
2	Electron Multiplier	When charged particle strikes the detector's surface, emission of secondary electron takes place from the detector's surface.	The secondary electron is amplified to more than million times by the cascade of discrete dynodes.	Suitable for all most all organic and inorganic mass spectrometers, where simultaneous multi-collection is not required. Used for the characterization of low abundant species
3	Channel Electron Multiplier		The secondary electron is amplified by single dynode made from a resistive film on an insulating surface in the form of a curved tube or convoluted channel	
4	Daly Detectors		Secondary electrons are accelerated towards a scintillator, and upon striking generation of photons takes place. These photons are detected by Photo Multiplier Tube (PMT)	
5	Faraday cups	Incident ions strike the electrode surface. Electric current flows away from the electrode surface through high ohmic resistor, across which a potential difference is created. This potential difference is measured.		Used for Simultaneous multi-collection instruments
6	Focal pane array detectors	It consists of an array of $10^4 – 10^7$ miniaturized channel electron multipliers. The individual channels are orientated in parallel to each other. Principle is similar to CEMs.		Mass Spectrometers with Mattauch-Herzog geometry, used for simultaneous multi-collection of large number of ions Ion imaging (in microscope mode) for Secondary Ionization Mass Spectrometers (SIMS)
7	Cryogenic detectors / Super Conducting Tunneling Junction (STJs)	The impact of ions or particles on the superconducting thin film creates phonons, which are subsequently absorbed by breaking Cooper pairs. This results in the electron-hole excitations (quasi particles), which can quantum mechanically tunnel through the existing barrier, creating a measurable signal.		Used for i) neutral and molecular beam spectroscopy ii) Particle physics and astrophysics iii) DNA sequencing by STJ detector with MALDI-TOF MS

Table 1.4. List of various detectors with principles of detection and their application

Table 1.5. Variations of lithium isotopic ratios in different types of samples and their measurement techniques

S. No.	Nature of the sample	Ion source loading material	Monitoring ion	Method of analysis	Natural variations (in ‰)	Reference
1	Sargasso sea water, Basalt, Volcanic Arc, Fe/Mn Crust, P. Obliquiloculata, Mid Ocean Ridge Basalt (MORB)	Li_3PO_4	Li^+	TIMS	δ^6Li = -40.7 to -4	[65]
2	Seawater, basalt, granite and chondrite	Li_3PO_4	Li^+	TIMS	δ^6Li = -31.5 to 1.2	[92]
3	Basalt, hydrothermal fluids, marine evaporites, carbonates, black shales	Li_3PO_4	Li^+	TIMS	δ^6Li = -32 to -4	[93]
4	High temperature vent fluids	$LiBO_2$	$Li_2BO_2^+$	TIMS	δ^6Li = -11 to -6	[94]
5	Seawater, basalt	Li_3PO_4	Li^+	TIMS	δ^7Li = +4.9 to + 30.0	[95]
6	Lava samples	Sample solution	Li^+	MC - ICPMS	δ^7Li = +3 to +4.8	[96]
7	Ridge and Vent fluids	Li_3PO_4	Li^+	TIMS	δ^7Li = +7.2 to +15.4	[97]
8	Flood basalt	Sample solution	Li^+	MC - ICPMS	δ^7Li = +3.5 to +4.0	[98]

9	Arc volcanics from subduction zones	Li_3PO_4	Li^+	TIMS	δ^7Li = +1.1 to +7.6	[99]
10	Alkaline lavas, adakite lavas and MORB	Sample solution	Li^+	MC - ICPMS	δ^7Li = +1.4 to +11.2	[100]
11	Lava samples	Li_3PO_4	Li^+	TIMS	δ^7Li = +4 to +6	[101]
12	MORB	Li_3PO_4	Li^+	TIMS	δ^6Li = -13.7 to +1.4	[102]
13	Sediments from hydothermal fluids	Lithium sodium borate	$LiNaBO_2^+$	TIMS	δ^6Li = -11 to +1	[103]
14	Pore waters (Greenland)	Li_3PO_4	Li^+	TIMS	δ^6Li = -42 to -25	[104]
15	Pore fluids (Escanba)	Li_3PO_4	Li^+	TIMS	δ^6Li = -26.8 to -0.6	[105]
16	Clays and sediments	Sample solution	Li^+	MC - ICPMS	δ^7Li = -1.6 to +12.8	[106]
17	Sedimentary granites, Shales for upper continental crusts	Sample solution	Li^+	MC - ICPMS	δ^7Li = -5 to +5	[107]

Table 1.6. Variations of boron isotopic ratios in different types of samples of boron and their measurement techniques

S. No.	Nature of the sample	Monitoring ion	Method of analysis	Natural variations (δ^{11}Bin ‰)	Reference
1	Geothermal waters	BO_2^-	N-TIMS	-22 to 25	[108]
2	Industrial vent fluids	BO_2^-	N-TIMS	-4.8 to +0.9	[109]
3	Saline ground water and sediments	BO_2^-	N-TIMS	-10.2 to +26.3	[110]
4	Tourmaline samples	B^+	Ion microprobe	-2 to +30.0	[111]
5	Rain water	$Cs_2BO_2^+$	P-TIMS	+38	[112]
6	Seepage water	BO_2^-	N-TIMS	-5.7 to +9.6	[113]
7	Sea water	B^+	MC-ICPMS	+39.61	[114]
8	Surface and ground water samples	B^+	MC-ICPMS	-0.8 to +20	[115]
9	Fossil corals	$Cs_2BO_2^+$	P-TIMS	23.3 to 25.5	[116]
10	Tourmaline samples	B^+	Ion microprobe	-15 to -5	[117]
11	Marine carbonates	BO_2^-	N-TIMS	+22.1	[118]
12	Fresh and transition zone water	BO_2^-	N-TIMS	+20 to 30	[119]

From the Tables 1.5 & 1.6, it is evident that, irrespective of the nature of the sample, Thermal Ionization Mass Spectrometry (TIMS) and Inductively Coupled Plasma source Mass Spectrometry (ICPMS) are widely used for high precision measurement of isotopic ratios of lithium and boron. A few reports have also been published using Ion microprobe as a measurement technique. Owing to 100% (nearly) ionization efficiency, high sample through put with achievable

precision in isotope ratio measurement comparable to TIMS (0.01% or better) the magnetic sector based ICP systems with multi-collector assembly are gaining popularity. However, it suffers from certain disadvantages such as i) huge spectral and non-spectral interferences ii) large but constant instrumental mass bias up to 25% for lighter elements especially lithium which depends on the matrix and concentration of the sample [62] iii) memory effects which can affect accuracy for samples with widely varying ^{10}B content and iv) need for matrix matched standard, as the behavior of analyte is affected by the type of matrix. Standard-Sample-Standard bracketing approach has to be used for correction of this instrumental mass bias.

On the other hand, TIMS has been internationally recognized as a gold standard for isotope ratio measurements, due to the high accuracy and precision obtained during isotope analysis. Owing to the low operational temperature of the ionization filament (~2000^{o}C), singly charged ions are produced which makes the interpretation of spectrum is very simple [63]. Every time a fresh filament is used for the sample loading procedure, therefore the measurements are not affected by memory effects of previous sample during analysis by TIMS. One of the drawbacks of TIMS measurement is isotope fractionation which is as a result of preferential evaporation of lighter isotope relative to the heavier ones, leading to the continuous decrease in the measured isotopic ratio with time. The severity of the fractionation is high for lighter elements such as lithium. This can be reduced by monitoring their polyatomic molecular ions having higher masses relative to their atomic ions.

1.7. Isotopic analysis of Li & B using molecular ions

Isotopic measurement of various elements by TIMS can be carried out by monitoring either atomic or polyatomic molecular ions. The term Atomic Ion Beam Method (AIBM) is

normally used for atomic ions while Poly Atomic Molecular Ion Beam Method (PAMIBM) is used when molecular ions are monitored. Each method has its own associated merits and demerits. The ion intensity ratio measured by AIBM is a direct measure of isotope ratio and is normally preferred for high Z elements with reasonably low ionization potential whereas PAMIBM is used for low Z elements to reduce fractionation effects or for elements with high ionization potential.

Adoption of AIBM for the precise isotopic measurement of lithium isotopes is a challenging task because of mass dependent isotopic fractionation which is induced by the lower atomic mass of lithium and also due to the high relative mass difference (17%) between the isotopes of ^{6}Li and ^{7}Li. Though the sensitivity of AIBM is high, precision and accuracy depend on a large number of parameters such as; the amount of sample loaded on the filament, the nature of chemical compound of lithium, purity of the sample and the time of collection of the data etc [64 - 67].

Production of atomic ions of boron (B^{+}) is not possible in the thermal ion source due to its high first ionisation potential (8.1eV). Isotopic analysis of boron is usually carried out by monitoring alkali metaborate ions $M_2BO_2^{+}$ (M = Na, Rb or Cs) or BO_2^{-} ions in positive mode of TIMS or negative mode of TIMS respectively. Isotopic analysis of boron using BO_2^{-}, by N-TIMS is very sensitive and requires 5 -10 ng of boron for comfortable analysis. However, a high-level operator skill and strict analytical protocols such as amount of boron deposited on the filament and heating conditions etc are required for precise analysis [68 - 72]. Positive mode of TIMS using alkali metaborate ions, gives precise and accurate results though the amount of boron on the filament has to be at µg levels.

In the present studies the possibilities of using PAMIBM as an alternate method for precise and accurate isotopic measurement of lithium has been further explored whereas for boron

isotopic analysis, PAMIBM is the only method of choice. In our laboratory, $Na_2BO_2^+$ ions at *m/z* 88 and 89 are being conventionally monitored for boron and $Li_2BO_2^+$ at *m/z* 54 to 57 for lithium.

1.8. Determination of total number of polyatomic molecular ion species

Prior to any measurement, it is essential to determine the total number of ionic species formed for a specific polyatomic ion being employed. Sodium and cesium, being mono-isotopic; boron and oxygen being di - and tri - isotopic elements respectively, the total number of species (for such type of isotopic combination of elements) will be calculated as follows:

$$total\ no.of\ species = a_{Na,Cs}^2 * (a+b)_B * (a+b+c)_O^2 \quad \text{-------- Eqn. 1.2}$$

where a, b and c are the different isotopes of the element represented in the molecular species

Upon expanding the terms, we get

$$total\ no.of\ species = a_{Na,Cs} * (a+b)_B * (a^2+b^2+c^2+2ab+2bc+2ca)_O \text{ --- Eqn 1.3}$$

On addition and multiplication of the terms in the equation, we get total number of species formed (12 for $Na_2BO_2^+$ and $Cs_2BO_2^+$) whereas for lithium and rubidium being bi-isotopic

$$total\ no.of\ species = (a+b)_{Li,Rb}^2 * (a+b)_B * (a+b+c)_O^2 \text{ ----- Eqn. 1.4}$$

For potassium being tri-isotopic we get

$$total\ no.of\ species = (a+b+c)_K^3 * (a+b)_B * (a+b+c)_O^2 \text{ ------ Eqn. 1.5}$$

Table 1.7, gives the total number of species formed for a particular alkali metal atom, if we employ alkali metaborate ions for the isotopic measurement.

Table 1.7. Number of species can be formed for different alkali borate ions

S. No.	Molecular ion	No. of species
1	$Li_2BO_2^+$	36
2	$Na_2BO_2^+$	12
3	$K_2BO_2^+$	72
4	$Rb_2BO_2^+$	36
5	$Cs_2BO_2^+$	12

1.9. Determination of elemental isotope abundance ratios from polyatomic molecular ion ratio

Isotopic measurement of boron using $M_2BO_2^+$ (M – alkali metal Na / Rb / Cs) as monitoring ions by TIMS is commonly used method among researchers [73 - 82]. Sodium and cesium being mono-isotopic, the appropriately chosen ion intensity ratios directly yield the boron isotopic ratio i.e., $^{10}B/^{11}B$ from ion intensity ratios at *m/z* 88, 89 when sodium is the alkali used and at *m/z* 308, 309 when cesium is used, viz. $^{88}I/^{89}I$ and $^{308}I/^{309}I$ respectively. Rubidium has two isotopes, resulting in distribution of boron among the 36 molecular species there by decreasing their intensities. However, since the two isotopes of Rb differ by 2 a.m.u. both $^{10}B/^{11}B$ and $^{85}Rb/^{87}Rb$ ratio can be distinctly obtained from the $^{212}I/^{213}I$ and $^{213}I/^{215}I$ respectively. This enables correction for fractionation using the correlation between the two ratios using SRM 951 and natural Rb [83]. Whereas the mass difference between the two isotopes of ^6Li and ^7Li is 1 a.m.u. and therefore due to the Isotopic Abundance Distribution (IAD) pattern, the molecular ion intensity ratios do not directly give the B and Li isotopic ratios. The mathematical equation required to

obtain the $^{6}Li/^{7}Li$ and $^{10}B/^{11}B$ ratio is complicated due to this distribution of the isotopes among the different molecular species formed [84 - 89]. $Na_2BO_2^+$ was the first alkali borate ion used for measurement of boron Isotopic Composition [90]. With multi-collection detectors, simultaneous collection of these polyatomic ion is easily possible unlike the case of $Cs_2BO_2^+$ where state of art instrument is required due to the small dispersion at *m/z* 308 & 309. Though high sensitivity with $Cs_2BO_2^+$ method has been achieved by researchers, with modifications in the existing methodology, the sensitivity of $Na_2BO_2^+$ method has also been improved considerably to sub - ppm levels since the time it was first used [91].

When the polyatomic molecular ion $Li_2BO_2^+$, is used for isotopic analysis of Li, neither Li nor B isotopic ratios can be obtained directly from their polyatomic ion intensity ratios due to their overlapping spectra even if ^{16}O is considered to be monoisotopic. $^{6}Li/^{7}Li$ can be obtained from the polyatomic ion ratios such as $R_{56/57}$, $R_{55/57}$ and $R_{55/56}$ from the following equations

$$2Li + B - R_{56/57} = 0 \longrightarrow \text{Eqn. 1.6}$$

$$Li^2 + 2B * Li - R_{55/57} = 0 \longrightarrow \text{Eqn. 1.7}$$

$$Li^2 + 2\left(B - R_{55/56}\right) Li - B * R_{55/56} = 0 \longrightarrow \text{Eqn. 1.8}$$

where Li = $^{6}Li/^{7}Li$ and B = $^{10}B/^{11}B$

Isotopic ratio of lithium can be determined from any of the above polyatomic ion ratios $R_{56/57}$, $R_{55/57}$ and $R_{55/56}$ by substituting the numerical value (0.2473) of SRM-951 (an isotopic standard of boron), which is added to the lithium sample (mole ratio B/Li ~ 5), for the production of lithium metaborate ions. Even though, the determination of the isotopic ratio of $^{6}Li/^{7}Li$ from $Li_2BO_2^+$ appears to be complicated due to the nature of the quadratic equations involved, the method is robust and the conditions for analysis are not as stringent as that required for atomic ions. However, during the mass spectrometric analysis, both Li & B isotopes suffer from isotopic

fractionation due to preferential vaporization of the lighter isotopes of the constituent elements of $Li_2BO_2^+$ ions at ion source. Hence in the determination of lithium isotope abundance ratio, the fractionation of boron isotopes cannot be account since the experimental observed value cannot be independently determined. Moreover, in case of any inadvertent contamination of boron during the sample preparation, the true Li isotopic abundance ratio cannot be determined even if boron of known isotopic abundance ratio is used for the analysis of Li as $Li_2BO_2^+$. This limits the accuracy of the method.

1.10. Scope & aim of Present work

The objective of the present thesis is the application of molecular ions for precise and accurate determination of isotopic ratios of Li and B in various types of samples used for nuclear industrial applications. Thermal ionization mass spectrometry has been employed in the entire work for the isotopic ratio measurement. Owing to the various advantages of molecular ions over atomic ions, the present work focuses on the application of molecular ions of lithium and boron for the isotopic ratio measurement of lithium and boron. Sodium metaborate ion ($Na_2BO_2^+$) for the boron isotopic analysis, Lithium metaborate ($Li_2BO_2^+$) and also Sodium lithium metaborate ions ($NaLiBO_2^+$) have been used for the isotopic analysis of lithium.

The present work gives an insight into the selection of a particular pair of polyatomic ion ratios of $Li_2BO_2^+$ for the simultaneous determination of accurate isotopic ratios of both lithium and boron from the same filament loading. Theoretical calculations and its comparison with the results obtained from the experimental studies have been evaluated in the present study.

Details of the new method using $NaLiBO_2^+$ and $Na_2BO_2^+$ ions from lithium loaded as sodium lithium borate for determination of $^6Li/^7Li$ ratio is presented. The $LiNaBO_2^+$ method has

certain advantages over $Li_2BO_2^+$ as the cumbersome mathematical calculations could be avoided by application of the experimentally determined boron isotopic ratio (from same filament loading) to improve the accuracy of isotopic analysis of lithium. Ion source isotope fractionation for both boron and lithium was observed during the analysis and conditions were optimized for steady isotope ratio pattern for precise analysis.

Though adoption of molecular ions reduces the severity of isotopic fractionation by increasing the molecular mass of the species monitored this is at the cost of sensitivity. Analysis as atomic ions Li^+ requires only a few nanograms of the analyte, whereas if molecular ions such as $Li_2BO_2^+$ or $NaLiBO_2^+$ have to be monitored at least 1.5 µg Li is required on the filament. This requires processing of large sized sample which may not be possible when precious samples for geochronology and astrophysics have to be analyzed, where the sample amount is very limited. Total Evaporation and Ion Integration (TE & II), where data is acquired till all the sample deposited on the filament has exhausted completely, was developed for the sodium lithium borate ions. The method improves the accuracy since the intensity ratios measured are nearly free of fractionation and is also more sensitive than the conventional method of data acquisition.

Isotopic standards over wide range of ratios are required for calibrating the mass spectrometer for the determination mass discrimination factor and to validate the optimized experimental conditions of analysis of any newly proposed method (Analysis of Li using $NaLiBO_2^+$ as monitoring ions). Isotopic standards with varying abundances of ^6Li from 1%, 8%, 20%, 35%, 50%, 75% and 85% were prepared by mixing appropriate amounts of calibrated isotopic solutions of ^6Li and ^7Li. Calibration of these enriched stock solutions of lithium were carried out by isotope dilution thermal ionization mass spectrometry against Spec Pure Li_2CO_3 having natural isotopic composition using $NaLiBO_2^+$ ions.

The alkali borate ions were used for isotopic analysis of Li and B in refractory materials. For the production of alkali metaborate ions, boron (in the form of sodium borate) is added to lithium compound and sodium (in the form of sodium carbonate) is added to boron sample. Refractory samples of both boron and lithium were analyzed by direct fusion of the sample with sodium carbonate and sodium borate respectively. The experiments included validation of the method with dissolved samples and purified samples in the case of boron samples. For lithium samples total evaporation results were compared with the conventional method of analysis. Some compounds of lithium analyzed were Li_2TiO_3, $LiAlO_2$, $Li_2B_{10}O_{16}$ and boron compounds were B_4C, TiB_2, ZrB_2, LaB_6, CeB_6. The fusion route adopted for the refractory samples avoided dissolution and separation procedures that are conventionally used for analysis of samples by TIMS.

Chapter 2

Thermal Ionization Mass Spectrometry

Thermal ionization is considered to be one of the oldest sample ionization techniques that could be coupled to a mass spectrometer after the gas discharge tube. Though Gehrcke and Reichenheim observed the thermal emission of positive ions from a salt placed on a heated surface, the actual application of this ionization technique was developed by Dempster during his construction of first 180º sector magnetic field mass spectrometer [120, 121].

2.1. Principle of Thermal Ionization

2-5 µL solution containing ng to µg amounts of the analyte element is deposited on the filament surface and dried by means of resistive heating under atmospheric pressure. This loaded filament is further heated under high vacuum (~ 10^{-8} mbar). During the course of evaporation, when neutral atomic or molecular species of the vapor impinges on the hot metallic surface, according to Langmuir effect in addition to the neutrals there will be a small but a finite probability of the ion emission [122]. This ionization efficiency is different for different elements and can be calculated theoretically using Saha-Langmuir equation as given in Eqn. 2.1.

$$\alpha = \left(\frac{n^+}{n^o}\right) = \frac{g^+}{g^o} * exp\left[\frac{\Phi - E_i}{kT}\right] \quad \text{--------- Eqn. 2.1.}$$

Where α = ionization yield

n^+ and n^o = number of emitted positive ions and neutral atoms, respectively

g^+ and g^o = statistic weights of positive ion and atom, respectively

Φ = work function of the metal

E_i = first ionization potential of the element

k = Boltzmann constant

T = absolute temperature (in ºK) of filament surface

The choice of the filament material is based on the combination of work function and the melting point of the metal. It is desirable to have large values for work function and melting temperatures of the filament for high ion yield. The list of various filament materials that could be used for TIMS with their work functions and their melting points is listed in Table 2.1.

Table 2.1. Work function and melting points of various filament material

Element	Work function (eV)	Melting point (^{o}C)
Nickel	5.24	1453
Tantalum	4.30	2996
Tungsten	5.01	3410
Rhenium	5.10	3180
Platinum	6.27	1769

From Saha-Langmuir equation, it is evident that, elements whose first ionization potential values (E_i) are lower compared to the work function (Φ) of filament material would have high ionization efficiency (e.g. alkali and akali earth metals). However, for the elements with E_i values between that of alkali metals and 9 eV, the following modified loading conditions are adopted:

(i) Multiple filament (double or triple) geometry by Inghram and Chupka, where the sample solution is deposited on one of the filaments and heated to relatively lower temperatures when compared to another filament [123]. This way evaporation and ionization processes of the analyte element are decoupled. Neutral vapors controlled by the heating rate of the evaporation filament are directed towards to the other filament which operates at higher filament currents for

the effective ionization. Isotopic ratios of rare-earth metals and actinides, are being carried out using multiple filament geometries.

(ii) It is difficult to obtain a stable ion current for elements like lead, zinc etc with high volatility and high first ionization potential ~ 7eV, using thermal ionization. But with the application of filament surface modifiers such as Silica gel – phosphoric acid [124], an activator that produces a glassy type material on the filament, the volatility of these elements is possibly reduced to produce a stable ion current resulting precise isotopic ratio.

(iii) Isotopic analysis of non-metals such as boron with high E_i (8.1 eV) is not possible by monitoring its atomic ions (B^+). Therefore, isotopic measurement of boron is carried out using molecular ions $M_2BO_2^+$.

Improvement of analytical conditions of various elements for the precise isotopic analysis include the development of various conditions in which Saha-Langmuir equation strictly cannot applicable for the conditions whose ionization occurs from single filament assemblies by adopting surface modified filaments, polyatomic ion beam analysis and for the situations such as chemical and physical processes occur at ionization filament.

Though improvement in the precision and accuracy of isotope ratio measurement has been achieved by improving the ion-yield for various elements from single filament assemblies by adopting surface modified filaments and polyatomic ion beam analysis, application of Saha-Langmuir equation cannot be valid. This equation also does not hold for the condition of multiple filament geometries whose chemical and physical processes occur at ionization filament. However, this the equation still holds in the prediction of a gives a rough estimation in the comparison of ionization efficiencies of two or more elements [125, 126].

With slight change in the mathematical terms of the Saha-Langmuir equation the production yield of negative ions can be predicted for elements with high electron affinities (E_a> 2eV). Isotopic analysis of elements such as halogens, S, B, Se, Mo, Tc etc, can be analyzed by monitoring their molecular ions using negative mode of thermal ionization. The modified form of Saha – Langmuir equation is as follows:

$$\alpha = \left(\frac{n^-}{n^o}\right) = \frac{g^-}{g^o} * exp\left[\frac{E_{ea} - \Phi}{kT}\right] \qquad \text{---------- Eqn. 2.2.}$$

Where α = ionization yield

n- and n^o = number of emitted negative ions and neutrals respectively

g^- and g^o = statistic weights of negative ion and neutral species respectively

Φ = work function of the metal

E_{ea} = first ionization potential of the element

k = Boltzmann constant

T = absolute temperature (in ^oK) of filament surface

With the advancement in instrumentation, the scope of TIMS has widened to include elements that ionize to form both positive and negative species to cover most of the elements in the periodic table.

2.2. Developments of Sector Magnetic Field

Sir J. J. Thomson was the first person to develop the mass spectrograph of isotopes of element Neon in 1911 [127 - 129]. However, mass spectrometer with sector magnetic fields was first developed and used by Dempster [130]. A very brief history for the birth of sector magnetic field analyzers is given here. Thomson used Wien's filter for the deflection of the produced ions [131]. Under the influence of magnetic and electric fields (perpedicular to each other), ions gets

deflected tracing a parabolic path before it impinges on a photographic plates on a locus of points. Each parabola is a characteristic to an ion (isotope) of particular charge to mass (z/m) ratio in the given gaseous mixture [127 - 129]. This was the first Mass Spectrograph which gave evidence of the existence of isotopes of an element and subsquently turned out to be the key evolution point in the development of mass spectrometry.

Unlike "Thomson's first mass spectrograph", where the electric and magnetic fields were perpendicular to each other (Wien's filter), Aston made his mass spectrometer (1919) with an "energy filter" (electric field in form of parallel plates) placed prior to the strong magnetic coil (as a mass analyser) [132]. This was the first time that the velocity filter was adopted for the ion collimation rather than slits. The greatest advantage gained by this arrangement in achieving "Aston's first mass spectrum" is that, there was a drastic improvement in the accuracy and the resolution of the instrument. This was possible due to the focussing all the deflected ions of same "z/m" to same point on the screen. Irrespective of the kinetic energy of the deflected ions, the position of this spot is exclusively mass dependent. During almost the same time period, Dempster (1918) had built a different type of mass spectrometer, in which, he used a sector based magnetic analyser with a deflection angle of 180^{o} [130]. Due to the peculiar property of the sector magnetic field, refocussing of the divergent ion beam could be possible, at the detector slit which is placed on the focal plane. This is called direction focussing and causes a significant enhancement in the sensitivity of the instrument. The birth of the Sector magnetic field had created revolution in the development of mass spectrometers.

Though direction focussing could improve the sensitivity in the Dempster's first mass spectrometer, the ionsource and the collector have to be placed at the boundaries of the sector magnet resulting in poor resolution which was also affected by the fringe magnetic fields. The

solution to this was provided by Herzog for a typical case of symmetrical 60º magnetic sector analyzer [133]. Based on the solutions to the equations of direction focusing qualities of magnetic sectors, he suggested that, for ions entering at angle of 90º to the magnetic field, the entrance and exit slits can be located at a distance of 1.7321 R_m on either side of the magnet, where R_m is the radius of the magnet. The solutions for 90º sector magnet analyzers gave similar symmetric footprints for placing the ionsource and collector at equal distances from the entrance and exit poles of magnetic, the only difference being the focal lengths [134]. This meant, smaller the deflection angle, larger will be the focal length (foot print) of the system. The details of the evolution of magnetic analyser to present day system is covered in in literature [134 - 136]. The working principle of the direction focussing for sector magnet analyzer is given in the section 2.3.

2.3. Principle of direction foucssing for Magnetic Sector anayzer

The ions entering the Sector magnetic field analyzer is subjected to a combination of prism effect and lens effect. The separation of the ion beam according to their mass to charge ratio (m/z) is due to the prism effect and the direction focussing i.e. collimation of diverging ions is due to the lens effect of the sector magnetic field.

Ions generated in the ion-source chamber will be directed towards the analyser region by the application of a high voltage (8 KV to 10 KV), between the sample filament and the exit slit of the ion-source housing. This causes ions to accelerate towards the analyzer region with kinetic energy given by

$$K.E. = \frac{1}{2}mv^2 = eV \quad \text{---------} \quad \text{Eqn. 2.3}$$

Where m = mass of the ion

v = velocity of the ion

e = charge of the ion

V = applied potential

These accelerated ions enter the analyser into a region of constant magnetic field. Here only ions of particular mass to charge ratio, whose Lorentz force (which is orthogonal to the direction of the field and direction of ion motion) is exactly balanced by a centripetal force, will have a circular trajectory and pass through the analyzer tube. This is given by Eqn. 2.4.

$$Bev = \frac{mv^2}{r} \qquad \text{----------} \quad \text{Eqn. 2.4}$$

Where r = raidus of trajectory of an ion; up on equating the two equations and substituting for v we get

$$\frac{m}{e} = \frac{B^2 r^2}{2V} \quad \text{----------} \quad \text{Eqn. 2.5}$$

This basic equation (Eqn. 2.5.) shows the dependency of mass to charge ratio on either the strength of magnetic field or applied potential. The trajectory of the divergent ion beam from the point source to the collector plane by single (direction) focussing characteristics of magnetic analyzer is as shown in Fig. 2.1.

Direction focusing collimates the ion beam in y-axis which is perpendicular to the direction of the magnetic field. Ions in the z-direction are not collimated since there is no component of magnetic field in this direction. The sensitivity of the measurement is therefore affected. Then the concept based on Legler's theory of Stigmatic focusing on electric fields was applied to sector magnets with a slight modification in their angle of incidence.

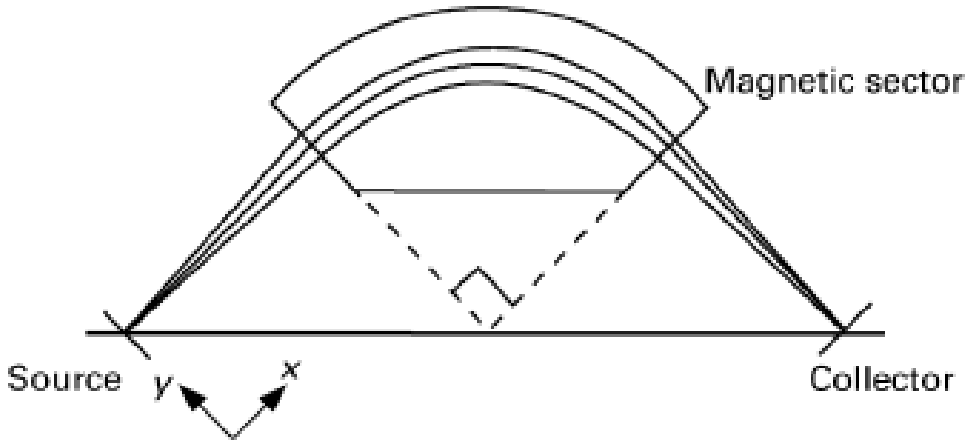

Fig. 2.1. Trajectories for the ion beam incident normal to the pole face of 90º sector magnet

2.4. Stigmatic focusing [137, 138]

In contrast to conventional focusing where the incident ions are perpendicular to the plane of sector magnet, in stigmatic focusing the ions are made incident at an angle of 26.6º to the pole face. This was achieved by machining the sector magnets for shaping the pole faces. This generated a component of magnetic field in orthogonal direction to the plane of the sector magnet due to which the ions in the z-direction were brought to focus at the collector resulting in more efficient transmission of ion from source to detector. The pictorial trajectories for the ion transmission from both directions (y and z- direction) with stigmatic focusing is given in Fig. 2.2 & 2.3. Application of stigmatic focusing improved the sensitivity and increased the dispersion due to extension in the effective radius of the curvature of the analyzer.

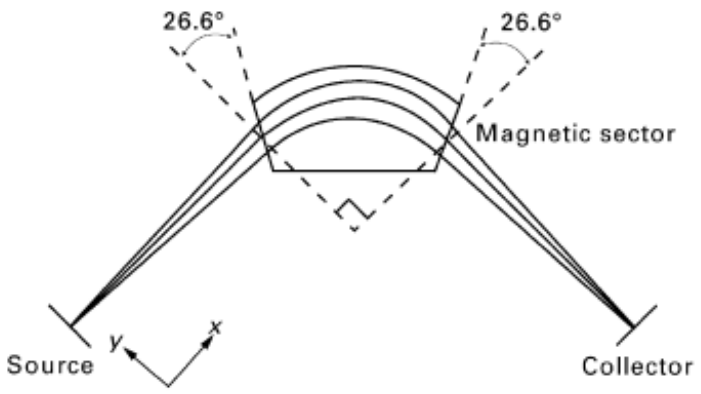

Fig. 2.2. Trajectories of the ion beam focused in Y-direction with an incident angle of 26.6º

Fig. 2.3. Ion transmission due to Z- focusing

2.5. Detectors

Among the various available detectors mentioned in the Table 1.3, Faraday Cups, Electron Multipliers, and Daly Detectors are commonly used in Thermal Ionization Mass Spectrometers. Measurement of signal intensity is carried out either in pulse counting, where individual ions are counted, or in analog mode (direct mode), where incident ion beam intensity is measured as an ion current (charge per unit time). A brief discussion on the ideal characteristics which are shown in the Fig. 1.4 and the advances carried out in the development of these detectors are given below.

2.5.1 Faraday Transducer

Faraday cup detectors are inevitable choice for accurate measurement of relatively high ion currents of the separated beams in the analog mode, due to the following advantages a) response of faraday cup detector is independent of ion energy, mass and the chemical nature of ions. b) Accurate output, constant sensitivity and low electric noise c) possibility of simultaneous multi-collection. Faraday detectors are usually designed as "cup-shaped" rectangular metal box opened at one end through which the separated ions are impinged. These ions get neutralized by the electrons supplied through the ground. This electron current is recorded after passing through the high-ohmic resistor. Typically, $10^{11}\,\Omega$ resistors are used. Faraday detectors can operate in two modes Static and Dynamic.

i) Static mode: This is the most common mode of operation of faraday detector in most of the commercial mass spectrometers when the ion currents in the range of 10^{-14}A to 10^{-10}A. In this mode the separated ion beam is incident on the metal electrode and the measurement is carried by charge transfer of the charged particle.

ii) Dynamic mode: This mode of operation is chosen when the ion currents are far higher than 10^{-10}A where the detector response is saturated. Here the charged particles are allowed to have a free passage through the cup. During this passage, there will be induced current developed which is proportional to the magnitude of the charge transported [139].

In static mode operation when the accelerated ion beam strikes the electrode surface, they get neutralized, in addition significant emission of secondary electrons also takes place. Substantial development has been carried out to offset this effect and also improve other aspects of the counting system. A few of them are described below:

An Electron repeller / suppressor, which is an additional slit connected to a negative potential is placed near the entrance of the Faraday cup which causes the emitted secondary electrons to be repelled back to the electrode. The secondary electron emissions are also hindered by the application of small magnets. Increase in the aspect ratio (depth/width) and graphite coating for the inner layers of the faraday bucket also prevents the secondary electron emissions [140].

In most of the multi-collection systems of inorganic mass spectrometers such as MC-TIMS and MC-ICPMS, typical range of ion currents measured by regular faraday cups are 10^{-14} A to 10^{-10} A after amplification by high ohmic feedback resistor (10^{11} Ω). But for special applications to measure the low abundant isotopes, now a days, amplifiers with 10^{13} Ω resistors are available which can measure very low signal intensities (30 kcps) with external precisions close to limits of counting statistics [141, 142].

Apart from the amplification, faraday cups are often affected by their response time. The response time of a typical faraday cup is in the range 0.2 sec (for an ohmic feedback resistor 10^{11} Ω with a combination of 2 pF capacitance). That means, detector has to wait for the Current to Voltage Converter (CVC) to respond to changes in beam current, while switching masses, etc. In the recent times, fast response faraday cups with about 10 nsec response times are manufactured for the measurement of electron beam experiments [143].

2.5.2 Electron Multipliers (EMs)

The working principle of an electron multiplier is based on the emission of secondary electrons from the surface of the metal electrode. When an ion impinges on a metal surface, the emission of electrons takes place from the surface layer of the electrode which are called “Secondary Electrons”. The number of secondary electrons emitted from the surface depends on the nature of the incident charged particle, its energy and the nature of the surface of the electrode

material. The multiplication of these secondary electrons is carried out in two types. 1) Discrete dynode Secondary Electron Multiplier (SEMs) 2) Continuous dynode or Channel Electron Multiplier (CEMs). A SEM has a dynode array which typically consists of 12 to 24 dynodes to which a high voltage is applied. Charged particles that are impinged on the first dynode (conversion dynode) releases secondary electrons. These are further accelerated by virtue of electron optics to the next dynode which is operated at successively higher voltage. Thus, an electron cascade is achieved with the several dynodes which results in a gain between 10^4 to 10^8 electrons per single incident ion. Detector's output is characterized by its gain, which is defined as the average number of electrons collected for each incident charged particle.

In contrast to Faraday cup detector which operates only in analog mode, Electron Multipliers can be operated in both modes i,e analog and pulse counting mode. In analog mode, relatively higher signal intensities are amplified to a medium gain of about $10^3 – 10^5$ with the conventional amplifying techniques such as Current to Voltage Converter (CVC). For lower signal intensities higher amplification up to $10^6 – 10^8$ is attained. At such high amplification, the gain is large enough to distinguish, individual electron pulses from the instrumental noise allowing pulse counting technique to be used. The pictorial representation of the Dual mode of operation of an EM is given in Fig. 2.4. Although the sensitivity of EM is better in comparison with Faraday cup by a factor of $10^5 – 10^8$ and the response times faster, they suffer from various disadvantages such as mass discrimination effects, deterioration in peak shapes and dead time of the detector. However, with the application of dual detector modes (faraday and EM), the dynamic range of a mass spectrometer is extended up to 10^9 which increases the measurement range from 1000 μgml^{-1} (1000 ppm) to as low as 1 $pgml^{-1}$ (ppt) [135, 136, 144].

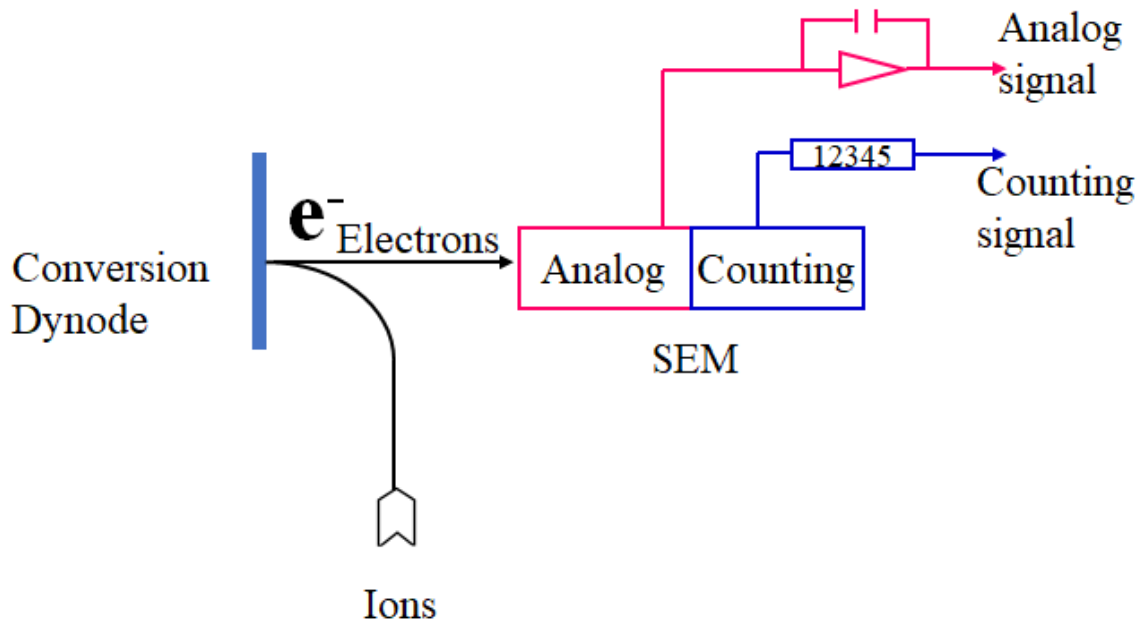

Fig. 2.4. A typical schematic of an ion counter which operates in both analog and digital mode.

2.6. Instrumental Parameters affecting the precision of isotope ratios

TIMS is an inevitable choice and a benchmark technique for the high precision and accurate isotope ratio measurement of various elements due to various advantages like low instrumental background, production of mostly singly charged particles, element selectivity and element specificity, minimal spectral interference (isobaric) due to molecular ions. However, the measurement precision in the isotope ratio analysis is affected by various instrumental parameters which are discussed below.

2.6.1 Peak shape

One of the reasons for high precision and accuracy of thermal ionization mass spectrometric measurement is the flat-topped peak as shown in Fig. 2.5. The combination of narrow entrance slit width and wide collector slit width, makes the ion beam acquire a trapezoidal

shape with flat-topped peaks. The advantage of the flat-topped peaks is that the ion intensity can be measured accurately despite small fluctuations in magnetic field or acceleration voltage.

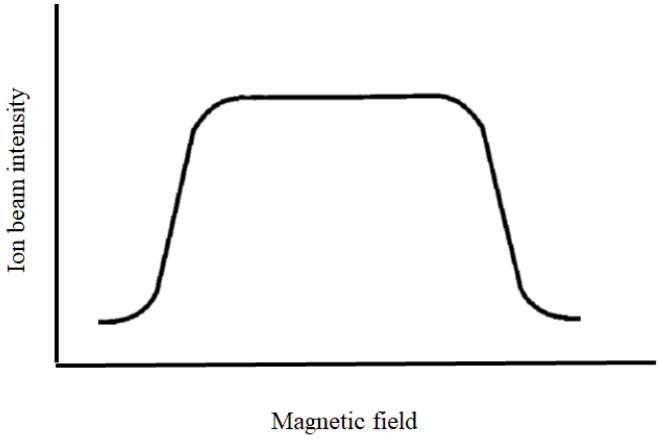

Fig. 2.5. Trapezoidal shaped flat-topped peak

2.6.2 Gain Calibration of Faraday transducer

Due to their small width multi-collector faraday cup assemblies are employed for simultaneous multi-collection of isotopes to give very precise isotopic ratios. However, the measurement accuracy is limited to the differences in the response factors / efficiencies of the individual collectors. This can be overcome by performing cross-calibration of all the faraday detectors with respect to the reference cup. Generally, a constant current of 2×10^{-12}A on the lower side and 9×10^{-11}A on the higher side generated externally by an amplifier source is fed to all the individual amplifiers connected to the respective faraday cups. The response of all the amplifiers is measured for both lower and higher constant currents. The average of the ratios of the response of the individual amplifiers with respect to the reference cup yields the cross-calibration (gain calibration) factors [145].

2.6.3 Virtual amplifiers (Matrix calibration) for Faraday detector

In contrast to classic approach of cross-calibration, a relay matrix has been used in this design, where the amplifiers can be switched between different Faraday cups. The bias caused by the uncertainties associated in the amplifier cross-calibration can be greatly minimized using this approach [146].

2.6.4 Plateau voltage of Electron Multiplier

Electron multipliers yield high gains in the range of 10^8 -10^9. For providing such high gains, successive increase in the voltage is applied for the cascade of dynodes. The optimization of the operating voltage is crucial for accuracy of the measured counts and to prevent sudden aging of the detector. As shown in the Fig. 2.6, below the threshold voltage, actual signal pulse and pulse from unwanted sources (noise pulses) cannot be distinguished. With the increase in the voltage above the threshold, there will be continuous increase in the measured count rate. Further increase in the operating voltage will have a little effect on detector response. On still further increase of the operating voltage a sharp increase in the count rate is observed due to some adverse effects such as “ion-feedback” and “electronic double counting of pulses (after pulsing effects)”. Though the gain of the detector is increased at operating voltages higher than the plateau voltage, the best analytical attributes such as linearity, stability in the gain and detector’s aging is achieved when the operating voltage is just above the knee of the plateau region [136]

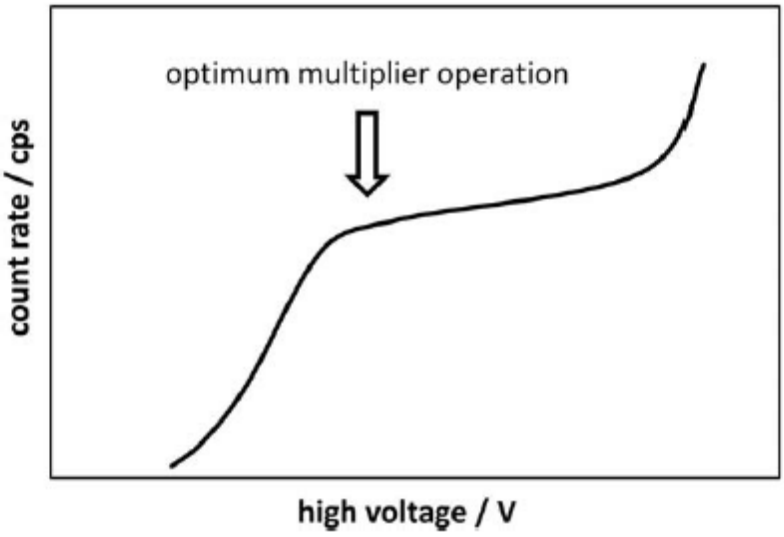

Fig. 2.6. Ion counting plateau of SEM

2.6.5 Linearity of Electron Multiplier

A linear relationship between analyte ion current supplied to the electron multiplier and its output count rate is a pre-requisite analytical condition for the accurate pulse-counting measurement using Electron Multipliers. In an ideal condition, the intercept of the linear relationship plot represents the EM's dark noise. The slope of this plot represents the relative yield of the electron multiplier, which is the ratio between the measured count rate and the true rate of ions incident on the detector. If the EM is calibrated to maintain its linearity, the yield is independent of the count rate applied to the EM. However, count rate response is strongly affected by dark noise as well as dead-time of the detector. The choice of EM is very crucial with respect to low dark noise levels for the accurate measurement of isotopes having extremely low relative abundances such as ^{230}Thand ^{236}U in natural samples. Of the two manufacturers, EM from ETP offers relatively lower dark noise (< 1cpm) when compared to EM from MasCom [147]. On the

other hand, if the count rate is too high the detector's dead-time will affect the linearity of the measurement. It was observed that non-linearity starts at a moderate count rate of 2 X 10^4 cps and requires significant correction as it increases beyond 10^5 cps. In addition to this, the count rate of EM is also dependent on following physical processes:

i) Velocity and angle of incidence of the analyte ions impinging on the conversion dynode

ii) Acceleration of the secondary electrons between the dynodes

iii) Surface charge effects on the last dynode of the electron multiplier.

2.7. Isotopic fractionation

For any mass spectrometric measurement, various random and the systematic source of uncertainties are responsible for the deviation of the measured isotopic ratios from the true ratios. This deviation is referred as mass bias factor. In MC-TIMS, as all the isotopes of an element are being collected simultaneously any fluctuation in the ion current due to changes in instrumental parameters will not result in any loss in the precision. In the thermal ionization source, the process of evaporation from single or multiple filament assembly follows Rayleigh's distillation law according to which the rate of evaporation is inversely proportional to the mass of an isotope. During the course of evaporation, with the increasing amount of sample removed from the filament, there will be a continuous depletion of the lighter isotope in the residue. This process of mass dependent differential evaporation of lighter isotope over the course of evaporation is termed as ion source fractionation which is the main source of uncertainty in TIMS measurements. Consequent to this, the observed ratio (lighter/heavier) is positively biased during the early stage of evaporation, equals the true ratio at 63% consumption of the sample from the reservoir and is negatively biased towards the end of the measurement [148, 149]. Due to this phenomena, the

observed isotope amount ratio changes with time which affects the accuracy of acquired data since the ion intensities are recorded only for a certain period of time for common modes of data acquisition. A brief discussion on various modes of data acquisition is given below.

2.8. Modes of data acquisition

Two Thermal Ionization Mass Spectrometers of make Isoprobe-T (VG, UK) and Triton-Plus (Thermofisher, Germany) with salient features listed in Table 2.2 were employed during the work presented in this thesis. Data acquisition which is software controlled can be carried out by 3 modes of operation.

2.8.1 Static mode of multi-collection

Prior to data acquisition, the faraday cups are adjusted in accordance with the configuration given by the software for the collection of atomic or molecular ions of interest so that, there is a perfect alignment of the peak-shapes of the isotopic ion beams. The magnetic field is set for the reference mass to be collected in the reference (axial) cup and the rest of the isotopes are collected in the respective cups accordingly. Ion currents of all the isotopes are integrated for about 5 sec for each scan and 12 such scans are grouped to a block. For routine day-to-day analysis, to have a better statistics, data is acquired for 3 to 5 such blocks. Though static mode of multi-collection improves the measurement precision by collecting all the ion beams simultaneously, the measurement accuracy is affected by the individual response factors of faraday cups. In order to account for this, gain-calibration of faraday cups are performed prior to data acquisition as detailed in section 2.6.2.

Table 2.2 Salient features of mass spectrometers employed

S. No.	Parameter	ISOPROBE-T (Make: VG, UK)	TRITON (Make: Thermofisher, Germany)
1	Radius of curvature	27 cm (effective = 54 cm)	23 cm (effective = 81cm)
2	Ion beam incidence Angle & Foot-print	26.5º (Stigmatic focusing) & Symmetric	26.5º (Stigmatic focusing) & Asymmetric
3	Slit widths	Entrance = 0.3mm; Exit = 1 mm	Entrance = 0.3 mm; Exit = 1.7 mm (Adjustable slit)
4	Resolution	400 (10% valley at mass 238)	470 (10% valley at mass 238)
5	Dispersion	17% (for simultaneous collection of ^{6}Li &^{7}Li)	17% (for simultaneous collection of ^{6}Li & ^{7}Li)
6	Sensitivity	1 ion in 300 atoms of uranium	1 ion in 200 atoms
7	Accelerating voltage	Up to 8 kV	Up to 10 kV
8	Sample loading	Single or triple filament assemblies	Single or double filament assemblies
9	Data handling system	Completely automated via Mass Lynx software	Completely automated via Triton software
10	Vacuum system	One rotary pump, one turbomolecular pump, two ion pumps	One rotary pump, one turbomolecular pump, two ion pumps
11	Abundance sensitivity (contribution of ion current of mass M at M±1)	2 ppm at mass 237(due to ions of m/z 238) and 20ppb with WARP filter	1 ppm at mass 237(due to ions of m/z 238) and 2ppb with RPQ
12	Detectors	9 movable faraday cups	9 movable faraday cups; 1 SEM
13	Others		Zoom-Optics (for peak jumping)
			TE and II acquisition mode is available in the software.

2.8.2 Dynamic mode of multi-collection by peak jumping

In this mode, the reference cup is assigned to different masses of the ions to be collected in different sets. In each set, proper peak-shape alignment of the isotopes is required. During the measurement, the magnetic field is changed by peak jumping so that the ions of the different isotopes are collected as defined in the set. Usually, a delay time of 1 sec is given between the measurement of replicate sets in each scan. This delay time is required to settle the magnetic field that has been changed according to the requirement of the set. Integration time, number of scans and blocks to acquire the data is similar to the static mode of multi-collection. As the replicate sets of data have to be collected for each scan and due to the delay time between these sets per scan, the time taken for the data acquisition for dynamic mode is much more compared to that of static mode of multi-collection. However, since the same ion beam is measured by different faraday cups, the response factors of individual transducers are nullified with this mode of data acquisition.

2.8.3 Total evaporation and Ion-integration method (TE & II)

Unlike routine day-to-day analysis, where the data acquisition is restricted to a limited number of scans, in TE & II method the data is acquired till the sample is completely exhausted. In this method, the data acquisition is carried out by integrating the ion currents for all the isotopes being monitored. The ratio of the integrated ion currents at the end of the measurement gives the isotope amount ratios of an element under study. Since the ions are collected till the sample is completely exhausted, the isotope ratios will not be affected by ion source fractionation and yields isotope ratios closer to the true value. Only a few nanogram amount of sample are required for

analysis by this method of data acquisition. Since the ions are integrated, this method of acquiring data is appropriate for minor isotopes. Ideally the method is suitable for sample evaporating as single ionic species, though it is also being used for elements evaporating as multiple species which have low abundance compared to the species being collected. Small corrections may be required to account for residual ions which is done using isotopic standards.

2.9. Correction methodologies

Correction methodologies are required for isotopic measurement carried out using either static or dynamic mode of multi-collection as both are affected by isotope fractionation. Methods such as external normalization and internal normalization using a known / certified ratio are employed to obtain a correction factor (K) which is the ratio of certified ratio to the observed ratio. These normalization methods use suitable algorithms such as linear, exponential, power, linearized Rayleigh and Rayleigh for obtaining the fractionation factor per unit mass. A brief discussion of these methodologies is given below.

2.9.1 External normalization

In this approach, mass spectrometric measurement is carried out for the isotopic Standard Reference Materials (SRMs) of the analyte element prior to the sample analysis. From the observed ratio and the certified ratio of the isotopic standard, the fractionation factor (K) can be easily calculated using the following formula

$$K = \frac{\left(\frac{R_{observed}}{R_{true}} - 1\right)}{\Delta m}$$

Where K = mass discrimination factor

$R_{observed}$ = measured isotopic ratio (m_L/m_H ratio of the lighter isotope to heavier)

R_{true} = certified isotopic ratio of SRM

Δm = mass difference between the two isotopes in an isotopic ratio considered

This is the most widely used method for obtaining K, provided isotopic standard reference materials are available. The main drawback of this method is that the sample and standard should be analyzed under identical conditions which requires stringent control of various parameters.

2.9.2 Internal normalization

This technique is applicable for the elements with three or more isotopes of which at least a pair of isotopes should have an invariant / constant ratio. For example, $^{88}Sr/^{86}Sr$ isotopic ratios = 8.375209 [150] and $^{146}Nd/^{144}Nd$ = 0.7219 [151, 152] are invariant and their experimentally observed ratio is used to obtain the fractionation factor calculated using appropriate fractionation laws as given below. This is used to correct the other ratios of interest to the two elements. The process of internal normalization to give accurate values for isotopic ratios of interest is carried out using any of these empirical algorithms given below [142]. Strontium is used as an example.

Rayleigh law:

$$\frac{r_1}{S_1} = \frac{\beta_1}{(\beta_2)^x}\left(\frac{r_2}{S_2}\right)^x \qquad\qquad x = \frac{\beta_2(\beta_1 - 1)}{\beta_1(\beta_2 - 1)}$$

Exponential law:

$$\frac{r_1}{S_1} = \left(\frac{r_2}{S_2}\right)^x \qquad x = \frac{ln(\beta_1 - 1)}{ln(\beta_2)}$$

Power law:

$$\frac{r_1}{S_1} = \left(\frac{r_2}{S_2}\right)^x \qquad x = \frac{m_2 - m_1}{m_3 - m_1}$$

Linear law:

$$\frac{r_1}{S_1} = (1 - x) + x\left(\frac{r_2}{S_2}\right) \qquad x = \frac{m_2 - m_1}{m_3 - m_1}$$

where

r_1 and S_1 is the measured and normalized $^{87}Sr/^{86}Sr$ ratio respectively

r_2 and S_2 is the measured and true invariant $^{88}Sr/^{86}Sr$ ratio respectively

m_1, m_2 and m_3 are the nuclidic masses of ^{86}Sr, ^{87}Sr and ^{88}Sr respectively

β_1 is the $(m_2/m_1)^{1/2}$ and β_2 is $(m_3/m_1)^{1/2}$.

As the experimental conditions for measurement of the reference ratio and the ratios of interest of the element are the same, stringent analytical protocols during analysis are not required.

Chapter 3

Development of precise and accurate methods using molecular ions for isotope ratio measurement of Lithium by TIMS

3.1. Introduction

Isotopic measurement of lithium and boron is required in the field of astrophysics, geochemistry, biomedicine and nuclear technology. Thermal Ionization mass spectrometry (TIMS) is the method of choice for providing data on the isotopic measurement of samples which require high precision and accuracy. Isotopic ratios of light elements affected by instrument-based fractionation can be analyzed as molecular ions by TIMS which improves the precision of the isotopic measurement. For eg. precise determination of the isotopic ratio employing atomic ions of lithium, with two isotopes ^{6}Li and ^{7}Li is a challenging task because of the high relative mass difference (17%) between these two isotopes, which results in a large time dependent isotopic fractionation during its evaporation in the ion source. This causes the $^{6}Li/^{7}Li$ atom ratio monitored as atomic ions Li^{+} at *m/z* 6 and 7, to decrease with time resulting in high uncertainty in the measured $^{6}Li/^{7}Li$ ratio. To circumvent this limitation, Lithium is analyzed as molecular $Li_2BO_2^{+}$ ions formed by reaction of lithium carbonate with boric acid loaded on single Rhenium filament assembly. The lithium tetraborate formed produces $Li_2BO_2^{+}$ in the ion source at *m/z* 54 -57 [84, 153, 154]. The different molecular species in mass range 54 - 57 and their isotopic -abundances are shown in Table 3.1. Employing $Li_2BO_2^{+}$ molecular ion method and by monitoring any of the single polyatomic ion pair R_i, ($R_i = I_x/I_y$, where I is the ion intensity, 'x' is mass number in the mass range from 54 to 57, 'y' is mass number within this mass range other than 'x') and knowing the isotopic abundance ratio of boron, the isotopic abundance ratio of lithium can be computed or vice versa [153]. The method gives better precision due to lower isotope fractionation at higher m/z of $Li_2BO_2^{+}$ ions than at *m/z* 6, 7. However, during the mass spectrometric analysis, both Li & B isotopes suffer from isotopic fractionation during the vaporization of the $Li_2BO_2^{+}$ ions in the ion

Table 3.1. Isotopic pattern of $Li_2BO_2^+$, various species and their natural abundances

S.No.	Mass No.	Species	Abundance (in %)
1	54	$Li^2{}_6B_{10}O^2{}_{16}$	0.11
2	55	$2Li^2{}_6B_{10}O_{16}O_{17}$ $Li^2{}_6B_{11}O^2{}_{16}$ $2Li_6Li_7B_{10}O^2{}_{16}$	3.2
3	56	$2Li^2{}_6B_{10}O_{16}O_{18}$ $Li^2{}_6B_{10}O^2{}_{17}$ $2Li^2{}_6B_{11}O_{16}O_{17}$ $4Li_6Li_7B_{10}O_{16}O_{17}$ $2Li_6Li_7B_{11}O^2{}_{16}$ $Li^2{}_7B_{10}O^2{}_{16}$	28
4	57	$2Li^2{}_6B_{10}O_{17}O_{18}$ $2Li^2{}_6B_{11}O_{16}O_{18}Li^2{}_6B_{11}O^2{}_{17}$ $4Li_6Li_7B_{10}O_{16}O_{18}$ $2Li_6Li_7B_{10}O^2{}_{17}$ $4Li_6Li_7B_{11}O_{16}O_{17}$ $2Li^2{}_7B_{10}O_{16}O_{17}$ $Li^2{}_7B_{11}O^2{}_{16}$	68.24

source. Since the isotope ratio of boron is not independently determined, the instantaneous contribution of boron isotopes to R_i cannot be determined. Moreover, in case of any inadvertent contamination of boron during the sample preparation, the true Li isotopic abundance ratio cannot be determined even if boron of known isotopic abundance ratio is used for formation of $Li_2BO_2^+$. Hence two analytical methodologies to simultaneously measure the isotopic ratios of both B and Li from the same loading using two different molecular ions have been proposed in the present study.

3.1.2 Methodology I ---- Application of $Li_2BO_2^+$ ions

Instead of adopting a single polyatomic ion pair from the $Li_2BO_2^+$ ions formed at *m/z* 54 to 57, by recording two sets of polyatomic ion ratios and solving the two equations, isotopic abundance ratios of both lithium and boron can be simultaneously determined from the same filament loading [154]. However, as the lithium isotopic ratio is being derived from a mathematical equation, the uncertainty associated with the measured polyatomic ion ratio is propagated to the computed isotopic abundance ratio of the lithium [84 - 89]. A systematic evaluation on the error propagation for the determination of the isotopic ratio of lithium and boron simultaneously was carried out previously considering natural isotopic composition for lithium and boron [88, 89]. The present study was carried out to check whether the observations reported for Li and B having close to natural abundances is applicable in special cases as shown below, when any of the two elements have isotopic abundances different from natural.

Case 1. Lithium isotopic abundance of natural composition (^{6}Li 7.5% &^{7}Li 92.5%) and varying ^{10}B atom percent abundance as given (10%, 50%, 70% & 90%).

Case 2. Boron isotopic abundance of natural composition (^{10}B 19.9% &^{11}B 80.1%) and ^{6}Li atom percent abundance varying as given (10%, 50%, 70% and 90%)

Case 3. Equal atomic abundances of both ^{6}Li &^{10}B with each of them as given (10%, 20%, 50%, 70% and 90%)

3.1.3 Methodology II ---- Application of $NaLiBO_2^+$ ions

The $Li_2BO_2^+$ methodology involves rigorous mathematical calculations for the selection of the correct combination of molecular pair which will give good precision for ^{6}Li/^{7}Li ratio. The very low abundance of one of the polyatomic molecular ions for the combinations of highly enriched isotopes of either of the element (Li or B), results in poor measurement precision, making the judicious selection of molecular ion pair even more difficult. So as an alternative to this, a new approach has been explored in the present study by mixing sodium borate to the lithium compound to form sodium lithium (mixed alkali) borate which would produce $NaLiBO_2^+$ molecular ions (mass range of major abundant species 71 - 73), $Li_2BO_2^+$ (mass range 54 - 57) along with $Na_2BO_2^+$ (88 - 89) in the ion source [155 - 158]. Lithium isotopic ratio can be obtained by monitoring the $NaLiBO_2^+$ ion using the equation

$$\frac{72_I}{73_I} = \frac{6_{Li}}{7_{Li}} + \frac{10_B}{11_B} \quad \text{---------- Eqn. 3.1}$$

The lower fractionation of the molecular ions at mass 72 - 73 is expected to result in better accuracy and precision for lithium isotopic ratio. ^{10}B/^{11}B ratio in Eqn. 3.1 can be independently determined by monitoring $Na_2BO_2^+$ to measure ^{88}I/^{89}I ion intensity ratio simultaneously instead of directly using the constant / certified as in the previously developed $Li_2BO_2^+$ ion method [84]. The advantage of using experimentally determined values is that there is no compulsion to use standard

boric acid with known isotopic composition and variation in isotopic composition of boron due to environment contamination or experimental conditions would be accounted to give accurate $^{6}Li/^{7}Li$.

3.2. Experimental

ISOPROBE – T (Make: GV instruments) and TRITON - PLUS (Make: Thermo Fisher Scientific Pvt. Ltd.) Thermal Ionization Mass Spectrometer equipped with multi-collector assembly having 9 movable faraday cups and a Secondary Electron Multiplier (for TRITON - PLUS) was used during the analyses for both the methodologies. The instrument (TRITON – PLUS) is also provided with zoom-optics for the better peak alignment during dynamic mode of multi-collection (peak jumping mode). The detailed experimental procedures which include sample treatment, loading procedures and TIMS analysis is presented in the Table 3.2.

3.3. Results & Discussions

3.3.1 Methodology – 1 ($Li_2BO_2^+$)

By monitoring any two molecular ion pair of $Li_2BO_2^+$ in the mass range 54 – 57, one can determine the isotopic ratios of both lithium and boron simultaneously. Theoretical calculations (see Appendix 3.1) were performed for judicious selection of ion pair combinations ($R_i = I_x/I_y$ and R_i) based on their measured uncertainty which would be propagated to the computed $^{6}Li/^{7}Li$ ratio. The solution to the polynomial equation obtained from a particular Combination of Two Molecular ion Pairs (CTMPS) from the nine CTMPS (given in Table 3.3) gives the $^{6}Li/^{7}Li$ isotopic ratio. On substituting this $^{6}Li/^{7}Li$ isotopic ratio in the polyatomic ion ratios of the chosen CTMPS, two corresponding $^{10}B/^{11}B$ isotopic ratios are generated. Hence from a single data acquisition of six polyatomic ion ratios ($^{54}I/^{55}I$, $^{54}I/^{56}I$, $^{54}I/^{57}I$, $^{55}I/^{56}I$,$^{55}I/^{57}I$, $^{56}I/^{57}I$) we obtain nine

solutions for lithium isotopic ratio and eighteen solutions for boron isotopic ratio from the nine CTMPS. Among the different CTMPS, some yield significant difference between the $^{10}B/^{11}B$ isotopic ratios derived from the two polyatomic ion ratios (CTMPS) and some show negligible variation in the $^{10}B/^{11}B$ isotopic ratios derived from the two polyatomic ion ratios. Theoretically, for the same CTMPS, we have to calculate the Relative Uncertainty Magnification Factor (RUMF) for lithium ($[RUMF]_L$) and RUMF for boron ($[RUMF]_B$) using uncertainties in the polyatomic ion ratios R_i & R_j and the uncertainties propagated to the computed Li & B isotopic ratios. The selection of a specific CTMPS for all the three cases (mentioned in the section 3.1.1.) of different isotopic combinations of Li and B is very challenging and tedious as can be seen from Fig. 3.1 to 3.3. It is also observed that it is not always necessary for $[RUMF]_L$ and $[RUMF]_B$ to be either equal or close to each other for a specific CTMPS. For better representation, Fig. 3.1 & 3.2 were plotted by omitting out those CTMPS whose RUMFs are too high. For example, in Fig. 3.1, for the combination of natural Lithium and 90% ^{10}B, the value of $[RUMF]_{L7}$ is about 1 and $[RUMF]_{B7}$ (for CTMPS 7) is not shown since the value was too large for computing the isotopic abundance ratio. So, it is necessary to select the CTMPS by comparing the RUMFs for both the elements for a particular composition.

Theoretical calculations were performed for the all of the three cases detailed in section 3.1.1 for the uncertainty ratios δ_i/δ_j of 2, 4 and 6 (where δ_i and δ_j are the relative uncertainty on the polyatomic ion ratio R_i and R_j respectively). The results are graphically represented in Figs. 3.1 to 3.3. CTMPS with RUMF values less than 1 should be selected for the simultaneous determination of isotopic amount ratio of lithium and boron. This would mean that the experimental uncertainty in the calculation of isotopic ratio of Li & B is limited to the experimental uncertainty on the polyatomic abundance ratio.

Table 3.2. Details of the experimental conditions of both the methodologies to determine the optimum conditions of analysis for determination of $^{6}Li/^{7}Li$ ratio

S. No.	Parameter / Condition	Methodology 1 ($Li_2BO_2^+$)	Methodology 2 ($NaLiBO_2^+$)
1.	Reagents used	NIST RM – 9545 (L-Svec Li_2CO_3) NIST SRM – 951 (H_3BO_3)	NIST RM – 9545 (L-Svec Li_2CO_3) NIST SRM – 951 (H_3BO_3) Nat. Boric Acid (Sigma Aldrich) Na_2CO_3 (Sigma Aldrich)
2.	Mole ratio	B/Li ~ 5	Li/Na ~1; B/Na ~ 2, 5, 10 (during optimization) Li/Na ~ 1; B/Na ~ 10 (optimized)
3.	Experiments carried out during the investigations	Solutions of NIST RM – 9545 mixed with 10%, 50%, 70% 95% of ^{10}B	NIST RM – 9545 mixed with sodium tetraborate / sodium pentaborate or sodium decaborate (NIST SRM 951 with $^{10}B/^{11}B$ ratio = 0.2473 or (H_3BO_3 Sigma Aldrich with $^{10}B/^{11}B$ ratio = 0.2505) for borate formation
4.	Treatment	Solution mixtures shown in step 3 were prepared on a Teflon sheet, mixed and evaporated under IR lamp and treated twice with Millipore water for homogeneity	
5.	Loading	5 µL of the lithium borate solution or sodium lithium borate solution, containing 1.5 – 2 µg of lithium was loaded on the zone refined Rhenium (single) filament and evaporated to dryness at 1Amp current. Filament was further heated to 1.8A and held for 5 minutes and slowly heated to red hot for formation of the required alkali borate.	

TIMS analysis			
6.	Degassing	After achieving a sufficient vacuum in the ion source housing, the samples were degassed at 1.0 Amp for about 5 to 10 minutes	
7.	Initial focusing	Ion current of ^{23}Na	
8.	Ions monitored @ mass m/Z	$Li_2BO_2^+$ (54 -57) Different combinations of ratios R_i and R_j used to determine B IC from simultaneous equation	$NaLiBO_2^+$ (71 -73) $^{72}I/^{73}I$ and $^{73}I/^{71}I$ and $^{72}I/^{71}I$ $Na_2BO_2^+$ (88 – 89) $^{88}I/^{89}I$ recorded for independent determination of IC of boron.
9.	Data acquisition parameters	Peak centre, Auto focus, Baseline @ ± 0.5 a.m.u of the isotope of interest prior to the acquisition Integration time is about 5 seconds per each scan, 12 scans are grouped in to a block 3 – 5 block data was recorded for the measurement	
		Simultaneous multi-collection of all isotopes in each scan	Two sequences were carried out per scan by peak jumping mode Sequence 1: Simultaneous multi-collection of 71, 72 and 73 Sequence 2: Simultaneous multi-collection of 88 and 89
10.	Cup configuration	L_1, Ax, H_1, H_2 for 54 – 57 respectively Mass of reference cup (Ax) 55 a.m.u.	Sequence 1: L_1, Ax and H_2 for 71, 72 and 73; 72 (mass of Ax cup) Sequence 2: Ax, H_1 for 88 and 89; 88 (mass of Ax cup)

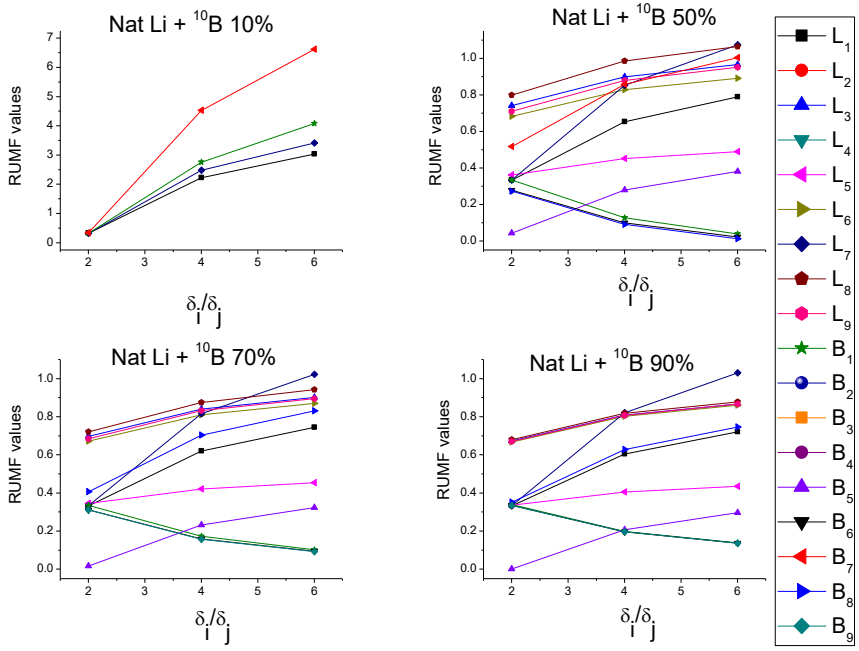

Fig. 3.1. RUMF obtained theoretically for natural $^{6}Li/^{7}Li$ and varying atom percent of ^{10}B

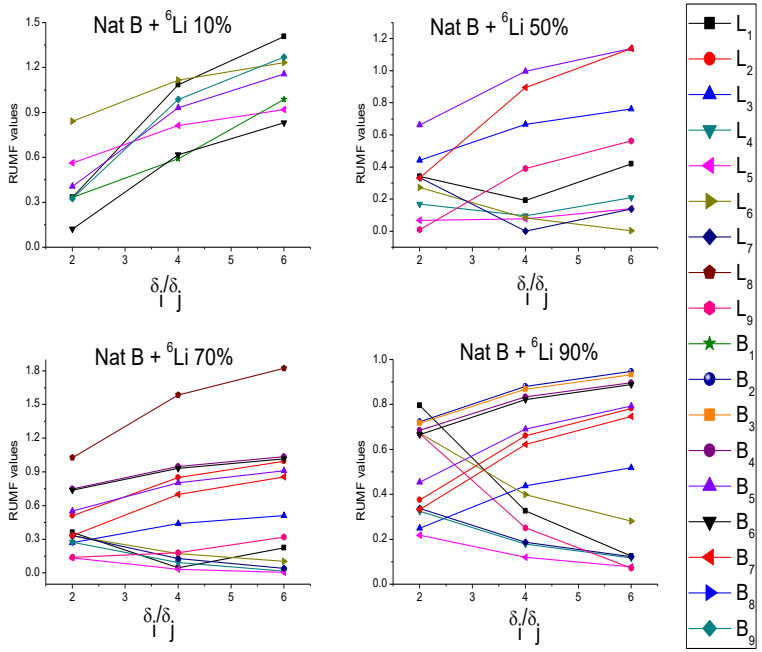

Fig. 3.2. RUMF obtained theoretically for natural $^{10}B/^{11}B$ and varying atom percent of ^{6}Li

Table 3.3. Description of various CTMPS (^{m}I is Ion intensity at given m/z)

Monitor Pair	CTMPS								
	1	2	3	4	5	6	7	8	9
R_i	$^{55}I/^{57}I$	$^{54}I/^{55}I$	$^{54}I/^{55}I$	$^{54}I/^{55}I$	$^{54}I/^{56}I$	$^{54}I/^{55}I$	$^{54}I/^{56}I$	$^{55}I/^{56}I$	$^{55}I/^{56}I$
R_j	$^{56}I/^{57}I$	$^{54}I/^{56}I$	$^{54}I/^{57}I$	$^{55}I/^{56}I$	$^{55}I/^{57}I$	$^{56}I/^{57}I$	$^{55}I/^{56}I$	$^{55}I/^{57}I$	$^{56}I/^{57}I$

From the Fig. 3.1 to 3.3, for all of the three cases, it is observed that some of the CTMPS display very large slopes for RUMF which indicates that a slight change in $\delta_i/\ \delta_j$ value, changes the RUMF values to a large extent, thus affecting the uncertainty in the isotopic ratio of lithium and boron. Hence the CTMPS have to be selected in such a way that the variation of RUMF with $\delta_i/\ \delta_j$ should either be zero or small. Based on these observations, the selection of CTMPS was carried out for the above-mentioned cases as below.

3.3.1.1. Case 1

Under this group, the results for the mixtures of natural lithium i.e. 7.5% of ^{6}Li ($^{6}Li/^{7}Li$ = 0.081081) with ^{10}B atom% varying from 50%, 70% and 90% were considered. ^{10}B atom % abundance of 10% is discussed under case 3 (of approx. equal abundances of ^{6}Li and ^{10}B) while 20% of ^{10}B is close to natural abundance of B for which detailed studies have already been reported [89, 159]. Theoretical values for the polyatomic ion ratios for varying isotopic content of ^{10}B with natural $^{6}Li/^{7}Li$ are listed in Table 3.4. Using these polyatomic abundance ratios for different isotopic contents of ^{10}B with natural $^{6}Li/^{7}Li$, theoretical estimation of RUMFs on Li & B were evaluated and represented in the Fig. 3.1. Selection of CTMPS for the simultaneous determination of isotopic ratio of Li & B was done based on the values of RUMFs (for Li & B) being less than 1 and this is listed in Table 3.5.

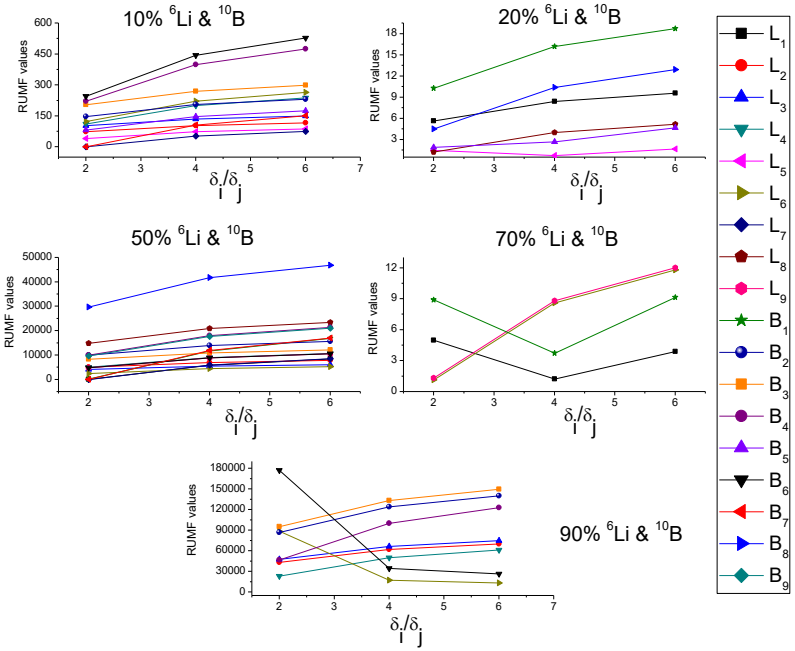

Fig. 3.3. RUMF obtained theoretically for equal compositions of ^{6}Li & ^{10}B

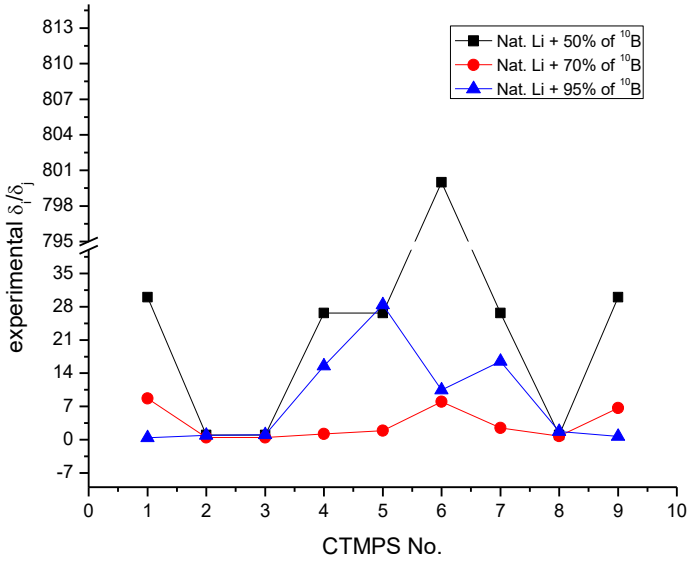

Fig. 3.4. CTMPS No. Vs experimental ratios of uncertainties on polyatomic ion ratios, R_i and R_j

Table 3.4. Theoretical values for various polyatomic ion ratios for different isotopic contents of ^{10}B with natural $^{6}Li/^{7}Li$

S. No.	Polyatomic ion ratio	10% ^{10}B	50% ^{10}B	70% ^{10}B	95% ^{10}B
1	$^{54}I/^{55}I$	0.029702	0.03896	0.039847	0.040453
2	$^{54}I/^{56}I$	0.002673	0.005656	0.006146	0.006518
3	$^{54}I/^{57}I$	0.00073	0.006564	0.015287	0.121627
4	$^{55}I/^{56}I$	0.089986	0.141576	0.154241	0.161114
5	$^{55}I/^{57}I$	0.024585	0.168478	0.383643	3.006635
6	$^{56}I/^{57}I$	0.273211	1.160507	2.487288	18.6616

Table 3.5. Selected CTMPS for Natural $^{6}Li/^{7}Li$ with different isotopic composition of boron

S. No.	Atom % of ^{10}B	CTMPS to be employed (theoretically calculated based on RUMFs for Li & B)	CTMPS to be employed (experimentally obtained based on the % deviation from true)
1	10	1^{*}, 5^{*}, 7^{*}	-------
2	50	1, 5, 6, 8, 9	1, 8, 9
3	70	1, 5, 6, 8, 9	1, 8, 9
4	90	1, 5, 6, 8, 9	1, 8, 9

*at uncertainty ratio$\delta_i/\ \delta_j = 2$

To compare the experimental data with the theoretical observations, one has to consider the % deviation of the observed ratio from true isotopic ratio (see Fig. 3.5) for RUMFs for lithium and boron obtained theoretically (see Fig. 3.1 to 3.3) using assumed values for δ_i/δ_j of 2, 4 and 6.

From Fig. 3.4, it is seen that uncertainty ratios (δ_i/δ_j) obtained experimentally for various CTMPS used for the different mixtures of lithium and boron are significantly different. The δ_i/δ_j values for the mixture containing Nat. Li and 50% of ^{10}B are very large (for all CTMPS except CTMPS no. 2, 3 & 8) when compared to rest of the mixtures. For each of the mixtures in this case, as mentioned earlier, nine solutions for lithium isotopic ratio and 18 values for boron isotopic ratio were computed from the respective polynomials obtained from the 9 CTMPS.

The % deviation of the experimentally obtained isotopic ratios from the true value was calculated and are depicted in Fig. 3.5. The observations are categorized based on the magnitude of the % deviation from the true values. It is clearly seen that the choice of selection of CTMPS for lithium isotopic ratio is relatively easier when compared to that of boron. From the Fig. 3.5, it can be seen that L_1, L_3, L_4, L_7, L_8 and L_9 can be selected for all categories under case 1 except for the mixture of natural lithium and 50% of ^{10}B, where CTMPS L_1, L_8 and L_9 can be considered.

In the case of boron, B_2, B_4 and B_7 cannot be considered for any of the mixtures since the two values derived for B isotope ratio from the selected CTMPS (i,e B_{2a} & B_{2b} or B_{4a} & B_{4b} or B_{7a} & B_{7b}) showed considerable deviation from true ratios. The variation between the two values of $^{10}B/^{11}B$ isotopic ratios obtained from CTMPS Nos. B_1, B_3, B_8 and B_9 are significantly different (about 2-5%) for some of the mixtures depending upon the isotopic abundance distribution pattern. From the Fig. 3.5, it is clearly seen that for the composition of

natural lithium with 50% of ^{10}B, the deviations of $^{10}B/^{11}B$ isotope ratios from true ratios are large for all the nine CTMPS compared to rest of the two compositions of ^{10}B. Among the CTMPS, the deviation from true ratio is less for CTMPS 1, 8 and 9. The CTMPS selected for experimental determination of Li and B isotope ratio is different from CTMPS selected based

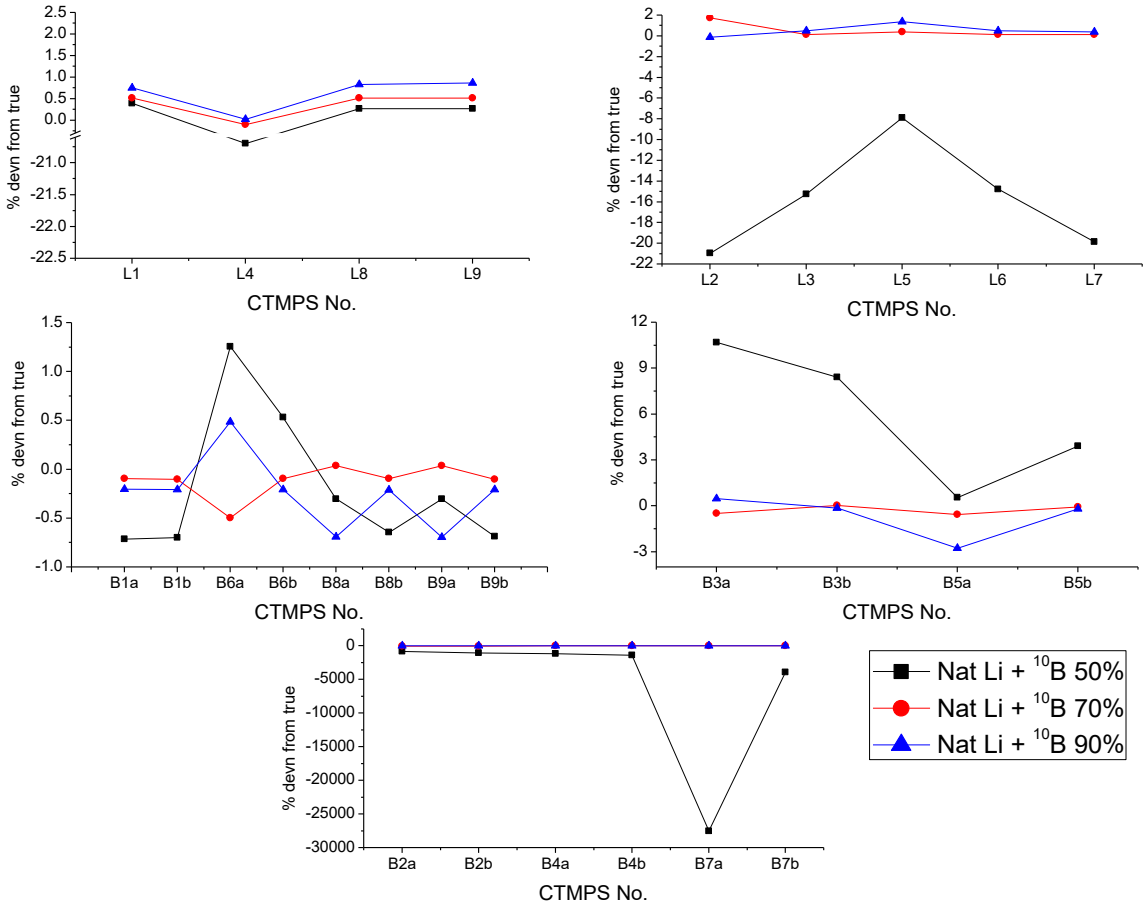

Fig. 3.5. CTMPS No. Vs % deviation of experimentally obtained $^{6}Li/^{7}Li$ & $^{10}B/^{11}B$ isotopic ratios from their true ratios

on the theoretical prediction which is due to the difference in the crucial parameter δ_i/δ_j. Earlier studies have shown that the accuracy of Li and B isotopic ratio is dependent on the ratio of the uncertainties in the experimentally obtained polyatomic ion ratios [89]. Fig. 3.4 shows the large difference in δ_i/δ_j between the calculations based on theoretical considerations (Fig. 3.1 to 3.3) and experimental observations (Fig. 3.4). For the mixture of natural lithium and 50%

abundance of ^{10}B, the experimentally obtained value for δ_i/δ_j is about 800 for CTMPS 6 and from the Fig. 3.5, a deviation of more than 10% from the true lithium isotope ratio can be seen for CTMPS 5 and 6. A comparison of the theoretical (Fig. 3.1) and experimental observations (Fig. 3.5) showed that CTMPS 1, 8 and 9 can be employed for the case 1, (as mentioned in Table 3.5). 10% abundance of ^{10}B falls under the category of case 3 since the isotopic abundance of ^{6}Li &^{10}B are close and hence reported separately below.

3.3.1.2. Case 2

The results for the mixture natural boron and 20% of ^{6}Li are considered under Case 3 (equal isotopic abundances of ^{10}B &^{6}Li). The CTMPS that can be employed under different categories of this case is mentioned in Table 3.6. From the Fig. 3.2, it can be seen that CTMPS - 5 and 6 can be employed for all compositions of Li since their [RUMF] and [RUMF] is less than 1.

Table 3.6. CTMPS to be considered for Natural $^{10}B/^{11}B$ with varying isotopic composition of lithium

S. No.	Atom % of ^{6}Li	CTMPS to be employed
1	10	5, 6
2	50	4, 5, 6, 7
3	70	2, 3, 4, 5, 6, 7
4	90	2, 3, 4, 5, 6, 7

3.3.1.3. Case 3

When the isotopic abundances ratios of both lithium and boron are equal, for certain compositions a few CTMPS yield infinite values of RUMF because of the specific isotopic abundance distribution pattern and for the remaining CTMPS the RUMF values are very large as seen in Fig. 3.3. When the atom percent of both ^{6}Li and ^{10}B are 10%, 50% and 90% the RUMF values are infinite for CTMPS – 1, CTMPS – 5 and CTMPS – 1, 5, 7, 8 & 9 respectively.

From this study, it was observed that when the isotopic abundance ratio of both lithium and boron are different, the possibilities of selecting the CTMPS are higher than when they are close to each other. When the isotopic abundance ratio of lithium and boron are equal as in the case 3, none of the CTMPS can be chosen for the accurate isotopic abundance measurements of lithium and boron because the RUMFs are high (Fig. 3.3).

These studies using $Li_2BO_2^+$ reveals that judicious selection of appropriate CTMPS is required for determination of $^{6}Li/^{7}Li$ ratio with low associated uncertainty.

3.3.2 Methodology ---- II ($NaLiBO_2^+$)

3.3.2.1. Sequence of ion formation

With the addition of sodium borate to the lithium compound, apart from 24 species of $NaLiBO_2^+$ (mass 71 to 77), 36 species of $Li_2BO_2^+$(mass 54 to 61), and 12 of $Na_2BO_2^+$ (88 to 93) are also formed in addition to Na^+ and Li^+ inside the thermal ion source. Only the major molecular species with ^{16}O as the one of constituent isotope (i.e mass 71-73) was considered for calculation and shown in the Table 3.7 as the abundance of the remaining species are insignificant. The relative abundance of different molecular ions calculated from the natural abundance of the constituent isotope is shown in Table 3.7. The ion intensity profile (in mV)

of the most abundant species of the different ions formed as a function of filament current for a typical mixture of lithium and sodium borate is presented in Fig. 3.6. As can be seen the sequence of ion formation with increasing filament current is in the order Na^+, $Na_2BO_2^+$, $NaLiBO_2^+$, Li^+ and $Li_2BO_2^+$. The ion intensities of Li^+ and $Li_2BO_2^+$ were significantly lower

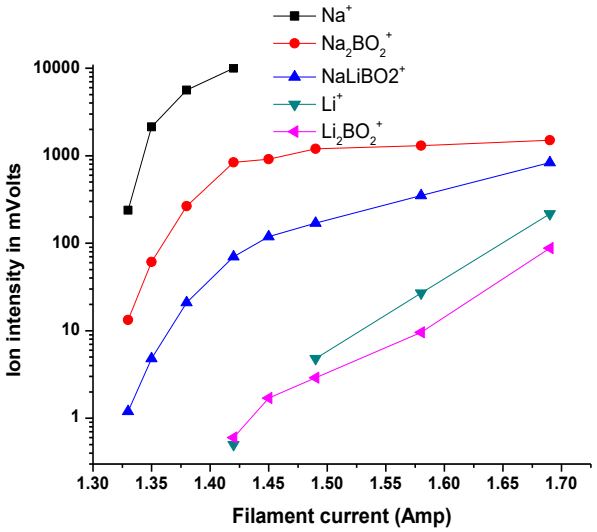

Fig. 3.6. Ion Intensity of the different molecular ions formed with increasing filament current

than $Na_2BO_2^+$ and $NaLiBO_2^+$. The reason for this order of ion formation could be i) Small differences in volatility of sodium borate and lithium borate [155] ii) Lower ionization potential of Na^+ (5.1eV) as compared to Li^+ (5.4eV). iii) Higher dissociation energy of lithium borate compared to sodium borate [157]. The fact that $NaLiBO_2^+$ ions appear after Na^+ but prior to Li^+, suggests that Na^+ must be bonding or associating with the un-dissociated $LiBO_2$ and $NaBO_2$ vapors to produce $NaLiBO_2^+$ and $Na_2BO_2^+$. As the filament current is increased, Li^+ and subsequently low intensity $Li_2BO_2^+$ molecular ions were observed. With Li^+ formation, association of Li^+ ions with $NaBO_2$ may also be contributing to $LiNaBO_2^+$ formation (detailed discussion is given below).

3.3.2.2. Possible ionization mechanism

To have a better understanding on the probable mechanism of formation of mixed alkali borate ions in TIMS, experiments were carried out using rhenium triple filament assemblies where the centre filament (CF) was loaded with lithium pentaborate and the side filament (SF) with sodium chloride. Heating CF/SF to1.58/1.58A produced $1x10^{-11}$A $Li_2BO_2^+$, 0.25×10^{-11}A $NaLiBO_2^+$ and 1×10^{-13}A $Na_2BO_2^+$. All the ion intensities increased with centre filament. This suggests that $NaLiBO_2^+$ & $Li_2BO_2^+$ ions are formed due to association of $LiBO_2$ evaporating from centre filament with vapors of Na^+ from side filament and Li^+ from centre filament respectively.

Table 3.7. The abundance of the different molecular ionic species obtained from sodium lithium borates

Molecular ions formed due to combination of constituent isotopes	**Mass**	**Abundance of species* (Natural abundances of Li, B and O)**
Lithium borate ions ($Li_2BO_2^+$)		
$^6Li^6Li^{10}BO_2$	54	0.12%
$2^6Li^7Li^{10}BO_2$, $^6Li^6Li^{11}BO_2$, $2^6Li_2{}^{10}B^{16}O^{17}O$	55	3.3%
$2^6Li^7Li^{11}BO_2$, $^7Li^7Li^{10}BO_2$, $4^6Li^7Li^{10}B^{16}O^{17}O$, $2^6Li^6Li^{10}B^{16}O^{18}O$, $^6Li^6Li^{10}B^{17}O^{17}O$, $2^6Li^{11}B^{16}O^{17}O$	56	28.26%
$^7Li^7Li^{11}BO_2$, $2^6Li_2{}^{10}B^{17}O^{18}O$, $2^6Li_2{}^{11}B^{16}O^{18}O$, $^6Li_2{}^{11}B^{17}O_2$, $4^6Li^7Li^{10}B^{16}O^{18}O$, $2^6Li^7Li^{10}B^{17}O_2$, $4^6Li^7Li^{11}B^{16}O^{17}O$, $2^7Li_2{}^{10}B^{16}O^{17}O$	57	67.89%
Sodium lithium borate ions ($NaLiBO_2^+$)		
$Na^6Li^{10}BO_2$	71	1.53%

$Na^{6}Li^{11}BO_2$, $Na^{7}Li^{10}BO_2$, $2Na^{6}Li^{10}B^{17}O^{16}O$	72	24.5%
$Na^{7}Li^{11}BO_2$,$2Na^{7}Li^{10}B^{17}O^{16}O$, $2Na^{6}Li^{11}B^{17}O^{16}O$, $2Na^{6}Li^{10}B^{18}O^{16}O$, $Na^{6}Li^{10}B^{17}O^{17}O$	73	73.53%
Sodium borate ions ($Na_2BO_2^+$)		
$Na_2{}^{10}BO_2$	88	20%
$Na_2{}^{11}BO_2$, $2Na_2{}^{10}B^{17}O^{16}O$	89	80%

^{10}B - 20%, ^{6}Li - 7.68% and ^{16}O - 99.76% used for calculation [O_2 stands for $^{16}O_2$]

The higher intensity of $Li_2BO_2^+$ is probably due to interaction of vapors in the immediate region of centre filament. The small signal of $Na_2BO_2^+$ must be due to combination of vapors of Na^+ from side filament with BO_2^- formed from the centre filament.

Similarly, ion association is likely to be the major source of $NaLiBO_2^+$ from the sodium lithium borates loaded on single filament. At lower temperatures Na^+ ions, $Na_2BO_2^+$ ions and $NaLiBO_2^+$ ions are observed which suggests the likely ion formation mechanism to be as follows:

$$NaBO_{2(g)} \xrightarrow{Absorbed\ on\ filament} NaBO_{2(a)} \xrightarrow{Ionisation} Na^{+}_{(a)} + BO^{-}_{2(a)} \xrightarrow{desorption} Na^{+}_{(g)} + BO^{-}_{2(a)}$$

Dissociative Ionisation

[160]

$$Na^{+}_{(g)} + NaBO_{2(g)} \rightarrow Na_2BO^{+}_{2(g)}$$

$$Na^{+}_{(g)} + LiBO_{2(g)} \rightarrow NaLiBO^{+}_{2(g)}$$

Alternatively, the association of the adsorbed $Na^{+}_{(a)}$ with adsorbed $LiBO_{2(a)}$ on the filament and subsequent desorption may also generate $NaLiBO_2{}^{+}_{(g)}$ as shown below

$(Na^{+}_{(a)} + LiBO_{2(a)} \rightarrow NaLiBO^{+}_{2(g)})$. At this stage of acquisition, $^{72}I/^{73}I$ should result in minimum fractionation for $^{6}Li/^{7}Li$ ratio.

On further heating the filament, dissociation of $LiBO_2$ also takes place to give Li ions which combine with lithium metaborate vapors resulting in the formation of $Li_2BO_2^{+}$ ions. At this stage the Li^{+} ions may also be combining with $NaBO_2$ vapors forming $LiNaBO_2^{+}$as shown below.

$Li^{+}_{(g)} + NaBO_{2(g)} \rightarrow LiNaBO^{+}_{2(g)}$ or $Li^{+}_{(a)} + NaBO_{2(a)} \rightarrow LiNaBO^{+}_{2(g)}$

$Li^{+}_{(g)} + LiBO_{2(g)} \rightarrow Li_2BO^{+}_{2(g)}$

Data acquisition at this stage could result in increased fractionation in $^{6}Li/^{7}Li$ ratios due to higher analysis temperatures. This is demonstrated in Fig. 3.7 where the isotopic ratio of L-Svec lithium and natural boron monitored as $Na_2BO_2^{+}$, $NaLiBO_2^{+}$, and $Li_2BO_2^{+}$ at increasing temperatures of the same filament.

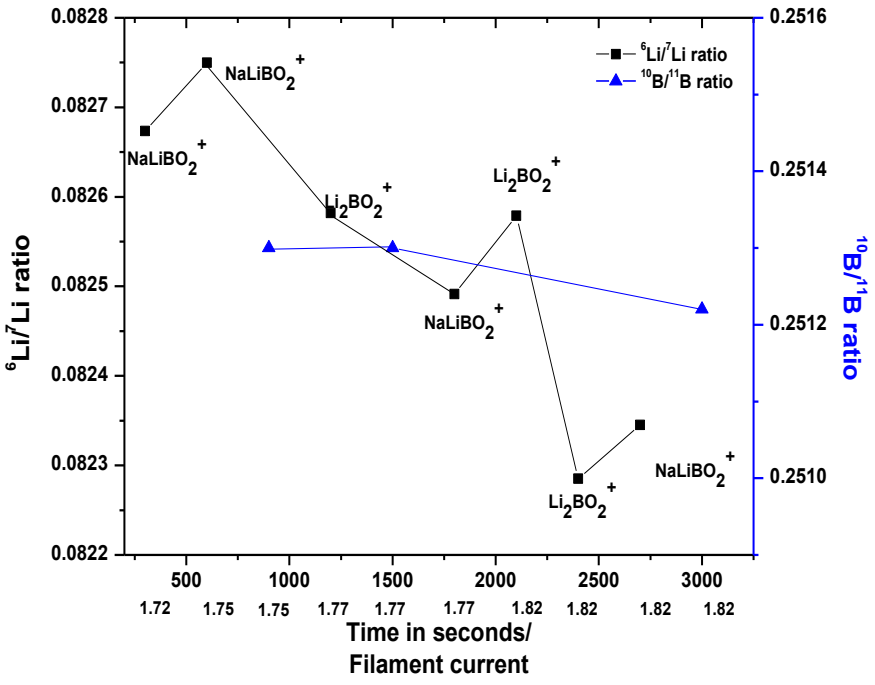

Fig. 3.7 Variation of $^{6}Li/^{7}Li$ (from $NaLiBO_2^+$ and $Li_2BO_2^+$) and $^{10}B/^{11}B$ isotope ratios Vs filament current

3.3.2.3. Derivation of $^{6}Li/^{7}Li$ isotopic ratio

From isotopic distribution pattern of the molecular ions summarized in Table 3.7, the $^{6}Li/^{7}Li$ and $^{10}B/^{11}B$ ratios can be derived from the ion intensity ratios $^{72}I/^{73}I$ or $^{72}I/^{71}I$ and $^{88}I/^{89}I$ respectively as shown below. Minor contribution of the molecular ions having ^{18}O or ^{17}O were included in the derivation. The contributions of the molecular ions involving ^{17}O and ^{18}O to the total ion intensities at ^{72}I and ^{73}I were calculated to be 0.005% and 0.034% respectively for natural compositions of Lithium and Boron. The relationship between ion intensity ratio and isotopic composition of lithium and boron are as given below.

$$\frac{^{72}I}{^{73}I} = \frac{^{6}Li\,Na^{11}B^{16}O_2 + {}^{7}Li\,Na^{10}B^{16}O_2 + 2*{}^{6}Li\,Na^{10}B^{16}O^{17}O}{{}^{7}Li\,Na^{11}B^{16}O_2 + 2*{}^{7}Li\,Na^{10}B^{16}O^{17}O + 2*{}^{6}Li\,Na^{11}B^{16}O^{17}O + 2*{}^{6}Li\,Na^{10}B^{16}O^{18}O + 2*{}^{6}Li\,Na^{10}B^{17}O^{17}O}$$

…… Eqn. 3.2

$$\frac{^{72}I}{^{71}I} = \frac{^{6}Li\,Na^{11}B^{16}O_2 + {}^{7}Li\,Na^{10}B^{16}O_2 + 2*{}^{6}Li\,Na^{10}B^{16}O^{17}O}{{}^{6}Li\,Na^{10}B^{16}O_2}$$ ---------- Eqn. 3.3

$$\frac{^{89}I}{^{88}I} = \frac{Na_2{}^{11}B^{16}O_2 + 2*Na_2{}^{10}B^{16}O^{17}O}{Na_2{}^{10}B^{16}O_2} = \left(\frac{^{11}B}{^{10}B}\right) - 2 * \left(\frac{^{17}O}{^{16}O}\right)$$ ------- Eqn. 3.4

Equation 3 was not used, due to the low intensity of ^{71}I for natural boron and lithium. In equation 2 the term ($2 * {}^{6}Li\,Na^{10}B^{17}O^{17}O$) has very low abundance and therefore ignored. The $^{6}Li/^{7}Li$ ratio derived from equation 3.2 is shown in equation 5 below.

$$L = \frac{[B - R - 2*RBO_a]}{[2*RO_a + 2*RBO_b - 1 - 2*BO_a]}$$ ------- Eqn. 3. 5

Where, L = $^{6}Li/^{7}Li$, R = $^{72}I/^{73}I$, B = experimentally determined $^{10}B/^{11}B$. $O_a = {}^{17}O/^{16}O$ and $O_b = {}^{18}O/^{16}O$ are constants = 0.00039 and 0.002 respectively

Since the abundances at mass 89, 88, 73 and 72 are high and comparable (Table 3.7), the ion intensity ratios $^{72}I/^{73}I$ and $^{88}I/^{89}I$ are obtained with good precision of better than 0.03%.

3.3.2.4. Effect of loading and analysis conditions on $^{6}Li/^{7}Li$ isotopic ratios

Initial feasibility experiments were carried out using L-Svec Lithium carbonate and sodium tetraborate mixtures with Li/Na mole ratio 1 and B/Na mole ratio 2. The pH of the borate solution was > 9 and the ion intensity of $NaLiBO_2^+$ was found to be unstable and decaying. Graphite loaded on the filament after fusion helped to stabilize the ion intensity though both $^{10}B/^{11}B$ ratio and $^{6}Li/^{7}Li$ ratio showed a high degree of fractionation [161]. Stable ion intensities for both $Na_2BO_2^+$ and $NaLiBO_2^+$ was observed when sodium pentaborate ($Na_2B_{10}O_{16}$) or sodium decaborate ($Na_2B_{20}O_{31}$) was added to the Li_2CO_3 solution. Conversion of either one of the alkali carbonates to chloride or nitrate improved the ionization behavior and further stabilized the ion intensity. Table 3.8 gives the details of the data obtained for L-Svec lithium carbonate. In column 1 and 2 of Table 3.8 the different forms of L-Svec lithium and sodium carbonate + boric acid used are given. Column 3 gives the B/Li mole ratio in the loaded sample. Columns 1 to 3 collectively influences the nature of mixed alkali borate formed on the filament. Column 4 gives the average ion intensity ratio, $^{72}I/^{73}I$ from three blocks which were measured with precision of better than 0.03% for a typical analysis. The ^{73}I during data acquisition was ~ 0.5 X 10^{-11}A. As shown in Eqn. 3.2 & 3.5 the $^{72}I/^{73}I$ ratio is the sum of measured lithium and boron isotopic ratios. The variations in $^{72}I/^{73}I$ due to two types of boron used, natural (row 2 to 5) and SRM 951(row 6 to 12) is evident. Column 5 gives the $^{10}B/^{11}B$

ratio determined by monitoring $Na_2BO_2^+$ ion intensity at mass 88 to 89. The ^{89}I was about 1 X $10^{-11}A$ and $^{88}I/^{89}I$ was measured with a precision of about 0.02% in most cases.

Table 3.8. $^6Li/^7Li$ and $^{10}B/^{11}B$ ratios obtained from sodium lithium borates prepared using L-Svec lithium and sodium salts with Natural boric acid or SRM-951 boric acid standard

Lithium compound	Sodium compound	B/Li atom ratio	$^{72}I/^{73}I$	$^{10}B/^{11}B$ ratio as $Na_2BO_2^+$	$^6Li/^7Li$ = from eqn.5 using constant $^{10}B/^{11}B^{\#}$ (0.2473 or 0.2505)	$^6Li/^7Li$ = from eqn 3.5 using exptly. determined $^{10}B/^{11}B$
Svec LiNO3	$Na_2B_{10}O_{16}$	5	0.33351	0.25073	0.08311	0.08288
Svec LiNO3	$Na_2B_{20}O_{31}$	10	0.33403	0.25137	0.08362	0.08276
Svec LiNO3	$Na_2B_{10}O_{16}$	5	0.33352	0.25086	0.08312	0.08276
Svec Li_2CO_3	$Na_2B_{20}O_{31}$	10	0.33379	0.25105	0.08339	0.08284
Svec Li_2CO_3	$Na_2B_{20}O_{31}$	10	0.33075	0.24802	0.08354	0.08283
Svec Li_2CO_3	$Na_2B_{20}O_{31}$	5	0.33081	0.24802	0.0836	0.08289
Svec Li_2CO_3	$Na_2B_{20}O_{31}$	10	0.33063	0.24795	0.08342	0.08278
Svec Li_2CO_3	$Na_2B_{20}O_{31}$	5	0.33046	0.24770	0.08326	0.08286
Svec Li_2CO_3	$Na_2B_{20}O_{31}$	10	0.33071	0.24794	0.08351	0.08287
Svec $LiNO_3$	$Na_2B_{20}O_{31}$	5	0.33063	0.24797	0.08342	0.08276
Svec Li_2CO_3	$Na_2B_{20}O_{31}$	10	0.33122	0.24844	0.08402	0.08288
Mean $^6Li/^7Li$					0.0834 ± 0.4%	0.08283 ± 0.07%

$^{\#}$ $^{10}B/^{11}B$ NIST 951 standard=0.2473 ± 0.0002,

$^{10}B/^{11}B$ in H_3BO_3 Sigma Aldrich = 0.2505 ± 0.0002

Column 6 gives the $^{6}Li/^{7}Li$ ratio obtained by substituting the standard value $^{10}B/^{11}B = 0.2473$ for NIST 951 and 0.2505 for natural boron where ever used. Column 7 gives $^{6}Li/^{7}Li$ obtained by substituting the experimentally determined $^{10}B/^{11}B$ ratio (column 5) in Eqn. 3.5. Comparison of the external precision of $^{6}Li/^{7}Li$ ratio given in Column 6 (0.08339 ± 0.00035) and column 7 (0.08283 ± 0.00006) of Table 3.8 shows a poorer precision for the mean $^{6}Li/^{7}Li$ ratios in column 6. This is because the standard $^{10}B/^{11}B$ ratio is directly substituted in equation 5 and its share of fractionation in $^{72}I/^{73}I$ is not taken into account resulting in erroneous values for $^{6}Li/^{7}Li$ ratio. This is depicted in Fig. 3.8 for a large number of analysis which shows the resulting precise $^{6}Li/^{7}Li$ ratio, when the contribution of small variations in $^{10}B/^{11}B$ ratio (determined from $^{88}I/^{89}I$) to $^{72}I/^{73}I$ ratio is accounted. The effect of sample loading condition on the ion source fractionation in $^{6}Li/^{7}Li$ ratio and $^{10}B/^{11}B$ ratio is shown in Fig. 3.9 and 3.10. The two plots show the observed fractionation per unit mass for B and Li with increasing temperature of filament when the pH of loaded solution was >9 and < 8 respectively. The fractionation factor was calculated as $(1-^{10}B/^{11}B_{obs} / {}^{10}B/^{11}B_{std})$ for boron, where $^{10}B/^{11}B_{std}$ is 0.2473 and similarly for lithium, $(1-^{6}Li/^{7}Li_{obs} / {}^{6}Li/^{7}Li_{std})$ where $^{6}Li/^{7}Li_{std} = 0.0832$. The points in the line are average B and Li isotopic ratios observed for a sample at increasing filament currents beginning with $^{73}I \sim 0.5 \times 10^{-11}$ A to higher ion intensities. Stable ratios for both B and Li are observed when the loading medium has pH $\leq$ 8 (Fig. 3.10) whereas high pH of the loading solution showed decaying ion intensities and high fractionation for both B and Li isotopic ratios (Fig. 3.9). The studies show that a mildly alkaline solution of sodium lithium borate is desirable for obtaining stable ratios which is possible when $Na_2B_{10}O_{16}$ or $Na_2B_{20}O_{31}$ are used for fusion with lithium salt for forming the mixed alkali borates, whereas $Na_2B_4O_7$ when used results in higher fractionation. Fig. 3.11 shows stable $^{72}I/^{73}I$ ratio for 10 blocks of 12 scans each, for L-Svec lithium nitrate mixed with sodium pentaborate. The mean $^{6}Li/^{7}Li$ isotopic ratio for Svec Li_2CO_3 determined from several analysis under optimized condition was 0.08283 ± 0.00006

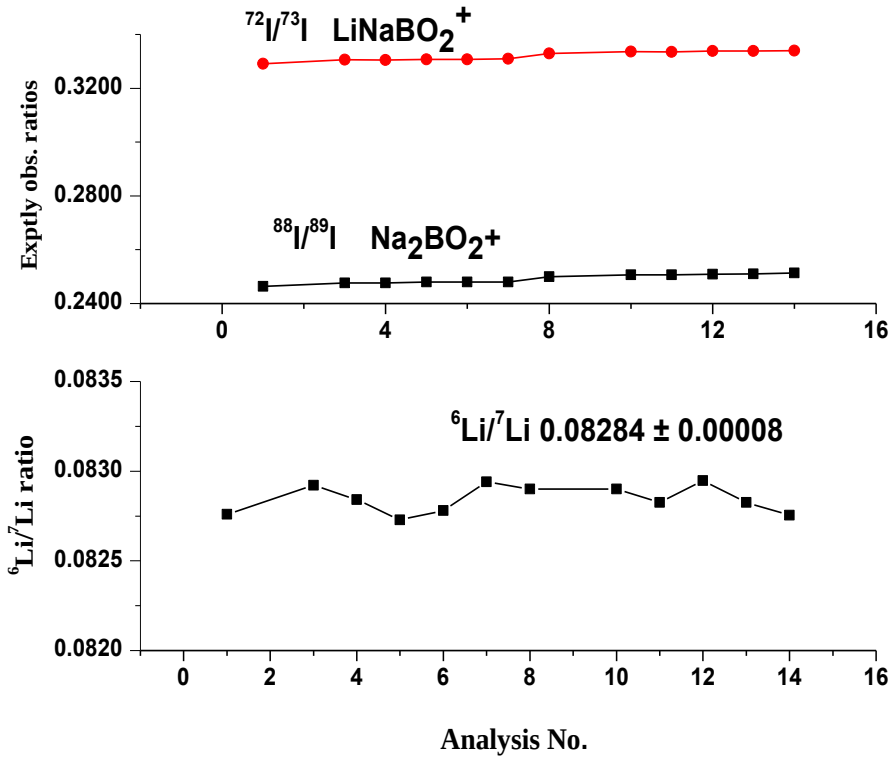

Fig. 3.8 Precise $^6Li/^7Li$ ratio obtained for L-Svec Li_2CO_3 after subtracting the experimentally obtained $^{10}B/^{11}B$ ratio of two different sources

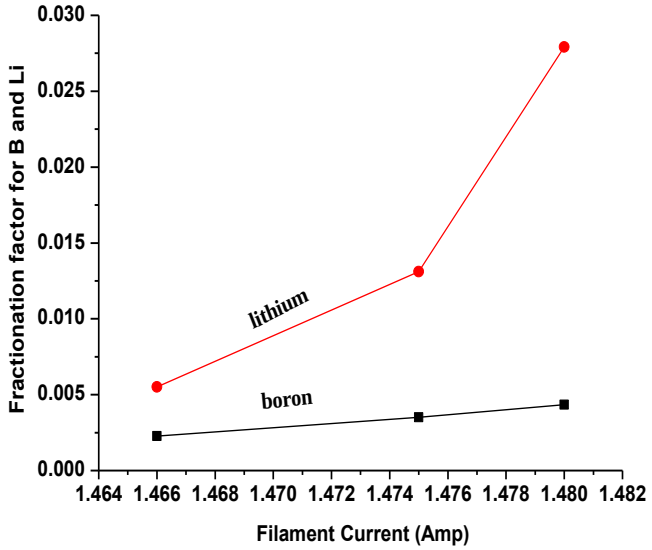

Fig. 3.9. Fractionation pattern for L-Svec lithium and NIST SRM-951 boron in $NaLiBO_2^+$ & $Na_2BO_2^+$ (for Li_2CO_3 and $Na_2B_4O_7$, Na/Li mole ratio =1, solution pH > 9)

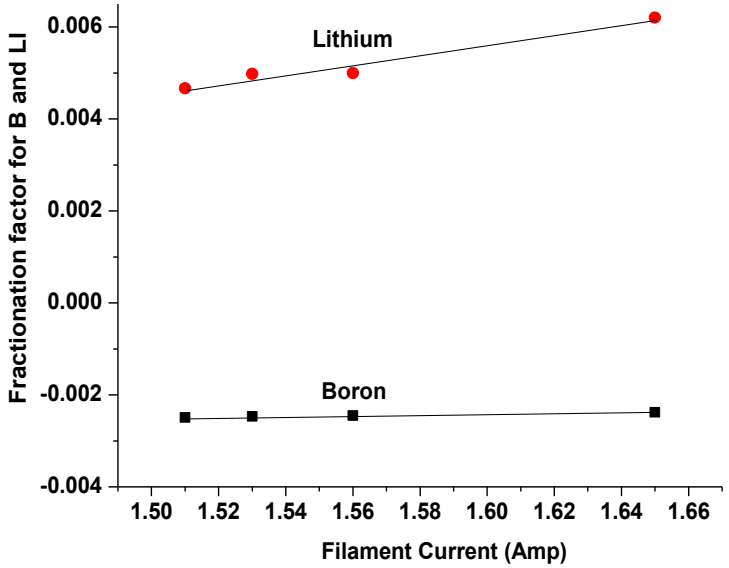

Fig. 3.10. Fractionation pattern for L-Svec lithium and NIST SRM-951 boron in $NaLiBO_2^+$ & $Na_2BO_2^+$ (for Li_2CO_3 and $Na_2B_{20}O_{31}$, Na/Li mole ratio =1, solution pH< 8)

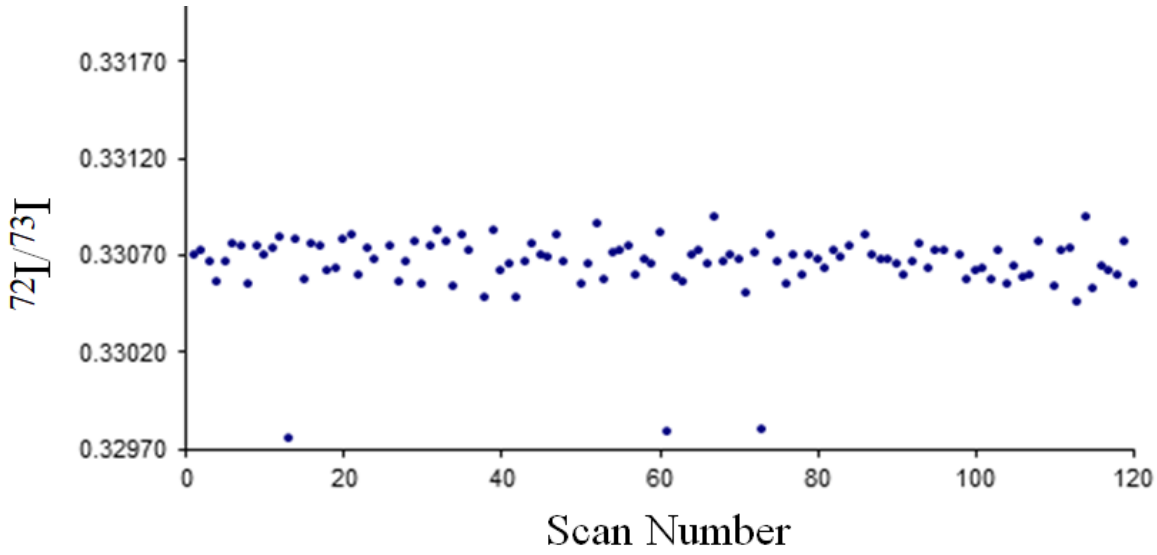

Fig. 3.11. The stable ion intensity ratio for L-Svec $LiNO_3$ sample analysed as $NaLiBO_2^+$ is seen. (for L-Svec lithium and $Na_2B_{10}O_{16}$, Li/Na ratio ~ 1, pH < 8)

[0.00011]. The value in parentheses is the propagated error from Eqn. 3.5. A comparison of the $^{6}Li/^{7}Li$ ratio for L-Svec Standard determined in this work and some previous researchers are shown in Table 3.9. The large variations among the $^{6}Li/^{7}Li$ ratios could be attributed largely to the chemical treatment preceding the analysis and instrumental biases during measurement. The value determined in this work assumes significance as boron isotopic abundance required for computing $^{6}Li/^{7}Li$ ratio by monitoring $NaLiBO_2^+$ is experimentally obtained by simultaneously monitoring $Na_2BO_2^+$ in-situ, also formed during the analysis. Since sodium is added intentionally thorough purification from sodium will not be required during analysis of actual samples.

Table 3.9. $^{6}Li/^{7}Li$ isotope ratio obtained for L-Svec lithium from different laboratories

Reference [no.]	Chemical form	Filament assembly	Monitoring ion	$^{6}Li/^{7}Li$ ratio
*Flesch et al [162]	LiI	Re-Re-Re	Li^+	*0.0832 ± 0.0002
Chan et al [153]	$Li_2B_4O_7$	Ta	$Li_2BO_2^+$	0.0828 ± 0.0001
Green et al [64]	LiF	Ta-Re-Ta	Li_2F^+	0.08201 ± 0.0001
Xiao et al [66]	$Li_2B_4O_7$	Ta-Re	Li^+	0.08221 ± 0.00002
#Datta et al [84]	$Li_2B_{10}O_{16}$	Te	$Li_2BO_2^+$	0.0834 ± 0.00011
Moriguti et al [67]	Li_3PO_4	Re-Re	Li^+	0.082543 ± 0.00002
Sahoo et al [154]	$Li_2B_4O_7$	Re	$Li_2BO_2^+$	0.082289 ± 0.000043
Sahoo et al [163]	Li_3PO_4	Re-Re-Re	Li^+	0.08258 ± 0.00009
Chen et al [65]	Li_3PO_4	Re-Re	Li^+	0.08261 ± 0.00003
S.Duta et al [164]	$Li+H_3BO_3$	Re-Re-Re	Li^+	0.08215 ± 0.00023
This work	NaLiO $X.B_2O_3$	Re	$NaLiBO_2^+$	0.08283 ± 0.00006

*Value of SVEC Li standard

3.4. Conclusions

A thorough investigation has been carried out for precise and accurate isotopic ratio measurement of Lithium using the two molecular ions $Li_2BO_2^+$ and $NaLiBO_2^+$. The robustness of the method using $Li_2BO_2^+$ ions depend on the judicious selection of ion pair combination from the nine combinations for different isotopic abundances of lithium and boron. The final propagated uncertainty is largely affected by the measurement uncertainty in the detection of low abundant species [165].

The computation of $^6Li/^7Li$ using $NaLiBO_2^+$ ions is simple as boron isotopic ratio is independently determined simultaneously from the same sample loading by monitoring $Na_2BO_2^+$ ions. Good ion intensities are obtained for $NaLiBO_2^+$ and $Na_2BO_2^+$ when the B/alkali atom ratio ≥ 5 resulting in high precision in the measured ion intensity ratios [166].

Analyses of Li as molecular ions, $Li_2BO_2^+$ or $NaLiBO_2^+$ under optimized analysis conditions produces stable ion intensity ratios less effected by ion source fractionation compared to atomic ions and the methodology has significantly improved the precision of $^6Li/^7Li$ isotope ratio measurement.

Chapter 4

Total Evaporation for the accuracy and sensitivity enhancement of $NaLiBO_2^+$ molecular ion method for the isotope ratio measurement of $^6Li/^7Li$

4.1. Introduction

Conventionally isotope ratio measurement of lithium is carried out using atomic ions (Li^+). Though atomic ion analysis of Lithium is very sensitive, as only a few nano gram amounts are required, stringent analysis conditions with respect to sample amount, the type of lithium compound, loading conditions and a high level of operator skill are required to have a reasonably good precision in the measurement. Further, faraday cups have to be adjusted to their extreme positions for simultaneous collection of $^6Li^+$ and $^7Li^+$ which requires state of art instruments having dispersion of 17%. On the other hand, analysis as high molecular weight ions such as $Li_2BO_2^+$ (*m/z* 54 to 57) and $NaLiBO_2^+$ (71 to 73) reduces the severity of fractionation. Simultaneous collection of the molecular ionic species that are required for determining $^6Li/^7Li$ isotope ratio is easily possible when $Li_2BO_2^+$ and $NaLiBO_2^+$ are used. Among the two molecular ions, $NaLiBO_2^+$ is a method of choice for the isotopic measurement of lithium because of the following advantages: i) mass numbers of monitoring ions of $NaLiBO_2^+$ from m/z 71 to 73 is relatively higher to that of m/z 54 to 57 (in the case of $Li_2BO_2^+$), which reduces the severity of ion-source isotope fractionation ii) as sodium is deliberately added for the formation of sodium lithium borate, there is a relatively high tolerance for sodium in the sample iii) contribution from isotopes of boron can be accounted from in situ measurement of $^{10}B/^{11}B$ ratio obtained from $Na_2BO_2^+$ ion (m/z 88, 89) which is formed along with $NaLiBO_2^+$. However, in spite of the several advantages offered by the molecular ion methods they are not widely used among the geological communities as it is not as sensitive as atomic ions requiring 2 to 3 µg amount of lithium on the filament.

Some of the shortcomings of limited scan acquisition can be addressed by adoption of Total Evaporation and ion integration (TE) or flash evaporation technique wherein, the ions emitted from the heated filament are simultaneously collected and integrated in multi-collector

assembly till the sample is completely exhausted [167, 168]. The scope of this method includes nearly fractionation free isotopic analysis as well as enhancement of detection limits to nanogram level sample size because of the augmentation in the ion intensities of the isotopes since all the ions formed are integrated. Total evaporation as well as the modified TE techniques have been used for analysis of minor isotopes of U and Pu for nuclear safeguards with improved accuracy [169 - 171]. Unlike in conventional method where the ion collection is limited to a few blocks of steady ion current, in total evaporation, since most of the emitted ions are collected, the fractionation factor is considerably reduced. This results in improved accuracy in the isotope ratios of elements. This method of acquisition is only possible with Thermal ionization source with multi collector detector assembly. The advantages of Total Evaporation technique are 1) the isotopic measurement is almost fractionation free (minor corrections due to residual sample remaining on the filament) 2) Since the ion current is integrated till the sample is completely consumed, the correction factors are less dependent on the amount of sample loaded on the filament 3) the sensitivity of the monitored ions are enhanced. The method has also been used for analysis of sub-nanogram sized samples of boron as molecular BO_2^- by N-TIMS [72].

The objective of the present work was to explore the possibility of using the total evaporation and ion integration method (TE & II) also called flash evaporation for improving the accuracy as well as the sensitivity for isotopic analysis of Li using $NaLiBO_2^+$ ions. To the best of our knowledge no reports have been published based on TE&II for the isotopic measurement of lithium using molecular ions. L-SVEC Lithium (NIST RM 8545) and Specpure lithium (spectroscopic grade pure lithium) both lithium carbonate compounds of natural composition were analysed.

4.2. Experimental

4.2.1 Chemicals used and sample preparation

High Purity Spec Pure Li_2CO_3 with natural ^6Li content obtained from Johnson Matthey, isotopic standards of lithium and boron NIST-RM-8545 (L-SVEC Li_2CO_3) and NIST-SRM-951 (H_3BO_3) were also used during the present investigations. For preparing mixed alkali borates high purity Na_2CO_3 (Alfa Aesar) was used. Freshly deionized water (18.2 MΩcm) obtained from Milli Q system (Millipore) and quartz glassware were used for all dissolutions and dilutions. L-SVEC Li_2CO_3, Spec pure Li_2CO_3 were individually mixed with NIST-SRM 951 and high purity Na_2CO_3 in a proportion such that the mole ratio of B/Na ~10 and Li/Na ~ 1. The details of the sample preparation and loading procedure are discussed in Table 3.2 of chapter 3. During the present TE and II studies the amount of Li loaded was varied from 50 ng to 1.5µg in 5µL solution. The sample solution loaded on Re single filament was dried at 1A and heated slowly to red hot.

4.2.2 TIMS analysis

A thermal ionization mass spectrometer model TRITON-PLUS equipped with multiple faraday cups was employed in the present studies. The samples were analysed by both conventional method of limited blocks (3 to 5) each with 12 scans as well as by TE and II. The details of ion chemistry of the mixed alkali borate (sodium lithium borate) are already discussed in Section 3.3.2.1 to 3.3.2.2 of chapter 3. The loaded sample filament was heated slowly to 1 A and degassed for five minutes in the ion source. Na^+ ion was used for initial focusing of the

ion beam. On heating the filament further, $Na_2BO_2^+$ was obtained at a filament current of ~1.1 A immediately followed by $NaLiBO_2^+$.

For conventional method 1.5 µg to 2 µg of lithium was loaded on the filament and data was acquired when the ion intensity at *m/z* 73 ~ 0.5 X 10^{-11} A and the corresponding ion intensity at *m/z* 89 ~1 X 10^{-11}A. Data acquisition was carried out by dynamic mode of multi-collection in two sequences, in the first sequence, $NaLiBO_2^+$ ions at *m/z* 71, 72 and 73 were simultaneously collected in L_1, Ax and H_2 cups respectively and in the second sequence $Na_2BO_2^+$ ions at *m/z* 88 and 89, were collected in Ax and H_1 cups. The baseline measurement was made at the beginning of a block at *m/z,* M ± 0.5 for 10 s, where M is the isotopic mass of interest.

For TE and II the amount loaded varied from 100 ng to 1.5µg, few experiments were also carried out with 50 ng lithium on the filament. During acquisition using the TE&II procedure, the ion current at each faraday cup detector gets integrated with the subsequent next cycle. The ion current was recorded till it the ion current came down to 5 X 10^{-14} A. The data acquisition experiments were carried out individually for $NaLiBO_2^+$ ions at m/z 71, 72 and 73 and $Na_2BO_2^+$ ions at *m/z* 88 and 89 from the duplicate loadings. The various steps of the analysis protocol are detailed below:

After ensuring sufficient vacuum in the ion-source, sample filaments were initially heated with a rate of 200 mA/min until 1000 mA. Thereafter the filament current was programmed to increase till the sum of all intensities reaches to 12 X 10^{-14} A with a heating rate of 30 mA/min. Prior to acquiring the data, focusing and peak centering were carried out to have a maximum ion current at the nuclide mass of interest. During the Auto-acquisition, the filament heating current was programmed to ensure that it does not exceed the maximum pilot signal (sum of all intensities) of 40 X 10^{-11} A. The data acquisition terminated when the

recorded ion current reached below 5 X 10^{-14} A per cycle. Slope of heating rate maintained during acquisition was 1 mA per cycle. Signal intensities were integrated for 4.194 sec per cycle. On an average, analysis time is about one and half hour long for about 500ng of lithium on the filament.

4.3. Results and discussion

The results of conventional method (limited block) of analysis for SVEC lithium carbonate and Spec Lithium carbonate are represented in Fig. 4.1 and Fig. 4.2 series respectively. The figures depict the results of analysis under optimized condition as described in section 3.3.2.4 of chapter 3. Each data point in the Fig. 4.1 and Fig. 4.2 is the average of 3 blocks consisting of 36 scans of the measured data for $^{72}I/^{73}I$ and $^{88}I/^{89}I$. They. also give the average $^{6}Li/^{7}Li$ ratio obtained (from Eqn. 3.1 under section 3.1.2 of chapter 3) from five individual analysis along with their standard deviation. It has been observed that the effect of fractionation cannot be avoided but can be minimized when the pH of the loaded solution in the range 5 to 7. The Fig. 4.3 shows the measured $^{72}I/^{73}I$ and $^{88}I/^{89}I$ ratio of a sample of sodium lithium borate analysed at increasing filament current / ion intensity. It can be seen that the precision of the measured $^{72}I/^{73}I$ ratio is affected by fractionation. Of the two elements boron shows negligible fractionation as observed by the stable $^{88}I/^{89}I$ ratio recorded throughout the analysis. This is probably due to the vaporization behavior which depends on the stoichiometry of the borate compound formed, in the present case borate with B/M ratio ≥ 5 (M-alkali) [82, 172]. This implies that the fractionation in $^{72}I/^{73}I$ ratio is primarily due to the isotopes of lithium which effects the precision of the derived $^{6}Li/^{7}Li$ ratio (Fig. 4.3). TE and II method was therefore used to resolve the bias in the $^{6}Li/^{7}Li$ due to fractionation.

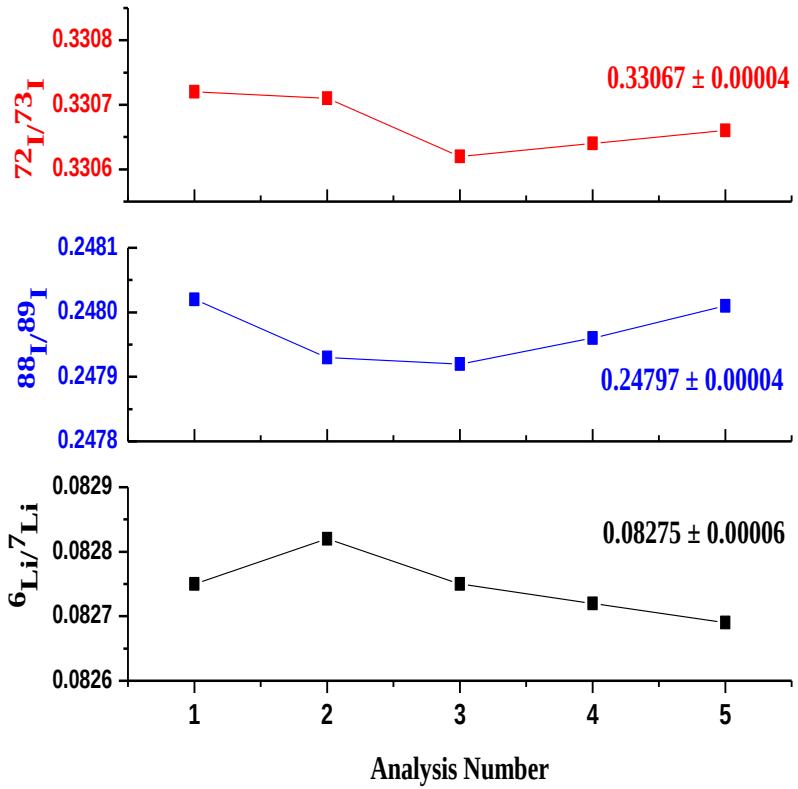

Fig. 4.1 Average $^{6}Li/^{7}Li$ ratio obtained for L-SVEC Li_2CO_3 from the measured $^{72}I/^{73}I$ and $^{88}I/^{89}I$ ratios from 5 individual analysis

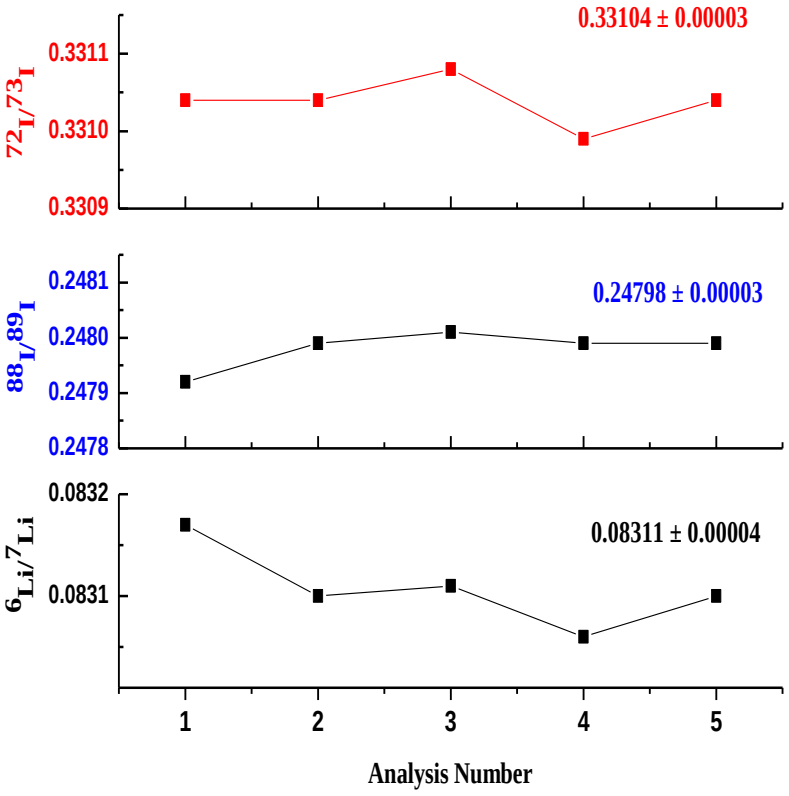

Fig. 4.2 Average $^{6}Li/^{7}Li$ ratio obtained for Specpure Li_2CO_3 from the measured $^{72}I/^{73}I$ and $^{88}I/^{89}I$ ratios from 5 individual analysis

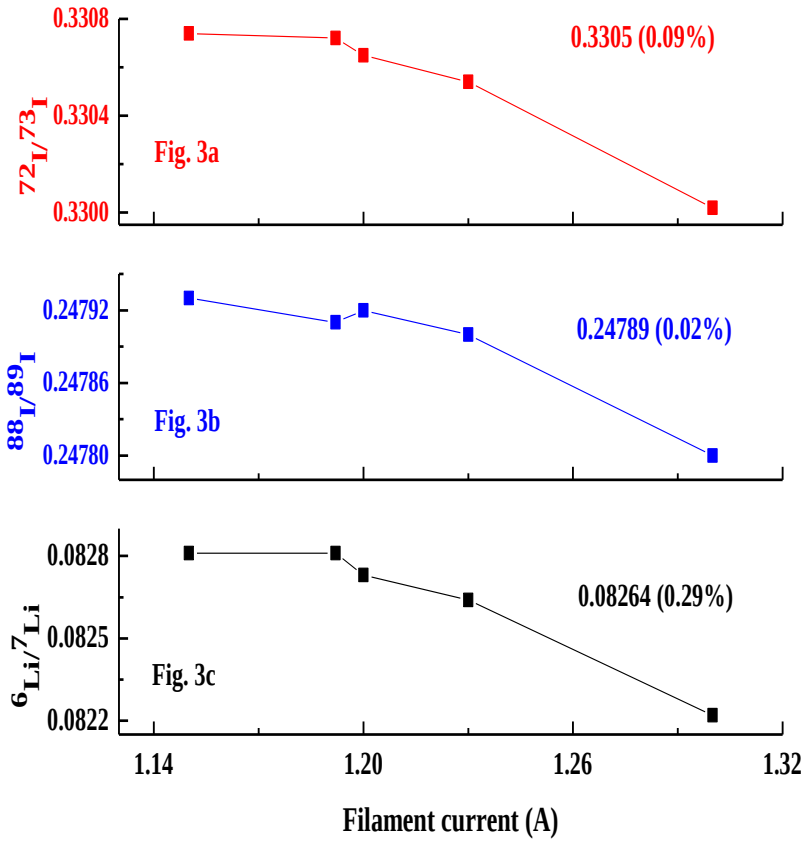

Fig. 4.3 Average $^{6}Li/^{7}Li$ ratio obtained for L-SVEC lithium acquired at increasing filament currents

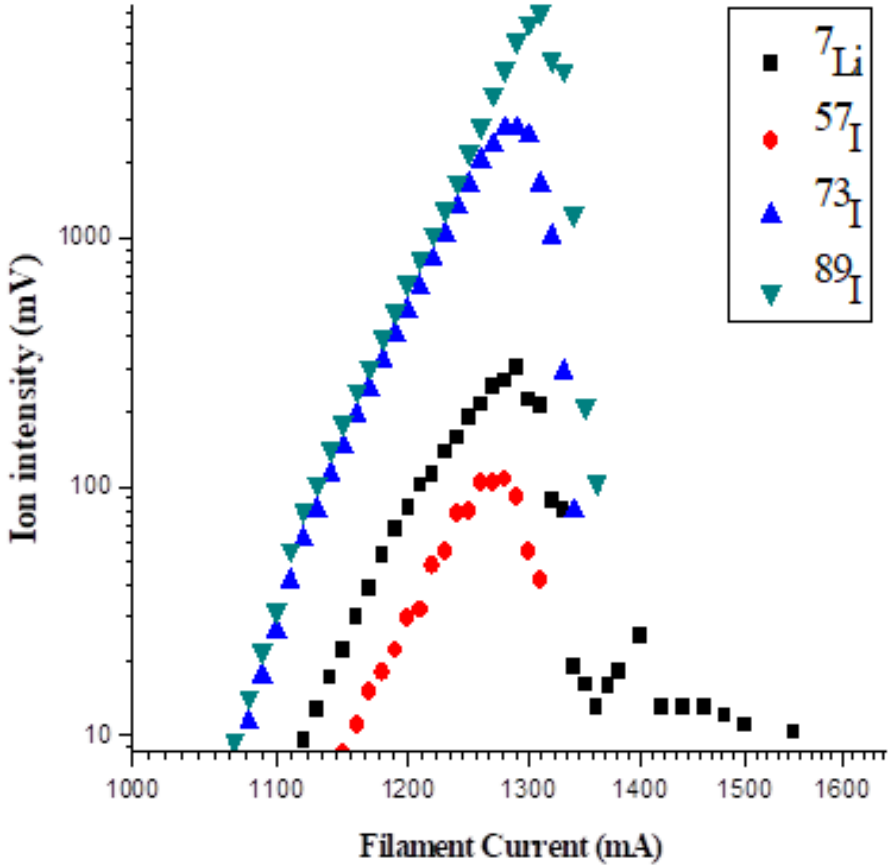

Fig. 4.4 Ion intensities of different molecular species formed from sodium lithium borate as a function of Filament current

4.3.1 TE and II method for $NaLiBO_2^+$ and $Na_2BO_2^+$

Ideally for adoption of total evaporation technique the element should evaporate and ionize as a single species to facilitate collection of all the ions of an element with no loss of sensitivity and accuracy. Li vaporizes as atomic species or molecular species depending on the type of compound loaded as well as the filament geometry. During our investigations the ion intensities of the different ionic species of lithium as a function of filament current was recorded which is shown in Fig. 4.4.

As can be seen in Fig. 4.4 at low filament current $NaLiBO_2^+$ ion is the major species formed with very minor contribution from Li^+ or $Li_2BO_2^+$. Inspite of the small loss in ion intensity during ion integration of $NaLiBO_2^+$ ions, no loss in accuracy is expected as these ions are evaporating together from the same source. During the present experiments a steady evaporation pattern was maintained by regulating the heating rate of the filament per scan to maximize collection of ions by the faraday cups. Among the 10 mA 5 mA, 3 mA, 1 mA per cycle heating rates investigated, 1mA was found to be most suitable. Fig. 4.5a and 4.5b shows the integrated $^{72}I/^{73}I$ ratio as well as the instantaneous $^{72}I/^{73}I$ ratio (i.e. ratio of each cycle) as a function of fraction of sample consumed for a typical analysis of 500 ng of L-SVEC Lithium and Specpure Lithium respectively. (Supporting spread sheet for calculation of typical ion intensity ratio profile is shown in Appendix 4.1) Fig. 4.5c shows both integrated as well as instantaneous $^{88}I/^{89}I$ ratio obtained by monitoring $Na_2BO_2^+$ ions from the loaded sodium lithium borate sample as function of fraction of sample consumed. The instantaneous $^{72}I/^{73}I$ ratio in Fig. 4.5a and 4.5b shows a steady decrease in ratio till about 85% sample has been consumed thereafter, the ratio changes steeply till most of sample has evaporated. Whereas for integrated $^{72}I/^{73}I$ ratio after initial fluctuations observed at low ion intensity (low sample

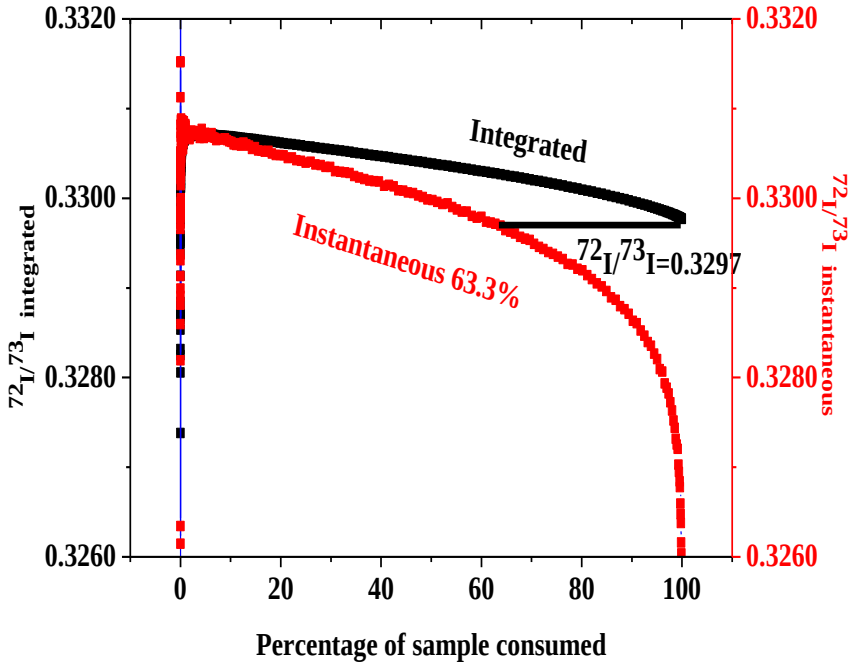

Fig. 4.5a Shows the fractionation profile of instantaneous and integrated $^{72}I/^{73}I$ ratio as a function of sample consumed for L-Svec lithium

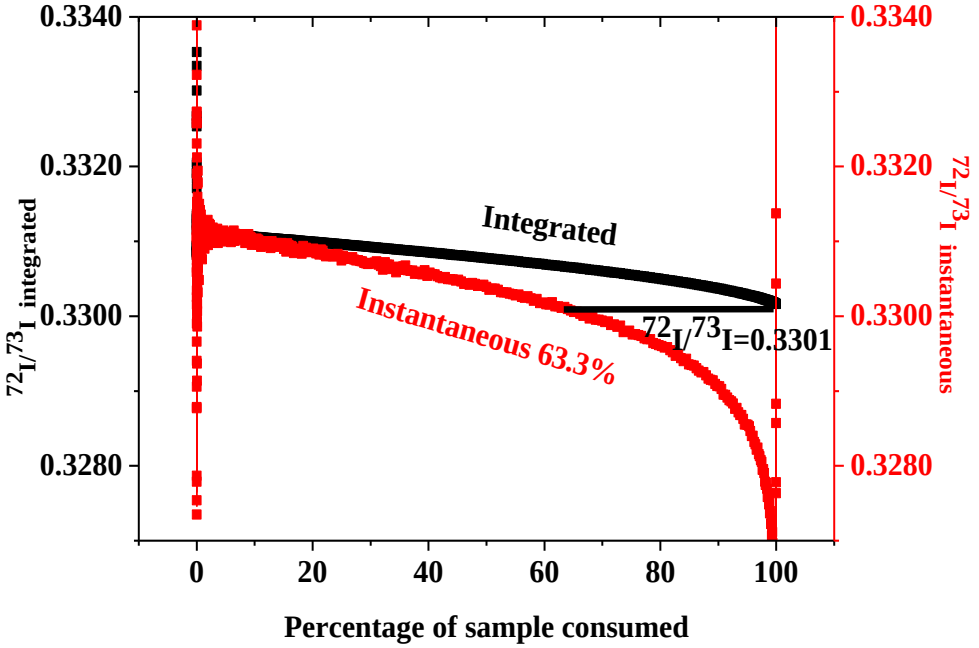

Fig. 4.5b Shows the fractionation profile of instantaneous and integrated $^{72}I/^{73}I$ ratio as a function of sample consumed for Spec pure lithium

consumption), the change in ratio is very gradual and remains constant after the sample has completely evaporated. This suggests that even if there is a small residual sample on the filament the affect on the final ratio is expected to be insignificant. At 100% sample consumption the measured integrated ratio should be equal to the true ratio. According to the Raleigh distillation law the measured ratio equals the true ratio when the ~ 63% of the sample has been consumed. It can be seen from Fig. 4.5a and 4.5b that at 63% sample consumption the instantaneous ratio is very close to the integrated value at 100% consumption. As seen in Fig. 4.5a and 4.5b the integrated $^{72}I/^{73}I$ ratios for L-Svec and Specpure differ by about 0.12%. As explained earlier, the measured $^{72}I/^{73}I$ ratio depends on the isotopic abundance of B and Li in the sodium lithium borate and their isotope fractionation behavior. There is no difference in the ion intensity ratio profile of $Na_2BO_2^+$ of the two lithium samples namely L-SVEC and Specpure as an aliquot of sodium borate prepared with NIST SRM-951 is added to both the samples (Fig. 4.5c). Except for the initial fluctuations the instantaneous measured $^{88}I/^{89}I$ ratio is nearly constant throughout the analysis. The integrated $^{88}I/^{89}I$ ratio pattern overlaps with the instant ratio values unlike the pattern observed for $NaLiBO_2^+$. It can therefore be concluded that the fractionation profile of $NaLiBO_2^+$ is primarily due to Lithium isotopes.

The $^6Li/^7Li$ isotope ratio from ion integration of the completely consumed sample is then calculated from the integrated $^{72}I/^{73}I$ intensity ratio and $^{88}I/^{89}I$ intensity ratio using Eqn. 3.1 under section 3.1.2 of chapter 3. Fig. 4.6a gives the integrated $^{72}I/^{73}I$ and $^{88}I/^{89}I$ values from five different analysis of L-Svec and Specpure lithium and Fig. 4.6b gives the respective $^6Li/^7Li$ ratio derived from equation. An external precision of better than 0.1 % was obtained for 500 ng of lithium for both L-Svec and Specpure lithium. For conventional analysis of the lithium at least 1.5 µg lithium is required to obtain similar precision in $^6Li/^7Li$ ratio. Average fractionation factor defined as $K = [^6Li/^7Li]_{Conventional} / [^6Li/^7Li]_{TE}$ for L-Svec lithium

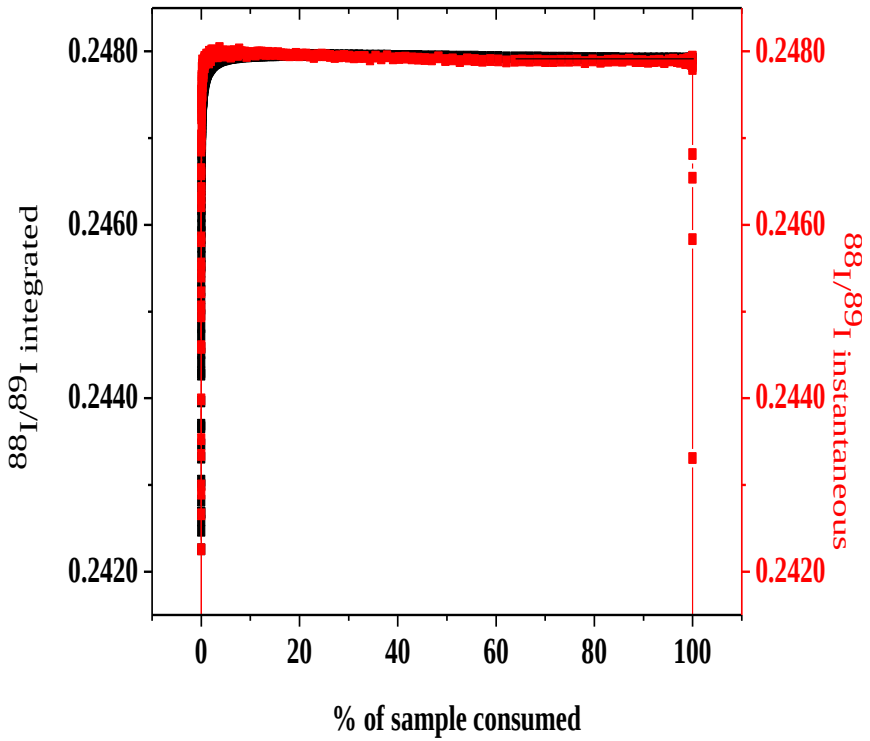

Fig. 4.5c Overlapping in the fractionation profile of instantaneous and integrated $^{88}I/^{89}I$ ratio as a function of sample consumed for typical sodium lithium borate sample

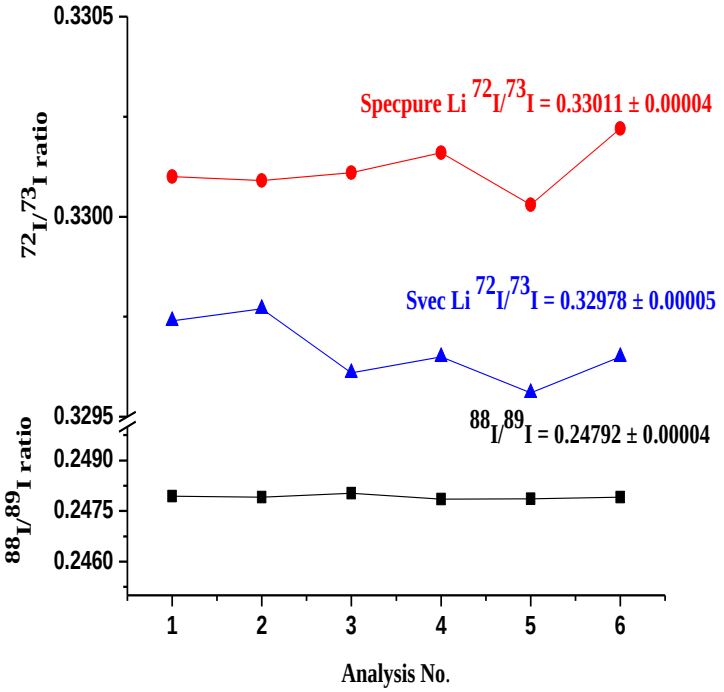

Fig. 4.6a Integrated $^{72}I/^{73}I$ and $^{88}I/^{89}I$ values from five different analysis for L-Svec and Specpure Lithium

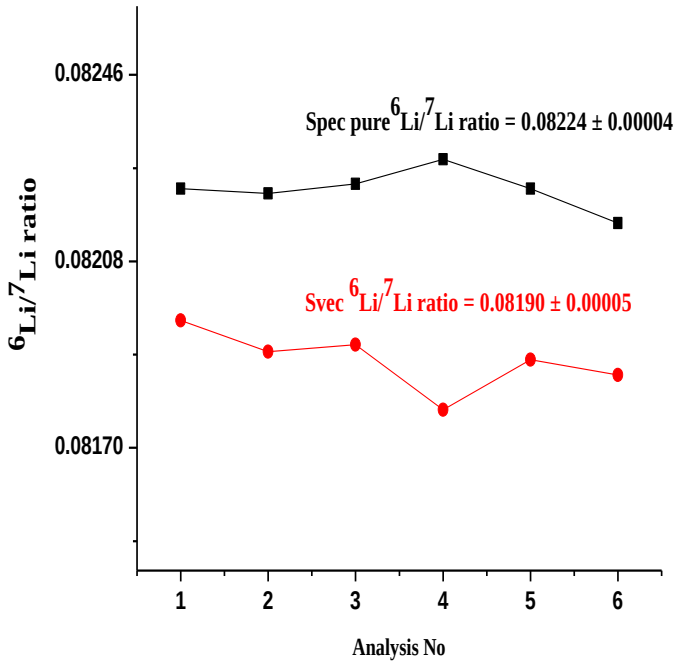

Fig. 4.6b $^6Li/^7Li$ ratio derived from eqn.1 for 500 ng Li on the filament for L-Svec and Specpure Lithium

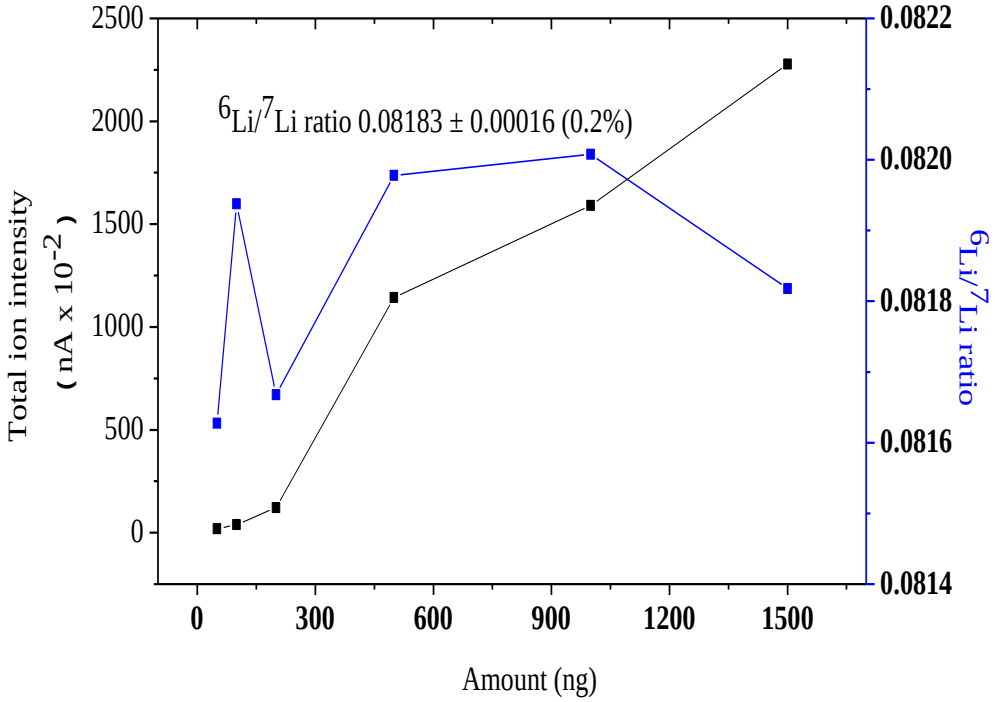

Fig. 4.7 Variation in total ion intensity and $^6Li/^7Li$ ratio with amount of lithium on the filament

= 0.08275 / 0.08190 = 1.0104 and for Specpure pure lithium = 0.08311 / 0.08224 = 1.0106 was obtained from analysis of 500 ng of lithium. Varying amounts of L-Svec lithium from 2 µg to 50 ng have been analysed by TE & II. Fig. 4.7 gives the variation in total ion current and $^{6}Li/^{7}Li$ ratio with the Lithium amount loaded on the filament. An average $^{6}Li/^{7}Li$ ratio of 0.08183 ± 0.2% was obtained irrespective of the amount of lithium loaded on the filament.

4.4. Conclusions

The possibility of using polyatomic molecular ions for isotopic analysis of lithium based on TE & II method has been explored for the first time. Both $NaLiBO_2^+$ as well as $Na_2BO_2^+$ formed from lithium loaded as sodium lithium borate were collected during the experiments. With a precision of 0.1% for the $^{6}Li/^{7}Li$ ratio employing 500 ng of lithium it is possible to differentiate among natural lithium samples having minor difference in their isotopic content. The developed TE & II method has improved the sensitivity as well as accuracy of the molecular ion method. It will be interesting to see if this fractionation profile is maintained over a wide range of lithium isotopic content.

Chapter 5

Preparation of Synthetic Lithium Isotope Mixtures (SLIMs)

5.1. Introduction

Thermal Ionization Mass spectrometry methodology using polyatomic ions such as $Li_2BO_2^+$ and $NaLiBO_2^+$ as monitoring ions have been developed to produce stable ion currents to give precise $^6Li/^7Li$ isotopic ratios for natural samples. It was observed that stable ion currents are obtained when the B/Alkali atom ratio was ≥ 5 for both these molecular ions. The overall fractionation observed was less than 1% with increase in temperature of the filament, which is much lower than the 9% fractionation observed for samples analysed by monitoring atomic ions Li^+ [67]. The value of $^6Li/^7Li$ for L-SVEC lithium assigned by two international certification laboratories National Institute for Standards and Technology, NIST RM 8545 and Institute for Reference Materials and Measurements, IRMM 016 are 0.0832 ± 0.0002 (1973) and 0.082154 ± 0.000099 (2005) respectively differ by more than 1%. Even though lithium was analyzed as Li^+ on single filament assembly by both the laboratories, the loaded form (LiI during NIST experiments and Li + H_3BO_3 during IRMM experiments), time of analysis, amount etc was probably the reason for the discrepancy in the L-Svec $^6Li/^7Li$ isotope ratio. The reference material NIST – RM – 8545 L-SVEC Li_2CO_3 having natural lithium composition yielded $^6Li/^7Li$ ratio of 0.08277 ± 0.00006 using $NaLiBO_2^+$ as monitoring ions under the optimized condition developed in this laboratory.

In Chapter 4 the role of Total evaporation and Ion integration with $NaLiBO_2^+$ as monitoring ion to arrive at an accurate and precise value which is almost fractionation free for the L-Svec Reference Material has been discussed. The highlights being a) simultaneous collection of ions at m/z 71-73 easily possible b) The analysis could be carried out comfortably with 500 ng Li with an external precision better than 0.1% (1σ) compared to the conventional fixed scan method which requires about 1.5 µg Li. c) The minimum sample requirement decreased to 50 ng from µg amounts required for the conventional molecular ion method d)

The $^{6}Li/^{7}Li$ ratio was independent of the amount of Li loaded and average $^{6}Li/^{7}Li$ ratio of 0.08183 ± 0.00016 was obtained for 1.5 µg to 50 ng lithium. The $^{6}Li/^{7}Li$ ratio of conventional vs TE method of acquisition for L-Svec i.e. K = 1.0104 ± 0.0010 obtained from five individual analysis of L-Svec by the two methods. The designated fractionation factor, K (considering $^{6}Li/^{7}Li$ by TE to be true value) should be applicable over a wide range of $^{6}Li/^{7}Li$ ratios and requires further experiments.

In view of the above reasons experiments were undertaken to prepare and characterize isotopic mixtures over a wide range of $^{6}Li/^{7}Li$ atom ratios for calibration of mass spectrometers over a wide range of ratios. This requires mixing of pure enriched calibrated isotope solutions of ^{6}Li and ^{7}Li on weight basis for making isotopic blends over a wide range of ratios. Isotope mixtures are being used determine the correction factor *K*, for mass discrimination of the measurement method and the mass spectrometer being used [173 - 178]. A.O. Nier performed the first measurements for isotope abundances, corrected for mass fractionation by means of synthetic mixtures of enriched isotopes [179]. This technology is being used since then for the determination of atomic weights and characterization of IRMs (Isotope Reference Materials). Highly enriched and chemically purified isotopes were used to gravimetrically prepare synthetic isotope mixtures, for which theoretical isotope abundance ratios can be calculated from the isotope abundances of the enriched isotopes [173 - 182].

The experiments presented here involved in the preparation of synthetic lithium isotopic mixtures (SLIMs) with ^{6}Li abundances ranging from 1% to 85% using the calibrated solutions of enriched ^{6}Li and ^{7}Li isotopes. Analysis was carried out by TIMS with $NaLiBO_2^+$ ion using both conventional and TE acquisition methods.

The objective of preparing synthetic lithium isotopic mixtures over a wide range of isotopic ratios and analyzing them using $NaLiBO_2^+$ as monitoring ions were:

1) Verify and confirm the constancy of isotope fractionation factor over a wide range of ratios for measuring the $^{6}Li/^{7}Li$ isotope ratio.
2) Identify reasons for non-linearity if any due to sample preparation, contamination, blanks, weighing errors etc.
3) Ascertain the accuracy of the measured isotope ratios in unknown samples over a wide range of ratios
4) To make available the isotopic working standards for quality control of data produced by other mass spectrometric methodologies such as P-TIMS using atomic ions and ICPMS
5) Calibration of additional working standards of pure Li_2CO_3 of non-natural isotopic compositions for routine use for economic viability.

5.2. Experimental

Li_2CO_3 95% enriched in ^{6}Li procured from M/s. ICON and Li_2CO_3 99.91% enriched in ^{7}Li from M/s. Eurotop. High Purity (99.998% purity) Spec Pure Li_2CO_3 with natural ^{6}Li content obtained from Johnson Matthey was used for calibration of the enriched solutions. Isotopic standards of lithium and boron NIST- RM – 8545 L-Svec (Li_2CO_3) and SRM-951 (H_3BO_3) were also used during the present investigations. High purity Na_2CO_3 (Alfa Aesar) was used for preparing mixed alkali borates. Freshly deionized water (18.2 MΩcm) obtained from Milli Q system (Millipore) and quartz glassware were used for all dissolutions and dilutions.

5.2.1 Calibration of Enriched $^{6}Li_2CO_3$ and $^{7}Li_2CO_3$ solutions and preparation of the synthetic isotopic mixtures

About 300 mg of each of Spec Pure Li_2CO_3 (Natural I.C. of Li), Enriched $^6Li_2CO_3$, and Enriched $^7Li_2CO_3$ were heated independently in an oven at 105°C for 2 hrs or till constant weight. This removed traces of moisture if any. Accurately weighed amount of each salt was dissolved in Millipore water in Quartz flask to prepare a solution of approximately 50 µg/gm of Li. Approximately one gm weighed aliquots each of both Spec Pure and ^6Li enriched Li_2CO_3 were mixed to prepare five Isotope Dilution Mass Spectrometry (IDMS) mixtures having $^6Li/^7Li$ ratio about one. The concentration of lithium in the ^6Li enriched stock solution was determined using Reverse – Isotope Dilution Mass Spectrometry (R-IDMS) equation. Similarly, five calibration blends of the Spec Pure and ^7Li enriched Li_2CO_3 were prepared with the ratio R_M (calculated) to be a geometric mean of the two for determining the concentration of lithium in $^7Li_2CO_3$ solution using the IDMS equation. The mass spectrometric analysis of the pure solutions and blends were carried out by Isoprobe-T TIMS and TRITON TIMS.

The Lithium isotopic mixtures to be used as isotopic working standards were prepared by gravimetric mixing of the highly enriched and calibrated ^6Li and ^7Li lithium carbonate solutions in fresh polypropylene bottles. Calculated aliquots of the enriched isotopes were mixed to give seven blends, SLIM - 1 to SLIM - 7, with ^6Li isotopic content of 1%, 8%, 20%, 35%, 50%, 75% and 85% respectively. The total lithium amount in each of the five mixtures was about 10 mg. All solutions were shaken for homogeneous mixing and kept aside for a week to allow complete isotopic equilibration.

5.2.2 Mass spectrometric analysis

The details of the chemical treatment, loading procedure and TIMS analysis protocol for analysis of Li with $NaLiBO_2^+$ ion is given in Table 3.2. The different molecular ionic species of $NaLiBO_2^+$ with their abundances is given in Table 3.7. The analysis was carried

out under the optimized conditions described in the earlier chapters, the stoichiometry of B/Alkali ratio was 5 and Na/Li ratio was 1 in the mixed alkali borate loaded on the single filament assembly. About 1.5 µg Li was loaded for analysis by conventional method. Data acquisition was carried out by dynamic mode of multi-collection in two sequences, as mentioned in Table 3.2. Ion intensity ratios for $^{72}I/^{73}I$ (R_1), $^{73}I/^{71}I$ (R_2), $^{72}I/^{71}I$ (R_3) and $^{88}I/^{89}I$ (R_B) were recorded during analysis. The data was acquired for 3 blocks of 12 scans each. Each scan consisted of 5 seconds of ion collection. The baseline measurement was made at the beginning of a block at *m/z*, M ± 0.5 for 10s, where M is the isotope of interest. All calibrations mixtures and the SLIMs were analysed following the analytical protocols mentioned in Chapter 3. The reproducibility of the analysis was obtained from four individual analysis of each of the SLIM's by the conventional limited block mode.

The seven SLIM's were also analysed by TE and II method, using the procedure given in chapter 4. Four individual analysis using 500 ng of each SLIM was carried out using TRITON TIMS to establish the reproducibility of this method.

5.3. Result and discussion

Since analysis involves non-natural lithium samples, the change in the Ion intensities at *m/z* 71, 72 and 73 as a function of fractional abundance of ^6Li is shown in Fig. 5.1. As can be seen the ion intensity at *m/z* 71 is less than 0.2% when the abundance of ^6Li in sample is 1% and increases to about 18% when the abundance of ^6Li increases to 100%. For natural lithium samples with ^6Li abundance of 7.6%, a very good precision is obtained for $^{72}I/^{73}I$ (R_1) during analysis. With increasing abundance of ^6Li it should be possible to use Ion intensity ratios $^{72}I/^{73}I$ (R_1), $^{73}I/^{71}I$ (R_2), $^{72}I/^{71}I$ (R_3) for deriving $^6Li/^7Li$ ratio in the sample from the equations given below.

$$L_1 = \frac{[B - R_1 - 2 * R_1 BO_a]}{[2 * R_1 O_a + 2 * R_1 BO_b - 1 - 2 * BO_a]}$$ -------- Eqn. 5.1

$$L_2 = \frac{[\frac{1}{B} + 2 * O_a]}{R_2 - 2O_b - 2 * \frac{O_a}{B} - O_a^2}$$ -------- Eqn. 5.2

$$\frac{1}{L_3} = R_3 - \frac{1}{B} - 2 * O_a$$ -------- Eqn. 5.3

Where R_1=$^{72}I/^{73}I$, R_2= $^{73}I/^{71}I$, R_3 = $^{72}I/^{71}I$ are the experimentally measured ratios and L_1, L_2 and L_3 are $^6Li/^7Li$ ratios derived from R_1, R_2 and R_3 respectively. $^{17}O/^{16}O$ = 0.00039 and $^{18}O/^{16}O$ = 0.002 denoted as O_a and O_b respectively. B = $^{10}B/^{11}B$ isotopic ratio (experimentally determined).

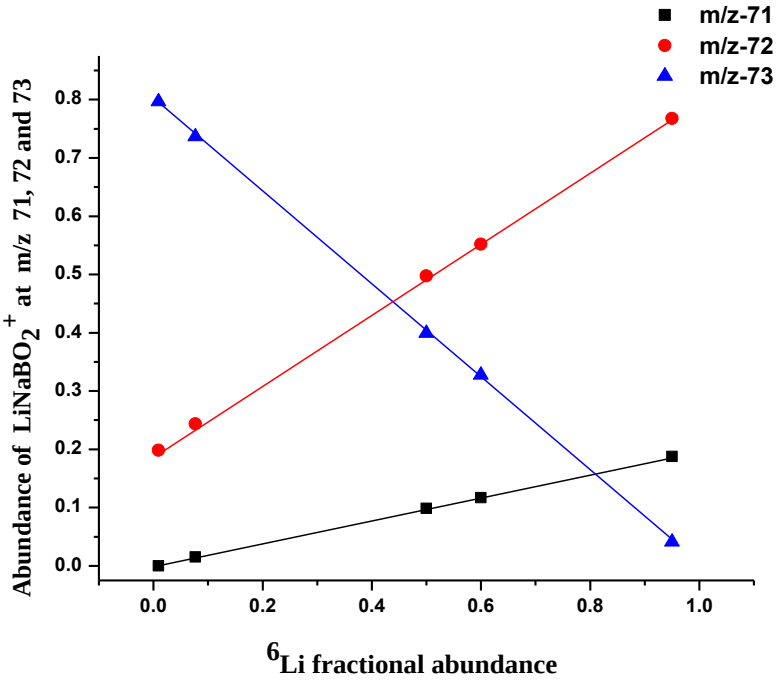

Fig. 5.1. Change in the Ion intensities at *m/z* 71, 72 and 73 as a function of fractional abundance of ^6Li

However, our detailed studies carried out to identify the ion intensity ratios for analysis of non-natural lithium samples showed that R_3 gave unacceptable values when it was used for deriving $^6Li/^7Li$ ratios in ^6Li enriched samples [183]. Though our studies showed that R_2 could be used for deriving $^6Li/^7Li$ ratios in samples with 50% abundance of ^6Li, all our experiments were carried our using $^{72}I/^{73}I$ (R_1), since it gave very satisfactory results and could be used universally for $NaLiBO_2^+$ ions, irrespective of ^6Li abundance in the sample.

The isotopic abundance of lithium in Spec pure natural Li_2CO_3, ^6Li enriched candidate spike and ^7Li enriched carbonate solution used in this work are given in Table 5.1. The Table 5.1 also gives the average atomic weight calculated from the isotopic analysis data. The footnote of the Table 5.1 gives the concentration of lithium in the high purity Spec Pure Li_2CO_3 standard solution calculated on gravimetric basis along with the uncertainty due to weighing errors. The uncertainty budget in preparation of specpure stock solution is given Table 5.2.

Table 5.1. Isotopic abundance of lithium in standard, ^6Li enriched and ^7Li enriched Li_2CO_3

Type of Li_2CO_3	$^6Li/^7Li$ isotopic ratio	Isotopic Abundance		Avg. atomic weight
		^6Li	^7Li	
^6Li enriched	21.48 ± 0.04	95.552 ± 0.007	4.448 ± 0.007	6.0596 ± 0.0001
^7Li enriched	0.00093 ± 0.00004	0.093 ± 0.004	99.907± 0.04	7.0151 ± 0.0001
Spec-Pure Natural	0.08311 ± 0.0001	7.67 ± 0.01	92.33 ± 0.01	6.9392 ± 0.00016

Stoichiometric concentration of lithium in standard Spec pure Li_2CO_3 = 47.738 ± 0.018[@]

[@] Uncertainties due to weighing error of the balance (0.0001g) and isotopic ratio measurement of natural Li in the standard used for calculation of average atomic weight.

Table 5.2. Uncertainty budget in the preparation of Specpure stock solution

Term	u = Uncertainity % (r.s.d.)
At Wt of natural Li in std	(u_1) 0.0022
Molecular weight of Li_2CO_3 Std	(u_1) 0.00033
Weight of Li_2CO_3 Std and its dilution	(u_2) 0.037
Uncertainty in concentration of Li_2CO_3 (u_{std})	$\sqrt{u_1^2 + u_2^2 + u_3^2}$ = 0.037

5.3.1. Determination of concentration of lithium in ^{6}Li and ^{7}Li enriched solution

Table 5.3 gives the details of the results of the spike calibration by Reverse-IDMS using Specpure natural lithium as standard. The average concentration obtained by analysis of the five blend aliquots along with the standard deviation (1σ) is given in the Table 5.3. Two ion intensity ratios $^{72}I/^{73}I$ (row 1) and $^{73}I/^{71}I$ (row 2) were measured during the analysis of each blend to give two independent $^6Li/^7Li$ ratio which were used for obtaining two independent concentration values for lithium in the spike. The detailed judicious selection and the experimental verification of the ion pairs was carried out during our studies [183]. As can be seen the reproducibility of lithium concentration determined from the five blends is better than 0.1% with the overall propagated uncertainty from the various terms of the IDMS equation being about 0.1%. Also, there is a close agreement between the concentration values obtained using the two ion intensity ratios R_1 and R_2. The concurrence of concentration values obtained from the two ion pairs $^{72}I/^{73}I$ and $^{73}I/^{71}I$ used for deriving $^6L/^7Li$ isotope ratio, indicates absence of any bias due to isobaric interference or isotope fractionation.

Table 5.3. Calibration of ^{6}Li enriched solution

Ion intensity Ratios used	^{6}Li - IDMS-1	^{6}Li - IDMS-2	^{6}Li - IDMS-3	^{6}Li - IDMS-4	^{6}Li - IDMS-5	Average
	(µg/gm Li)					
^{73}I/^{72}I	49.309	49.331	49.303	49.287	49.302	49.306 ± 0.019$^{\#}$
^{73}I/^{71}I	49.354	49.370	49.321	49.290	49.305	49.328 ± 0.033$^{\#}$

Table 5.4 gives the details of the results of the calibration of ^{7}Li enriched solution by IDMS using Specpure natural lithium as standard. The average concentration obtained by analysis of the five blend aliquots along with the standard deviation (1σ) is given in the Table 5.4. ^{72}I/^{73}I ratio was monitored and gave good precision during analysis. As can be seen here the reproducibility of lithium concentration determined from the five blends was better than 0.2%. This was because the ^{6}Li/7Li ratio (R_m) in the blends was about 0.009 and could only be measured with a precision of about 0.1%.

Table 5.4. Calibration of ^{7}Li enriched solution

Ion intensity Ratios used	^{7}Li - IDMS-1	^{7}Li – IDMS-2	^{7}Li – IDMS-3	^{7}Li – IDMS-4	^{7}Li - IDMS-5	Average
	(µg/gm Li)					
^{73}I/^{72}I	53.185	53.338	53.329	53.275	53.203	53.256 ± 0.09$^{\#}$

5.3.2 Mass spectrometric analysis of the synthetic isotopic mixtures by Conventional and TE acquisition

The results of the analysis of SLIMs - 1 to 7 by conventional method as well TE & II are given in Table 5.5. The expected value for the different SLIMs are calculated using the concentration data of the two enriched solutions (from Table 5.3 and 5.4), the weight of the aliquots of the two enriched solutions used for the particular SLIM and the isotopic content of the enriched isotopes using the formula

$$R^{6}/_{7}_{[AB]} = \frac{\left(\frac{[C*W*A.F.^{6}]_A}{[Av.At.Wt.]_A}\right)+\left(\frac{[C*W*A.F.^{6}]_B}{[Av.At.Wt.]_B}\right)}{\left(\frac{[C*W*A.F.^{7}]_A}{[Av.At.Wt.]_A}\right)+\left(\frac{[C*W*A.F.^{7}]_B}{[Av.At.Wt.]_B}\right)} \quad \text{--------- Eqn. 5.4}$$

where C denotes the concentration of lithium in the two enriched solutions A (6-Li solution) and B (7-Li solution) obtained from the IDMS experiments, W the aliquot weight of the each of the enriched solution in the given SLIM, A.F. is the atomic fraction of ^{6}Li and ^{7}Li in the two enriched Li_2CO_3 solutions and Av.At.Wt., is the average atomic weight of lithium in the enriched $^{6}Li_2CO_3$ and $^{7}Li_2CO_3$

The average bias factor $K_{bias} = R_{cal}/R_{obs}$, where R_{obs} is the ^{6}Li/^{7}Li ratio measured by conventional method and R_{cal} is the ^{6}Li/^{7}Li ratio calculated using Eqn. 5.4 for SLIMs 1 to 7. The K_{bias} (average) for SLIM 1 to 7 = 1.001436 ± 0.00236 (0.23%). As can be seen the calculated ratio for SLIM-1 is unexpectedly high and this is very likely to be due to human error in the weights of the aliquots recorded during preparation of SLIM 1. If SLIM 1 is excluded $K = R_{cal}/R_{obs}$ =1.00057 ± 0.00065 (0.06%). The closeness of R_{cal}/R_{obs} to one is expected as the enriched isotopes used for making the isotopic mixtures were calibrated by IDMS using natural Specpure Lithium as standard. The results of analysis of these mixtures validates the $NaLiBO_2^+$ method for measurement of lithium isotopic ratios over a wide range of ^{6}Li/^{7}Li ratio.

In addition to limited block measurement, TE & II mode of data acquisition was also carried out for all SLIMs 1 – 7 as a fractionation free $^{6}Li/^{7}Li$ ratio is possible using TE & II method. Column – 6 of Table 5.5 gives the fractionation factor $K_{ff} = R_{obs}/R_{TE}$ where R_{obs} is the $^{6}Li/^{7}Li$ determined by conventional method and R_{TE} the $^{6}Li/^{7}Li$ ratio measured by TE & II for the different synthetic mixtures. A very consistent ratio of K_{ff} was obtained over the wide range of $^{6}Li/^{7}Li$ isotope ratio of SLIMs. Average $K_{ff} = 1.0112 \pm 0.0015$ (0.15%) for SLIM - 1 to 7 demonstrates the reliability of the TE method over a wide range of $^{6}L/^{7}Li$ ratio.

The agreement of K_{ff} obtained for SLIM - 1 with the rest of the synthetic mixtures confirms that variation of R_{cal} from R_{obs} for SLIM - 1 seen in Table 5.5 is due to human error possibly while recording the weights of individual fractions of the enriched lithium solutions. The Table 5.5 also includes the fractionation factors (K_{ff}) obtained for L-SVEC lithium and Specpure Lithium recorded from conventional and TE analysis of the two natural Li samples. The Table also gives the isotopic ratios of L-SVEC (NIST- RM – 8545) and Specpure Lithium both having natural composition determined by Conventional and TE mode of acquisition. As can be seen the there is a very good agreement of Average $K_{ff} = 1.0112 \pm 0.0015$ of the seven SLIM's, $K_{ff} = 1.0106 \pm 0.0008$ of Specpure Lithium with K_{ff} of L-SVEC lithium which is 1.0105 ± 0.0010. The experiments establish the reliability of the procedure with $NaLiBO_2^+$ as monitoring ion for determining $^{6}Li/^{7}Li$ ratio in samples with varying ^{6}Li abundance. The constancy of $K_{ff} = R_{conventional}/R_{TE}$ over the range of $^{6}Li/^{7}Li$ ratios indicates that the fractionation profile does not change with $^{6}Li/^{7}Li$ ratios and therefore R_{TE} obtained for a unknown compound can be a good estimate of the true ratio.

Table 5.5. Results of K_{bias} and K_{ff} factors for various SLIMS

Blend No.	$^6Li/^7Li$ atom ratio			$K_{A/B}$ (K_{Bias})	$K_{B/C}$ (K_{ff})
	Theoretical calculation (A)	Ltd. Block Measurement (B)	TE & II (C)		
SLIM – 1	0.01095 ± 0.00003[#]	0.01087 ± 0.00004*	0.010755 ± 0.0003*	1.007 ± 0.004**	1.01 ± 0.03**
SLIM – 2	0.09580 ± 0.00029	0.09563 ± 0.00008	0.094532 ± 0.0002	1.002 ± 0.003	1.012 ± 0.002
SLIM – 3	0.28996 ± 0.00087	0.2899 ± 0.0002	0.286171 ± 0.0002	1.000 ± 0.003	1.013 ± 0.001
SLIM – 4	0.6366 ± 0.0019	0.6367 ± 0.00003	0.628684 ± 0.0003	1.000 ± 0.003	1.0127 ± 0.0005
SLIM – 5	1.1803 ± 0.0035	1.1796 ± 0.0006	1.1644 ± 0.0003	1.000 ± 0.003	1.0131 ± 0.0006
SLIM – 6	2.7429 ± 0.0082	2.7422 ± 0.0014	2.717912 ± 0.0003	1.000 ± 0.003	1.0085 ± 0.0005
SLIM - 7	6.6233 ± 0.020	6.618 ± 0.003	6.552864 ± 0.003	1.001 ± 0.003	1.0099 ± 0.0007
L-Svec (Li_2CO_3)	--------	0.08276 ± 0.00007	0.08190 ± 0.00005		1.010 ± 0.001
Specpure (Li_2CO_3)	--------	0.08311 ± 0.00004	0.08224 ± 0.00004		1.0106 ± 0.0007

[*]Std dev (1s) for four independent analysis; [**] propagated uncertainty

[#] The uncertainty in the ratios of the mixtures calculated from uncertainty for rest of the terms in the above equation

5.4. Conclusions

Seven isotope mixtures of lithium with varying ^{6}Li abundances were prepared by mixing known amounts of pre-calibrated pure ^{6}Li enriched solutions with ^{7}Li enriched solutions. The enriched isotopes were calibrated by IDMS using Specpure lithium as standard. These isotope reference materials were used to verify the constancy of fractionation factor over a wide range of $^{6}Li/^{7}Li$ determined by PTIMS using $NaLiBO_2^+$ as monitoring ion. The average bias factor for SLIM - 2 to 7 defined as $R_{calulated}/R_{observed}$ was 1.00057 (± 0.06%) which is very close to 1 as expected. The deviation of SLIM - 1 from this value was considered to be due to weighing errors during its preparation. The fractionation factor K_{ff} defined as $R_{observed}/R_{TE}$ for SLIM 1 to 7 = 1.0112 ± 0.0015 (0.15%) is in agreement with that of L-Svec =1.0105 ± 0.0010. A similar fractionation profile is obtained irrespective of the $^{6}Li/^{7}Li$ isotopic ratio and this observation underlines the fact that the $NaLiBO_2^+$ a reliable monitoring ion for determination of $^{6}Li/^{7}Li$ isotope ratio by TIMS. The consistency of K_{ff} for wide ratios authenticates the use of TE & II for determination of $^{6}Li/^{7}Li$ ratio in different samples as a good estimate of the true value.

Chapter 6

Fusion method for isotopic analysis of lithium and boron in refractory materials employing molecular ions

6.1. Introduction

Precise isotopic measurement of lithium or boron in various chemical compounds such as Li_2CO_3, LiOH, $Li_2B_{10}O_{16}$, $LiAlO_2$, Li_2TiO_3, H_3BO_3, B_2O_3, B_4C, TiB_2, LaB_6, CeB_6, ZrB_2 etc. is required in nuclear industry. Isotopic analysis of any element by TIMS requires the sample to be in the solution, possibly in its purest chemical form. Among the various chemical compounds, oxy-compounds of lithium and boron are easily soluble in water. A few µL solution containing 1 – 2 µg of the Li or B sample is mixed with calculated proportion of sodium borate or sodium carbonate respectively. By loading this mixture on rhenium single filament assembly and monitoring $NaLiBO_2^+$ and $Na_2BO_2^+$ molecular ions, precise isotopic measurement can be easily carried out. On the other hand, isotopic analysis of lithium and boron in refractory materials is tedious due to the difficulty associated with their dissolution. Conventionally alkali fusion, microwave assisted acid digestion are the techniques being used for the dissolution of refractory materials. There are some reports about the use of pyro-hydrolysis for extraction of boron from refractory materials [184 - 186]. Although these methods are reliable for ensuring the complete dissolution of the refractory materials or extraction of boron, they involve a number of steps and large quantities of reagents which make the sample processing laborious and can increase the reagent blank.

Instead of adding the alkali borate (alkali carbonate) to the dissolved sample solution of lithium (or boron), our laboratory has already explored the feasibility of addition of the sodium carbonate to the boron powder sample and directly fusing the sample slurry on the rhenium filament by heating it to red hot. Though this direct fusion method has been applied to boron carbide and acid leached irradiated TiB_2 chunk samples, the suitability of this method to the analysis of refractory lithium samples was to be still explored. Apart from that, adoption of this direct fusion for the isotopic ratio analysis of boron in some of the boron alloy

compounds and lanthanide borides has shown some erratic experimental results. So, present chapter describes the implementation of direct fusion to the refractory lithium compounds ($LiAlO_2$ and Li_2TiO_3) and the details of the challenges faced during the analysis of some of these different refractory boron powder samples using the direct alkali fusion method and also necessary modifications taken to overcome the difficulties.

In order to validate the fusion method used for formation and analysis as $Na_2BO_2^+$ in these refractory materials, the mass spectrometric measurements of the direct fusion method were compared with data obtained from analysis of the dissolved samples of these refractory powders and the purified fractions of boron extracted using 5% 2-Ethyl Hexane 1, 3 Diol (EHD) in chloroform. On the other hand, Total Evaporation and Ion integration (TE & II) method was carried out for the validation of the direct fusion method for the refractory compounds ($LiAlO_2$ and Li_2TiO_3) of lithium.

6.2. Experimental

6.2.1 Reagents and Materials

NIST – RM - 8545 (L-SVEC Li_2CO_3) and NIST – SRM – 951 (H_3BO_3) isotopic standards of lithium and boron respectively were used to check the performance of the methodology. $LiAlO_2$ (Alfa Aesar), Li_2TiO_3 (Sigma Aldrich), high purity analytical grade Na_2CO_3, 2-Ethyl hexane 1, 3 diol (EHD) and high purity acids procured from Merck were used. All the experiments were carried out using quartz beakers and separating funnels after leaching with 3M HNO_3. 1" X 1" inch Teflon sheets with a thickness of 0.2mm were used for treatment of lithium and boron samples prior to mass spectrometric analysis. For all the dilutions freshly deionized water (18.2 MΩ cm) obtained from a milli Q system was used. Various refractory materials of boron analyzed in this study are listed in Table 6.1. These were prepared in-house

by various pyrometallurgical routes. The details of the preparation for these samples are reported elsewhere [55 - 60].

Table 6.1. Refractory compounds of boron and their details

Sample	**Elemental composition**	**Form**	**Source**
B_4C	B-major, C	Pebble	Pvt. industries and In-house
B_4C	B-major, C	Crystalline	
LaB_6	La, B, C, O	Fine Powder	In-house
ZrB_2	Zr, B, C, O		
CeB_6	Ce, B, C, O		
TiB_2	Ti, B		
B-alloy-1	Ti major, Cr, Mo, B, C, Si, Fe, Ta, O		
B-Alloy-2	Ti major, Cr, Mo, B, C, Si, Fe, Ta, O		

6.2.2 Dissolution of boron samples

Around 0.1 g of each of these boron powder samples were fused with about 1.0 g of sodium carbonate for 2 hours in a platinum crucible uisng Bunsen burner. The fused mixture was allowed to cool and then leached in hot water. Digestion of these samples were carried out in a water bath maintained at 60°C and filtered to obtain the dissolved sample solution.

6.2.3 Separation of boron by EHD extraction

Dissolved solutions of the samples like LaB_6, CeB_6, TiB_2 and ZrB_2, B_4C were subjected to EHD extraction. 10 mL of solution of the dissolved boron acidified with 1M HNO_3 was equilibrated with 2 mL of 5% EHD in chloroform in a quartz separating funnel. After

equilibration for about 5 minutes, organic layer containing boron extracted as $B(OH)_3.2EHD$ complex was transferred into a quartz beaker after phase separation.

6.2.4 Instrumentation and Mass spectrometric analysis

TIMS instruments viz. Isoprobe - T and TRITON-PLUS each equipped with 9 movable faraday cups for the simultaneous multi-collection of ions were employed for the present work. TRITON-PLUS has 1 SEM for analysis of minor isotopes and a functional TE & II mode of acquisition in the software. Mass Spectrometric measurement has been carried out for isotopic composition of lithium and boron by monitoring $NaLiBO_2^+$ and $Na_2BO_2^+$ molecular ions respectively using two modes of data acquisition i) limited block measurement with 3 – 5 block data (each block consists of 12 scans) and ii) Total Evaporation and Ion Integration.

The details of the loading and treatment procedures along with the data acquisition parameters for limited block measurements of both the methods are given in Table 6.2. The details of TE & II mode of data acquisition are as given in section 4.2.2. of Chapter 4.

6.3. Results and Discussion

6.3.1 Refractory boron powder samples

Boron carbide samples are often available in different physical forms such as fine powder, crystalline powder and pebble forms as shown in Fig. 6.1. Initial experiments were carried out for the optimization of mole ratio of B/Na for the B_4C fine powder samples by varying B/Na from 5 to 0.5. Data acquisition was carried out at low filament currents (LFC ~ 1.3 A) and high filament currents (HFC ~ 1.7 A) in order to check the severity in the isotopic fractionation between the isotopes of boron. As seen from the Fig. 6.2, similar to the oxy

Table 6.2. Details of loading and treatment procedures & data acquisition parameters for limited block measurements of TIMS analysis

S. No.	Type of Sample	Treatment Procedure
1.	**Refractory Boron Powder samples**	About 5 mg of boron sample powder was taken on Teflon sheet and sodium carbonate solution was added in such a way that mole ratio of B/Na was in the range 5 to 0.5. A few µL of this slurry containing about 2 µg of boron was pipetted out and loaded on to the centre of the rhenium filament.
2.	**Dissolved boron samples**	5 µL of solution containing 2 to 3 µg of boron was directly transferred to the centre of the rhenium filament by means of a micro-pipette. After heating the loaded filament to red hot and the filament current brought down to zero ampere, about 2 – 3 µL of graphite (40 mg of graphite in 1 mL of 50% ethanol-water mixture) slurry was deposited on the filament and dried at 1.0 Amp current.
3.	**Purified Boron fractions**	The organic solvent, CH_3Cl was vaporised under the IR lamp leaving 100 µL of EHD containing the purified boron fractions in the quartz beaker. Millipore water treatment was given repeatedly to remove traces of dissolved acid. Sodium carbonate and mannitol solution were added so that the B/Na mole ratio was about 0.1 and mannitol/boron amount ratio about forty. This solution mixture was further heated for about 15 minutes on hot pate to decompose the EHD. The residue was dissolved in 20-50 µL of Millipore water. A few µL of this solution containing about 2 µg of boron was pipetted out onto the centre of rhenium filament. Graphite was deposited of the filament after heating the sample filament to red hot.
4.	**$LiAlO_2$ and Li_2TiO_3**	About 5 mg of lithium sample powder was taken on Teflon sheet and sodium borate solution was added in such a way that mole ratio of Li/Na ~ 1; B/Na ~ 10. A few µL of this slurry containing about 2 µg of lithium was pipetted out and loaded on to the centre of the rhenium filament and heated to red hot.
5.	Loading	5 µL of the lithium borate solution or sodium lithium borate solution, containing 1.5 – 2 µg of lithium was loaded on the zone refined Rhenium (single) filament and evaporated to dryness at 1Amp current.

		Filament was further heated to 1.8A and held for 5 minutes and slowly heated to red hot for formation of the required alkali borate.	
TIMS analysis			
	Condition	**$Na_2BO_2^+$**	**$NaLiBO_2^+$**
6.	Degassing	After achieving a sufficient vacuum in the ion source housing, the samples were degassed at 1.0 Amp for about 5 to 10 minutes	
7.	Initial focusing	Ion current of ^{23}Na	
8.	Ions monitored @ mass m/Z	$Na_2BO_2^+$ (88 – 89) $^{88}I/^{89}I$	$NaLiBO_2^+$ (71 -73) $^{72}I/^{73}I$ and $^{73}I/^{71}I$ and $^{72}I/^{71}I$ $Na_2BO_2^+$ (88 – 89) $^{88}I/^{89}I$ recorded for independent determination of IC of boron.
9.	Data acquisition parameters	Peak centre, Auto focus, Baseline @ ± 0.5 a.m.u of the isotope of interest prior to the acquisition Integration time is about 5 seconds per each scan, 12 scans are grouped in to a block 3 – 5 block data was recorded for the measurement	
		Simultaneous multi-collection of all ^{88}I and ^{89}Iin each scan	Two sequences were carried out per scan by peak jumping mode Sequence 1: Simultaneous multi-collection of 71, 72 and 73 Sequence 2: Simultaneous multi-collection of 88 and 89

compounds of boron, refractory powders of B_4C also showed ~ 0.2% variation in the isotopic ratio with the change in the mole ratio of B/Na.

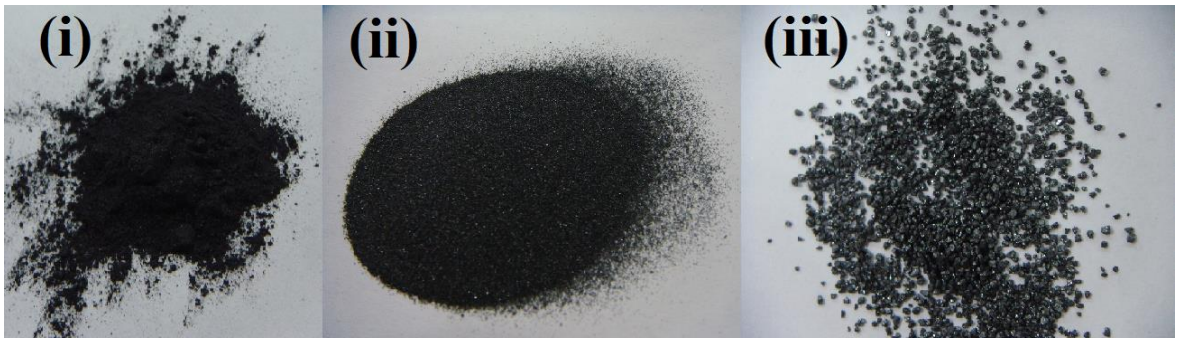

Fig. 6.1 Various forms of B_4C (i) fine powder (ii) Crystalline powder (iii) Pebbles

To understand the reason for the variations observed in the isotopic ratio of $^{10}B/^{11}B$ with the change in the mole ratio of B/Na, various sodium containing buffers effective in the pH range of 3 to 9 were employed, instead of the conventionally used sodium carbonate for formation of $Na_2BO_2^+$ ions in the ion source [172]. The use of buffer solution was to provide insights on the role of pH and B/Na mole ratio on the experimentally observed $^{10}B/^{11}B$ ratio. From the studies, it was concluded that, the foremost reason for variations in the isotopic ratio of $^{10}B/^{11}B$ is the amount of Na present as Na_2O on the filament i.e., the B/Na stoichiometry in the sodium borate compound formed on the filament. The outcome of this work has given us a better understanding of the experimental parameters that effect the $^{10}B/^{11}B$ isotopic ratio and procedures that have to be adopted to improve its precision during analysis of boron as $Na_2BO_2^+$ by P-TIMS [172]. Drop deposition of graphite after loading of the boron sample is required when the B/Na stoichiometry in the sodium borate compound is 0.5 or less (e.g. $2Na_2O.B_2O_3$) which would act as a reducing agent to form less volatile compounds of sodium borate.

From Fig. 6.2, it was observed that the difference in the analytical spread in the $^{10}B/^{11}B$ isotope ratios at mole ratio of B/Na 2 and 0.5 was very small when acquisition is carried out at high and steady intensity of the ion beam (2 x 10^{-11} A at m/z 89). A steady ion beam resulted in an internal precision of better than 0.01% in most cases. Therefore, to avoid the use of graphite, B/Na 2 was found suitable for routine analysis. The same strategy has been adopted for other forms of B_4C, crystalline powder and pebbles and the other refractory boron powder samples mentioned in Table 6.1. The B_4C pebbles were ground to fine powder before treatment. Enriched sample of B_4C was also analysed during the present investigations. The results of triplicate analysis of the different samples are shown in Fig. 6.3.

As can be seen the $^{10}B/^{11}B$ ratio for two samples ZrB_2 and LaB_6 were marginally higher than the isotope abundance ratio of natural Boron and in the case of CeB_6 and TiB_2 the $^{10}B/^{11}B$ were about 5% higher than expected data. All these samples were analysed with a precision better than 0.02%. During the analysis of two other alloy samples, we observed a steady increase in the$^{10}B/^{11}B$ ratio with time as well as with filament current contradictory to reverse trend normally observed. This continuous fractionation observed for the boron alloy resulted in very poor internal precision. Further investigations were carried out to resolve these discrepancies and ensure the authenticity of the fusion process followed for refractory compounds.

Case (i):

In the thermal ion source, the mass dependent isotope fractionation causes the lighter isotope to evaporate at a faster rate than that of heavier isotope leading to continuous decrease in the observed $^{10}B/^{11}B$ isotopic ratio due to the depletion of ^{10}B in the sample residue with time. However, a contradictory behaviour was observed for the two boron alloy samples

wherein the $^{10}B/^{11}B$ isotope ratios increased continuously with both time and filament current (Fig. 6.4a & 6.4b). This resulted in very poor internal precision of 5% during a single analysis.

The reason for this trend in the fractionation pattern is attributed to incomplete fusion of sample with sodium carbonate during loading stage. Other than Titanium, these alloys contained hard metals such as Cr, Mo, Ta (see Table 6.1) to increase the refractory character of these materials which possibly prevented complete fusion of the sample with the sodium carbonate. In all probability under the high vacuum and temperature conditions of the ion source the fusion process progresses further to form fresh sodium borate. This explains the observed fractionation behavior of increasing $^{10}B/^{11}B$ ratio as the fusion progresses. Increasing the sodium carbonate so that B/Na mole ratio was about 0.5 during fusion, had no effect on the fractionation pattern. The fusion method was further modified, wherein excess sodium as sodium carbonate was added such that B/Na was about 0.1. This step was carried out to make the fusion environment sufficiently alkaline to ensure complete reaction of the boron-based alloys in the sample with sodium carbonate during the loading stage. The fusion mixture was loaded on the filament and dried at 1 A and then raised to 1.8 A where it was kept on hold for 5 minutes. The filament was then heated to red hot and instantaneously brought down; this action was repeated twice for formation of homogenous melts. To avoid the formation of sodium rich borates such as $Na_4B_2O_5$ which are volatile in nature, the loaded filament was coated with graphite layer to reduce the excess sodium oxide. About 120 µg graphite in 2 µl of 1:1 ethanol was loaded on the filament and dried by passage of 1 A current through the filament for 5 min. The results of this modified treatment and loading procedures can be seen from the stable ratio obtained for the alloy shown in Fig. 6.5. The 100-scan data acquired at ^{89}I intensity of 2×10^{-11} A, gave a precision of 0.02%. Heating the filament further did not change the $^{10}B/^{11}B$ ratio.

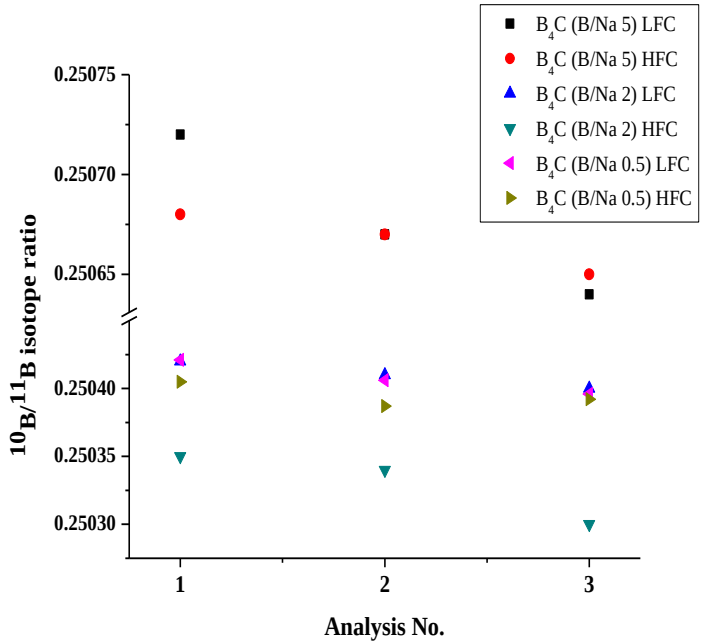

Fig. 6.2 Measured $^{10}B/^{11}B$ ratio in B4C powder at B/Na mole ratio 0.5 to 5

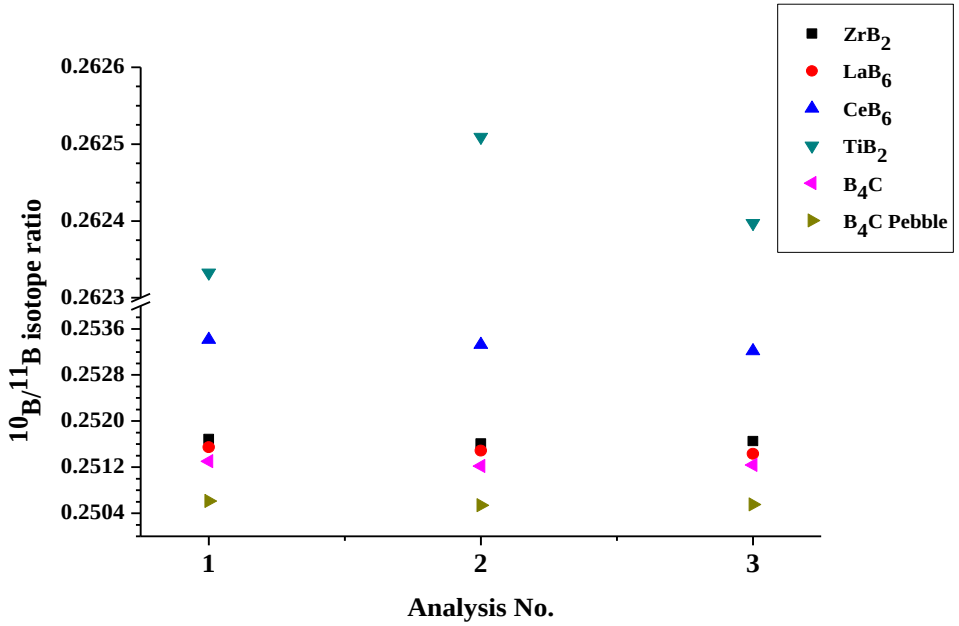

Fig. 6.3 $^{10}B/^{11}B$ ratios in different refractory boron powders at B/Na mole ratio 2.

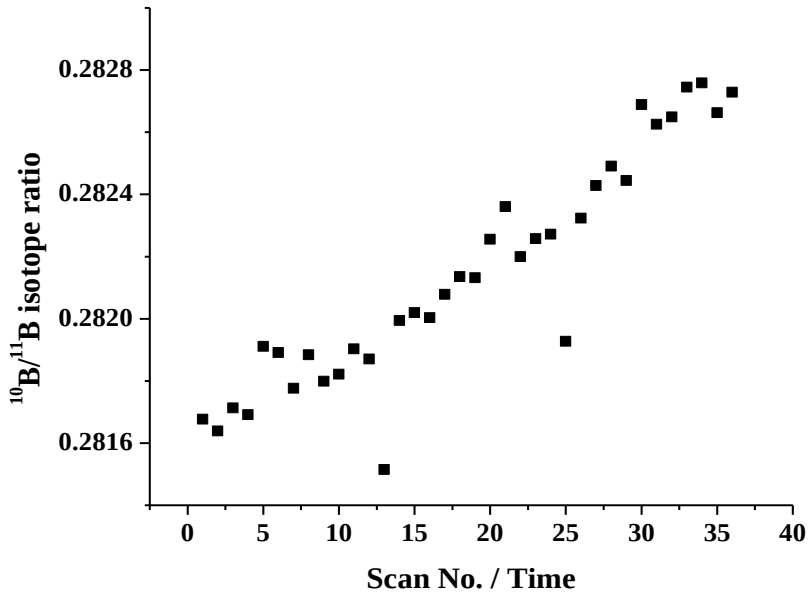

Fig. 6.4a Reverse fractionation resulting in increasing $^{10}B/^{11}B$ ratios with scan no. for boron alloy sample. Fusion of sample with Na_2CO_3, B/Na mole ratio 2.

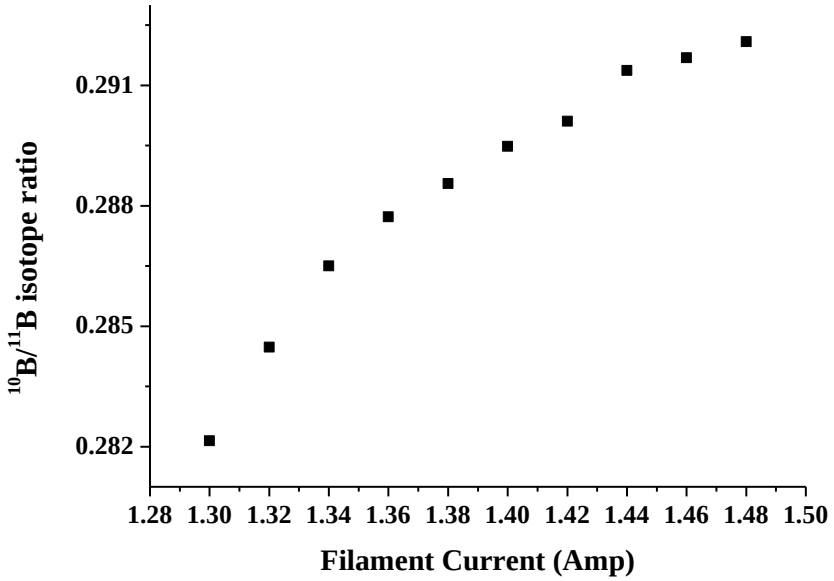

Fig. 6.4b Boron alloy sample showing reverse fractionation resulting in increase in $^{10}B/^{11}B$ ratio with filament current. Fusion of sample with Na_2CO_3, B/Na mole ratio ~ 2.

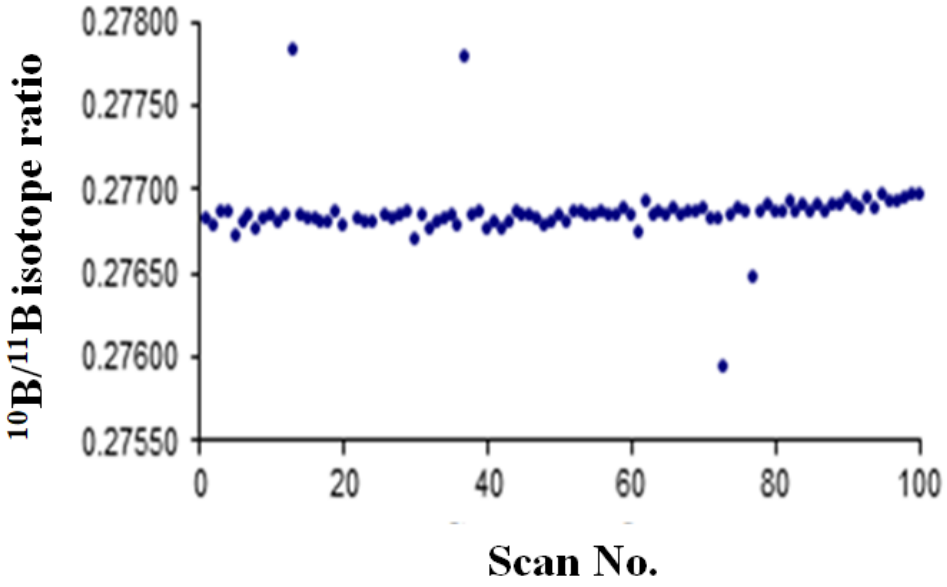

Fig. 6.5 100 Scans of B-alloy, B/Na mole ratio optimized at 0.1

Case (ii)

As mentioned in the previous section the isotopic composition of boron in LaB_6, ZrB_2 and B_4C showed natural variations, ^{10}B from (18.8% to 20.1%), whereas some other borides such as CeB_6 and TiB_2 showed unexpectedly higher values of $^{10}B/^{11}B$ with ^{10}B content as high as 21.7%. The measured values of $^{10}B/^{11}B$ were not affected by changing the B/Na ratio from 2 to 0.1. Further studies were therefore carried out to investigate whether this variation in the ratio was due to the direct fusion process followed during loading of these refractory samples or as a result of the synthesis processes involved in the formation of these compounds from their starting materials and therefore inherent to sample. To understand the reasons for the bias, both dissolved samples of the refractory compound and the purified boron samples were analyzed by TIMS. Analysis of dissolved samples would help to understand if the reason for observed bias was due to incomplete fusion. Also, to ensure that the observed deviation in the isotopic ratios is not matrix induced, the dissolved samples were subjected to solvent extraction of boron with 5% EHD in chloroform. The detailed procedures for the dissolution

of the refractory boron powders, solvent extraction and the respective treatment and the loading procedures listed in the sections 6.2.2 and 6.2.3 of this chapter. Table 6.3 compares the mass spectrometric results obtained for the samples carried out by these two procedures with the direct fusion method. The $^{10}B/^{11}B$ isotopic ratios of the NIST isotopic standard SRM-951 and Natural Boric acid (Merck) in the dissolved compound and after extraction with EHD are also given. The $^{10}B/^{11}B$ ratios for all the samples listed in the Table 6.3 obtained by the three procedures are in good agreement with each other. All the three treatment and loading procedures show similar deviation from natural $^{10}B/^{11}B$ ratio [187]. This signifies that the measured data is intrinsic to the sample itself and is neither matrix induced nor due to faulty treatment procedure. The investigations reaffirm the utilization of TIMS as reference technique for measurement of isotopic composition in various materials using appropriate loading techniques for different types of boron compounds.

Table 6.3. Comparison of $^{10}B/^{11}B$ ratio of various samples analysed by direct fusion, after sample dissolution and in the purified boron fraction of the respective samples

Sample	$^{10}B/^{11}B$ isotopic ratio (r.s.d 1σ)		
	Direct Fusion	Dissolved solution	Separated fraction using EHD in $CHCl_3$
SRM-951*	---	0.24761(0.01%)	0.24748(0.02%)
Nat H_3BO_3		0.2506(0.01%)	0.2503(0.02%)
LaB_6	0.2514(0.02%)	0.2512(0.03%)	0.2516 (0.04%)
TiB_2	0.2642(0.02%)	0.2643(0.04%)	0.2641 (0.03%)

CeB_6	0.2535(0.02%)	0.2532(0.03%)	0.2533 (0.03%)
B_4C	0.2505(0.01%)	0.2504(0.02%)	0.2504(0.03%)
B_4C	2.139 (0.02%)	2.134 (0.04%)	2.143(0.02%)

*$^{10}B/^{11}B$ isotopic ratio of NIST SRM – 951 = 0.2473 (0.08%)

6.3.2 For refractory Lithium powder samples

6.3.2.1. Limited Block Measurement

Based on the methodology developed for L-Svec Lithium standard, as mentioned in chapter 3, refractory powder samples of $LiAlO_2$ (Alfa Aesar) & Li_2TiO_3 (Sigma Aldrich) were analysed for $^6Li/^7Li$ using $NaLiBO_2^+$ molecular ions by limited block measurement mode of data acquisition. The samples were analysed using the three different sodium borate compounds having B/Na stoichiometry of 2, 5, 10 for fusion with the refractory materials. Sample amount containing about 1.5 µg of lithium was fused with the fusing agent so that the Na/Li mole ratio ~1 in the fusion mixture. Graphite had to deposited on the filament when the sample was fused with sodium tetraborate to obtain moderately stable ion intensities of $NaLiBO_2^+$, $Na_2BO_2^+$. Fusion with sodium pentaborate or sodium decaborate, did not require graphite for obtaining stable ion intensity ratios. The acquisition was carried out when the ion currents of $^{73}I \sim 0.5 \times 10^{-11}$ A and $^{89}I \sim 1 \times 10^{-11}$ A. Table 6.4 gives the $^{72}I/^{73}I$ and $^{10}B/^{11}B$ ratio determined for the two refractory compounds using the three forms of sodium borate for fusion. Sodium borate with B/Na ratio of 20, yielded low $NaLiBO_2^+$ ion intensity for lithium titanate, though for lithium aluminate fairly stable ion intensities for $NaLiBO_2^+$, $Na_2BO_2^+$ were obtained. Best results were obtained when sodium borate with B/Na ratio in the range 5 to 10

was used as fusion reagent. Average $^{6}Li/^{7}Li$ ratios, from three determinations using the three different sodium borate compound as fusing agent is shown in the Table 6.4. External precision of better than 0.07% was obtained for the $^{6}Li/^{7}Li$ ratio determined in $LiAlO_2$ & Li_2TiO_3. The isotopic composition of the starting material for synthesis of the refractory compound i.e. Li_2CO_3 are also given in the Table 6.4.

Table 6.4. Lithium and boron IC determined in Li_2TiO_3, $LiAlO_2$, $Li_2B_{10}O_{16}$ and Li_2CO_3

Lithium compound	Sodium compound used for fusion	Li/Na ratio	$^{72}I/^{73}I$	$^{10}B/^{11}B$ ratio as $Na_2BO_2^+$	$^{6}Li/^{7}Li$ (From Eqn. 3.5)
*Li_2TiO_3 (SigmaAldrich)	$Na_2B_4O_7$	1	0.32802	0.24623	0.08188
Li_2TiO_3	$Na_2B_{20}O_{31}$	1	0.33340	0.25164	0.08185
Li_2TiO_3	$Na_2B_{10}O_{16}$	1	0.33289	0.25118	0.08181
				Avg	**0.08185 ± 0.00004**
*$LiAlO_2$ (Alfa aesar)	$Na_2B_4O_7$	1	0.32993	0.24702	0.08301
$LiAlO_2$	$Na_2B_{20}O_{31}$	1	0.33441	0.25163	0.08288
$LiAlO_2$	$Na_2B_{10}O_{16}$	1	0.33389	0.25104	0.08295
				Avg	**0.08295 ± 0.00006**
Li_2TiO_3-a	$Na_2B_{20}O_{31}$	1	0.32964	0.24800	0.08174 ± 0.00011#
Li_2TiO_3-b	$Na_2B_{20}O_{31}$	1	0.33031	0.24808	0.08232 ± 0.00012
Li_2CO_3 (Merck)	$Na_2B_{20}O_{31}$	1	0.33017	0.24807	0.08220 ± 0.00009
Li_2CO_3 (SigmaAldrich)	$Na_2B_{20}O_{31}$	1	0.33031	0.24803	0.08238 ± 0.00012
Li_2CO_3 (Alfa aesar)	$Na_2B_{20}O_{31}$	1	0.33095	0.24790	0.08315 ± 0.00011
Li_2CO_3 (L-Svec)	$Na_2B_{20}O_{31}$	1	0.33075	0.24802	0.08282 ± 0.00012

* Graphite loaded on the filament after fusion

Propagated error from Eqn. 3.5

Small differences in the ratio between the ceramic compounds and starting material could be the due to the chemical processes involved in the formation of the compound. The table also gives the results of two additional Li_2TiO_3 samples which were analysed after fusion with $Na_2B_{20}O_{31}$. In all these samples both $^{72}I/^{73}I$ and $^{10}B/^{11}B$ ratio were measured with precision better than 0.03% for 3 blocks of 36 scans [166].

6.3.2.2. Validation of direct fusion method of loading for refractory compounds of lithium using TE & II mode of acquisition

TE & II mode of acquisition wherein the isotopes are simultaneously collected in multi-collector assembly till the sample on the filament is completely exhausted results in fractionation free isotopic ratios. In TIMS since fractionation is the major cause of bias, the isotope ratios obtained by TE are expected to be close to the true value. In chapter 4, we have seen that the fractionation profile for lithium evaporating as molecular species is in accordance with the theoretical prediction (Rayleigh distillation Law) and the $^6Li/^7Li$ ratio determined from TE and II shows a close representation of true ratio. In order to check the reliability of the direct fusion method adopted for loading the lithium refractory powder samples on the single Re filament assemblies, these samples were also analysed by TE & II mode of acquisition. The developed direct fusion method could be validated if the K_{ff} (fractionation factor) ($K_{ff} = [^6Li/^7Li]_{Conventional} / [^6Li/^7Li]_{TE}$) i.e. conventional limited block measurement Vs TE & II method for refractory materials is in agreement with L-SVEC Li_2CO_3 results [188]. The experiments involved five repeated analyses of Li_2TiO_3 and $LiAlO_2$ results of which are tabulated in Table 6.5.

Table 6.5. Comparison of $^{6}Li/^{7}Li$ ratio in different lithium compounds obtained from conventional and TE methods

Lithium compound	$^{6}Li/^{7}Li$ ratio (I) Conventional	$^{6}Li/^{7}Li$ ratio (II) TE & II	K factor (I/II)
L-Svec Li_2CO_3	0.08275 ± 0.00006*	0.08190 ± 0.00005*	1.0104 ± 0.0010**
Specpure Li_2CO_3	0.08311 ± 0.00004	0.08224 ± 0.00004	1.0106 ± 0.0008
Li_2TiO_3	0.08181 ± 0.00004	0.08086 ± 0.00004	1.0117 ± 0.0006
$LiAlO_2$	0.08299 ± 0.00005	0.08232 ± 0.00004	1.0081 ± 0.0007

*Uncertainty 1 σ from multiple analyses. ** propagated from I and II

The sample size of the refractory material to obtain steady ion current required for obtaining good analytical precision during conventional acquisition should contain at least 1.5 µg of lithium, whereas 500 ng of lithium was sufficient for obtaining reproducible results by TE & II. K_{ff} obtained for the two different refractory compounds analysed by both conventional and TE & II methods were in agreement with that obtained for L-SVEC Li_2CO_3. This indicated that fusion process opted for loading of the refractory material produces a homogeneous mixture of lithium and $^{6}Li/^{7}Li$ obtained by TE & II, a representation of the true value which is an essential requirement in the nuclear industry. This is depicted in Fig. 6.6, the average K factor = 1.0102 ± 0.0015 obtained for the different compounds of lithium implies that the fractionation profile is independent of the form of lithium compound and can be reliably used to differentiate between lithium compounds on the basis of natural variation in their $^{6}Li/^{7}Li$ ratios. The TE & II mode of acquisition therefore validated the use of direct fusion method for analysis of refractory materials of lithium. The other known benefits of TE & II being

improved sensitivity (minimum amount of sample required for analysis) and accuracy of the molecular ion method resulting in $^{6}Li/^{7}Li$ ratios with reduced uncertainty.

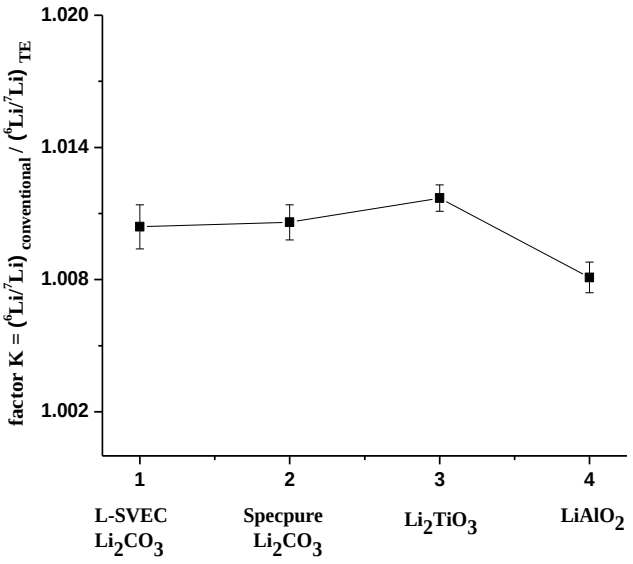

Fig. 6.6 The average fractionation factor K = 1.0102 ± 0.0015 obtained for the different lithium compounds shows that the fractionation profile is independent of the form of lithium compound.

6.4. Conclusions

Isotopic analysis of lithium and boron in refractory materials by the direct fusion method resulted in precise $^{6}Li/^{7}Li$ and $^{10}B/^{11}B$ ratios respectively. Agreement of the $^{10}B/^{11}B$ isotope ratio obtained by the direct fusion method with the $^{10}B/^{11}B$ isotopic ratio in dissolved samples as well as in the purified boron fraction of the respective samples has validated the direct fusion method as a rapid method for obtaining a homogenous solution of the refractory material during loading resulting precise $^{10}B/^{11}B$ ratio [187].

Agreement of the fractionation pattern of the refractory samples of lithium with NIST – RM - 8545 (L - SVEC Li_2CO_3) authenticated the use of direct fusion method as a rapid

analysis technique for precise analysis of lithium in refractory materials. This is demonstrated by the concurrence of the K factor ($K = [^6Li/^7Li]_{Conventional} / [^6Li/^7Li]_{TE}$) obtained for the refractory samples of lithium with the NIST – RM - 8545 (L - SVEC Li_2CO_3) [188]. The experiments authenticated the use of direct alkali fusion method as faster and reliable method for obtaining accurate and precise isotopic ratios in refractory samples of lithium & boron and thereby increasing sample throughput.

Chapter 7

Conclusions & Future Scope

7.1. Summary

The present dissertation focuses on the application of molecular ions for the development of robust methodologies for the precise and accurate isotope ratio measurement of lithium and boron using Thermal Ionization Mass Spectrometry. Both B and Li are preferably analysed as alkali meta borate ($M_2BO_2^+$, where M is Li, Na, Rb, Cs) ions owing to their higher molecular weight compared to the atomic ions. B cannot be analyzed as B^+ by TIMS due to its high first Ionization Potential (8.3 eV). Molecular ions such as $Na_2BO_2^+$, $Rb_2BO_2^+$, $Cs_2BO_2^+$ are used for the isotope ratio determination of boron. Though atomic ions of lithium (Li^+) have high sensitivity in the thermal ion source, stringent analysis conditions with respect to sample amount, the type of lithium compound, loading conditions and high level of operator skills of the analyst are required for obtaining high precision and accuracy in the $^6Li/^7Li$ isotope ratio. Analysis of Lithium using $Li_2BO_2^+$ molecular ion offers an alternative methodology for the thermal ionization mass spectrometric analysis of lithium. However, the accuracy in the isotope ratio of lithium is compromised since the fractionation of boron isotopes during analysis is not accounted and the value of the boron isotopic standard is directly used.

The aim of this thesis was to develop a robust methodology for precise and accurate isotope ratio analysis of lithium and validate the developed methodology using Synthetic Lithium Isotope Mixtures (SLIMs) having a wide variation in the atom percent abundance of ^6Li, prepared using calibrated fractions of enriched ^6Li and ^7Li solutions. The studies included experiments to explore the feasibility of adopting Total Evaporation and Ion Integration method to improve the sensitivity and accuracy of the molecular ion method. In addition to this, the application of direct fusion method, for loading of various refractory samples of lithium and boron using sodium borate and sodium carbonate as fusing agent respectively, for analysis using alkali meta borate ions was successfully carried out to give precise isotopic ratios

thus avoiding tedious sample dissolution procedures. The method was validated by carrying out analysis of dissolved as well as purified samples of Boron. The fused lithium samples were analysed by both conventional limited block as well as TE & II to compare the fractionation profile of sample with L-Svec lithium standard. Agreement among the K_{ff} values ($^{6}Li/^{7}Li_{conventional}$ /$^{6}Li/^{7}Li_{TE}$) would help to establish the reliability of the fusion technique used.

7.2. Conclusions

The focus of Chapter 3 was to develop a method for the simultaneous determination of $^{6}Li/^{7}Li$ ratio and $^{10}B/^{11}B$ ratio using the polyatomic molecular ion $Li_2BO_2^+$. This was necessary to account for contribution of $^{10}B/^{11}B$ ratio in the evaporating $Li_2BO_2^+$ ion, which was used for determination of $^{6}Li/^{7}Li$ ratio. A pair of polyatomic molecular ion ratios (R_i & R_j) were monitored instead of a single ratio R_i. As the polyatomic molecular ion ($Li_2BO_2^+$) is the combination of both lithium and boron, by solving the two equations generated from the pair of ratios R_i & R_j, simultaneous measurement of isotope ratios of both lithium and boron was carried out. However, it is obvious that the uncertainty in the final lithium or boron isotope ratio will be affected by propagation of the experimental uncertainties in the measured ratios R_i & R_j which depends on their specific isotope abundance distribution pattern. In this context, a detailed study was carried out for the selection of a pair of combination of two molecular ratios based on the magnitude of Relative Uncertainty Magnification Factors. The same criteria were applied for the various combinations of atom percent abundance of ^{6}Li and ^{10}B. Though this simultaneous measurement of lithium and boron improved the measurement accuracy, this method requires rigorous mathematical calculations in selecting the specific combination of a pair of polyatomic molecular ion ratios depending on the level of enrichment of ^{6}Li in the sample.

Alternate to alkali metaborate ion ($Li_2BO_2^+$), the application of mixed alkali borate ions ($NaLiBO_2^+$) for accurate isotope ratio measurement of lithium is also described. Of the two molecular ions studied, it was concluded that $NaLiBO_2^+$ used as monitoring ion for measurement of lithium isotopic ratio has the following advantages: i) higher mass numbers of $NaLiBO_2^+$, m/z 71 to 73 than $Li_2BO_2^+$ monitored m/z 54 to 57 which reduces the severity of ion-source isotope fractionation ii) as sodium is deliberately added for the formation of sodium lithium borate, there is a relatively high tolerance of sodium in the sample iii) contribution from isotopes of boron can be accounted from in situ measurement of $^{10}B/^{11}B$ ratio obtained from $Na_2BO_2^+$ ion (m/z 88, 89) also formed along with $NaLiBO_2^+$. Using this $NaLiBO_2^+$ method, it was possible to distinguish between the two lithium compounds (L-Svec Li_2CO_3 (NIST – RM – 9545) and Specpure Li_2CO_3) of natural origin with a difference of 0.5% in the $^6Li/7Li$ isotope ratio.

However, in spite of the several advantages offered by the developed $NaLiBO_2^+$ molecular ion method it cannot be directly adopted by various other fields of interest such as the geology, paleoceanography, as it is not as sensitive as atomic ions method, since it requires at least 2 µg amount of lithium on the filament. This shortcoming was addressed in chapter – 4, by the application of Total Evaporation and Ion Integration (TE & II) technique wherein, the ions emitted from the heated filament are simultaneously collected and integrated in multi-collector assembly till the sample is completely exhausted. With a precision of 0.1% in the $^6Li/^7Li$ ratio for 500 ng of lithium, TE & II mode of acquisition, improved both sensitivity and accuracy of the $NaLiBO_2^+$ method.

Reliability of isotope measurement of any new method has to be validated over a wide range of isotopic abundances. In this context, Synthetic Lithium Isotopic Mixtures (SLIMs) with varying isotopic abundances of ^6Li: 1%, 8%, 20%, 35%, 50% and 85% were prepared and analysed under the optimized conditions to assess the performance of the

$NaLiBO_2^+$ molecular ion method over a wide $^6Li/^7Li$ isotopic ratio. The experimental details are described in chapter – 5. Samples (SLIMs) were analysed using conventional limited block measurement as well as by TE & II methods. An average K factor ($K = [^6Li/^7Li]_{conventional} / [^6Li/^7Li]_{TE}$) $K_{SLIMs} = 1.0112 \pm 0.0015$ (0.15%) was obtained for all SLIMs which shows a very good agreement with the $K_{L\text{-}Svec} = 1.0105 \pm 0.0010$, obtained from replicate analysis of NIST – RM - 8545 (L - SVEC Li_2CO_3). The experiments established the reliability of the $NaLiBO_2^+$ methodology for measurement of wide range of $^6Li/^7Li$ isotope ratio.

For isotopic analysis of Boron and Lithium in refractory samples a sample dissolution step is normally required for analysis by TIMS. In chapter – 6, a direct fusion method developed for isotopic analysis of B and Li in the refractory samples was described. The refractory powder samples were directly fused with sodium borate and sodium carbonate respectively on the filament itself. This helped in avoiding the elaborate dissolution and purification procedures. The results of direct fusion method were validated by comparing the experimental results with the $^{10}B/^{11}B$ ratios determined in dissolved and purified samples of these boron-based refractory samples. For lithium based refractory samples the consistency of the K- factor i.e. ($K = [^6Li/^7Li]_{Conventional} / [^6Li/^7Li]_{TE}$) of lithium-based refractory samples with that of NIST – RM – 8545 L-SVEC Li_2CO_3 were examined to establish the reliability of the method to obtain accurate $^6Li/^7Li$ ratio.

7.3. Future Scope

Though the present investigations demonstrated the potential of using molecular ions for precise and accurate isotope measurement of boron and lithium, the present studies were restricted to nuclear industrial applications. For the other fields of interest such as hydrology, where elements are present in ppb/ppm quantities, the samples have to be subjected

to chemical treatment procedures for purification and preconcentration of lithium and boron to avoid adverse matrix effects. Conventionally a four-stage column separation is being employed to remove the matrix elements and the isotopic measurement is carried out using atomic ions of lithium (Li^+) using lithium phosphate as the ion source loading material. The time required to complete this separation is about 11-man hours and additionally to evaporate the volume generated in each of the stages and for the conversion of eluted lithium chloride to lithium phosphate, it takes about 5 - man hours. Since the conventional methodology is time consuming, an alternate methodology was developed during the present investigations for a quick and efficient separation of lithium from matrix and direct analysis of lithium in the eluent. We employed ion chromatography using Methane Sulphonic Acid (MSA) as an eluent on a weak cation exchanger column functionalized with carboxylic acid groups. The optimized conditions for the efficient and fast separation of lithium consisted of 1mM MSA at a flow rate of 1ml/min. The volume of the eluted fraction of lithium in 1mM MSA was about 5ml. The time taken for the collection was about 1 - 2 hrs. The eluted fraction was evaporated and treated with sodium borate solution so that the stoichiometry of Li/Na mole ratio ~ 1 and B/Na mole ratio ~ 10. The measurement was carried out by employing of $NaLiBO_2^+$ molecular ions to determine the $^6Li/^7Li$ ratio. Two synthetic ground water samples were prepared using high purity salts for the common cations and anions. One was spiked with Spec. Pure Li_2CO_3 and the other with Svec Li_2CO_3 to study the feasibility of the method.

Fig. 7.1 shows the chromatogram which shows a clear separation of lithium from sodium in the synthetic ground water samples. Collection of lithium fraction was done from 3.5 minutes to 4 minutes. In order to avoid fractionation of lithium isotopes during the column separation, sample collection was performed till complete recovery of lithium is achieved within the injection volume. Also, since sodium is added deliberately to the lithium sample for the formation of $NaLiBO_2^+$ complete separation of sodium is not required. Since the separated

lithium is present in 1mM MSA, its effect on the $^{6}Li/^{7}Li$ ratio determined using $NaLiBO_2^+$ ions was studied initially. Lithium carbonate solution, 5µL containing 5µg Lithium, in 20 mL 1 mM MSA was mixed the sodium borate (such that Li/Na mole ratio ~ 1 and B/Na mole ratio ~ 10) and evaporated to about 10 µL. This pre-concentrated solution was deposited on to the center of the rhenium single filament. Limited block measurement consists of 3 – 5 blocks was recorded using $NaLiBO_2^+$ ions. Good reproducibility of about 0.2% for $^{6}Li/^{7}Li$ isotopic ratio was obtained in the presence of reagents for about 2 - 4 µg Li on the filament [189].

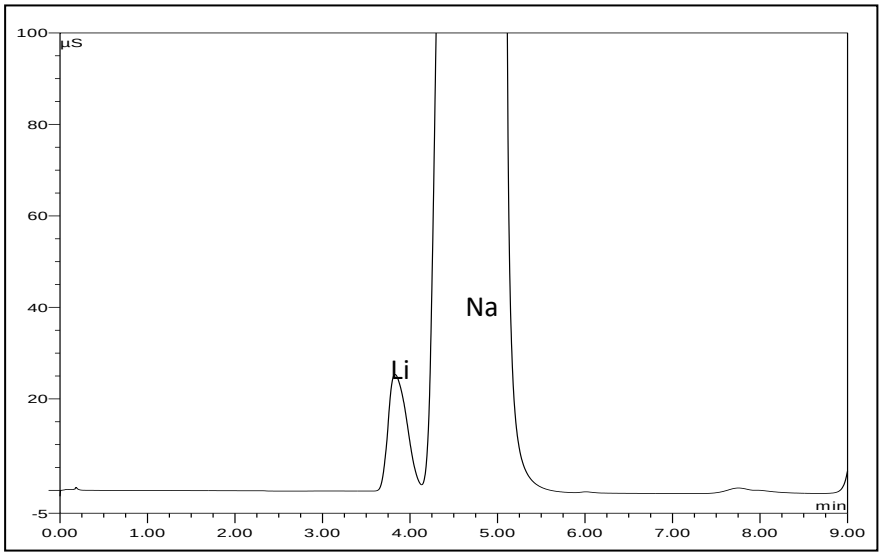

Fig. 7.1. Separation of lithium from sodium in synthetic ground water sample.

The Specpure lithium in 1mM MSA was also analyzed by TE & II mode of data acquisition for 500ng of lithium in ~5 µL solution. 5 µL solution of Specpure Lithium nitrate was also similarly analysed after treatment with sodium borate. A few analysis with 50 ng Li in MSA medium could also be analysed successfully. As shown from Fig. 7.2 and 7.3, there is a very good agreement between $^{72}/^{73}I$ and $^{6}Li/^{7}Li$ isotope ratios treated with MSA (as ion source loading material) and 1M nitric acid medium which helps us to conclude that the $^{6}Li/^{7}Li$ isotope ratios obtained by TE using $NaLiBO_2^+$ does not depend on the type of lithium compound loaded on the filament. Coupling of ion chromatography with TE & II technique

using $NaLiBO_2^+$ as monitoring ions for determination of $^6Li/^7Li$ ratio has the potential to increase sample throughput due to reduction in separation and treatment time for analysis by TIMS and also decreases the sample size requirement to a few hundred nanogram levels [190].

It is proposed to carry out the isotopic analysis of lithium in groundwater samples for the hydrological applications, rock and meteorite samples for geological and cosmology studies. Here the solid samples have to be subjected to microwave assisted acid digestion and thereafter lithium is to be separated by the developed ion chromatographic method and analysed for isotopic content by TIMS using TE & II of $NaLiBO_2^+$ ions. These feasibility studies reveal that geological samples containing trace quantities of lithium can be analysed efficiently using the developed methodology described above.

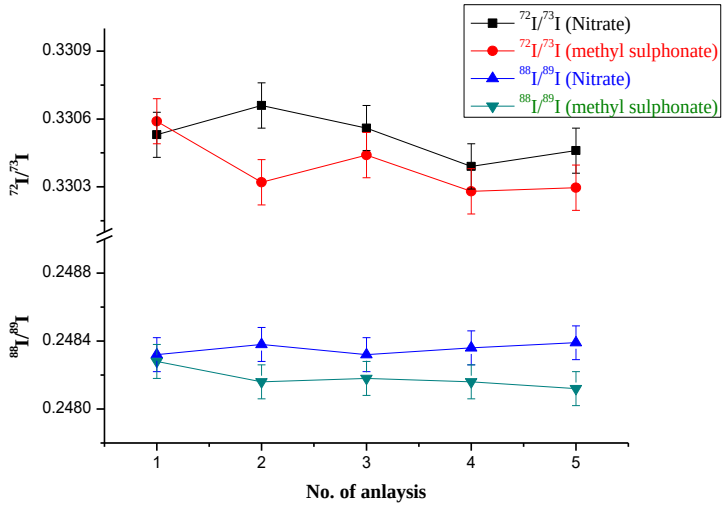

Fig. 7.2. Ion intensity ratio of $^{72}/^{73}I$ and $^{88}I/^{89}I$ obtained from TFE & II method in nitrate & Methyl Sulphonic Acid medium

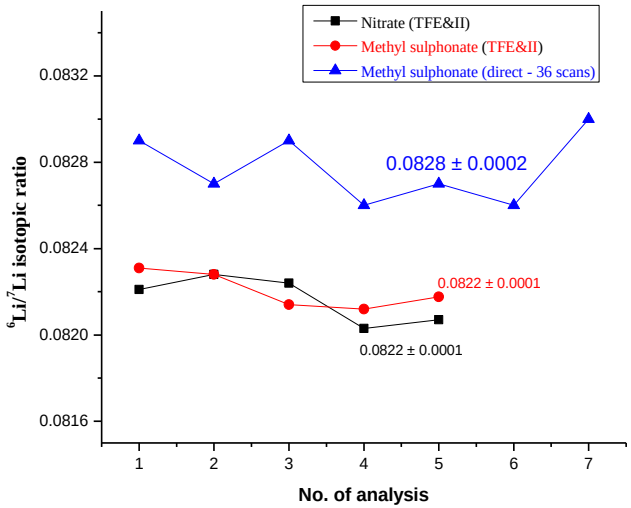

Fig. 7.3. Comparison of isotopic ratio of $^6Li/^7Li$ obtained from TE & II method for nitrate & MSA medium with direct measurement

Appendix 3.1

As the polyatomic ion abundance ratio (R_i) is a function of lithium (L) and boron (B) isotopic ratios, these ratios can be written as a function of both Li and B isotopic ratios, that is,

$f_i(L,B) = (R_i \pm \delta_{R_i})$ --------- Eqn. 3.1.1

$f_j(L,B) = (R_j \pm \delta_{R_j})$ --------- Eqn. 3.1.2

Where δ represents the experimental uncertainty on the particular polyatomic ion ratio R

Upon partial differentiation of Eqn. 3.1.1 and 3.1.2 with respect to R_i & R_j,

$\frac{d_{iL}}{d_i}\delta L + \frac{d_{iB}}{d_i}\delta B = \delta R_i$ & $\frac{d_{jL}}{d_j}\delta L + \frac{d_{jB}}{d_j}\delta B = \delta R_j$

On rearranging these terms, we get the uncertainty on lithium and boron isotopic ratio as

$$\delta L = \frac{(d_i * d_{jB} * \delta R_i - d_j * d_{iB} * \delta R_j)}{N}$$

$$\delta B = \frac{(d_j * d_{iL} * \delta R_j - d_i * d_{jL} * \delta R_i)}{N}$$

Where $N = d_{iL} * d_{jB} - d_{iB} * d_{jL}$

In the equations the terms d_i, d_j, d_{iL}, d_{jL}, d_{iB} and d_{jB} are constants for a polyatomic ratio under consideration and for a particular isotopic composition of lithium and boron. The relative uncertainty on lithium and boron abundance ratios are calculated as $\delta_L = \frac{\delta L}{L}$ & $\delta_B = \frac{\delta B}{B}$

Similarly, $\delta_i = \frac{\delta R_i}{R_i}$ & $\delta_j = \frac{\delta R_j}{R_j}$

The Magnification factors (MF) and Relative unceratinty magnification factors(RUMF) for lithium and boron can be computed using following formula:

$$[MF]_i^L = \frac{d_i * d_{jB} * R_i}{L * N} \text{ \& } [MF]_j^L = \frac{d_j * d_{iB} * R_j}{L * N}$$

$$[MF]_i^B = \frac{d_i * d_{jL} * R_i}{B * N} \text{ \& } [MF]_j^B = \frac{d_j * d_{iL} * R_j}{B * N}$$

$$[RUMF]_L = \frac{|\delta_L|}{|\delta_i| + |\delta_j|}$$

$$[RUMF]_B = \frac{|\delta_B|}{|\delta_i| + |\delta_j|}$$

Appendix – 4.1

Calculation of integrated ion intensity ratio, instantaneous (residual) ratio & fraction of sample consumed

Total number of scans = n

Total integrated ion intensity of ^{71}I = ${}_{total}^{71}I = \sum_{i=1}^{n} {}_{i}^{71}I$

Total integrated ion intensity of ^{72}I = ${}_{total}^{72}I = \sum_{i=1}^{n} {}_{i}^{72}I$

Total integrated ion intensity of ^{73}I = ${}_{total}^{73}I = \sum_{i=1}^{n} {}_{i}^{73}I$

Total integrated ion intensity (I) of all scans at 100% sample consumption = $I_{total} = {}_{total}^{71}I + {}_{total}^{72}I + {}_{total}^{73}I$

Integrated ion intensity ratio (^{72}I/^{73}I) at k of n cycles

Integrated Ion intensity of ^{72}I at k cycle = ${}_{kcycle}^{72}I = \sum_{i=1}^{k} {}_{i}^{72}I$ where 1 ≤ k ≤ n

Integrated Ion intensity of ^{73}I at k cycle = = ${}_{kcycle}^{73}I = \sum_{i=1}^{k} {}_{i}^{73}I$ where 1 ≤ k ≤ n

Integrated Ion intensity ratio at k cycle = (^{72}I/^{73}I) $K_{cycle} = \frac{{}_{kcycle}^{72}I}{{}_{kcycle}^{73}I} = \frac{\sum_{i=1}^{k} {}_{i}^{72}I}{\sum_{i=1}^{k} {}_{i}^{73}I}$

Total integrated Ion intensity ratio at n cycle $(^{72}I/^{73}I)_{total} = \frac{{}^{72}_{total}I}{{}^{73}_{total}I} = \frac{\sum_{i=1}^{n} {}^{72}_{i}I}{\sum_{i=1}^{n} {}^{73}_{i}I}$

Instantaneous ion intensity ratio $(^{72}I/^{73}I)$ at k of n cycles $= (^{72}I/^{73}I)_{instantaneous}$

$$= \frac{\left[{}^{72}_{kcycle}I\right] - \left[{}^{72}_{(k-1)cycle}I\right]}{\left[{}^{73}_{kcycle}I\right] - \left[{}^{73}_{(k-1)cycle}I\right]}$$

Sample consumption at kth cycle

Total integrated ion intensity (I) of all scans = $I_{total} = {}^{71}_{total}I + {}^{72}_{total}I + {}^{73}_{total}I$

Integrated ion intensity (I) at a particular cycle k = $I_{kcycle} = {}^{71}_{kcycle}I + {}^{72}_{kcycle}I + {}^{73}_{kcycle}I$ where $1 \leq k \leq n$

Fraction of sample consumed at kth cycle = $\frac{I_{kcycle}}{I_{total}} * 100 = \frac{\sum_{i=1}^{k} (71_I + 72_I + 73_I)}{\sum_{i=1}^{n} (71_I + 72_I + 73_I)} * 100$

Appendix 5.1

Uncertainty in concentration determination of Li enriched solutions of ^{6}Li & ^{7}Li

Term	Uncertainty % (r.s.d.) in 6-Li enriched [A]	Uncertainty % (r.s.d.) in 7-Li enriched [B]
Aliquot of enriched isotope W_A / W_B	(u_4) 0.037	(u_{11}) 0.037
Amount of standard $W_{std}C_{std}$	(u_5) 0.045	(u_{12}) 0.045
Concentration of the enriched solutions	(u_6) 0.04	(u_{13}) 0.17
A.F. of ^{6}Li	(u_7) 0.007	(u_{14}) 0.15
A.F. of ^{7}Li	(u_8) 4	(u_{15}) 0.004
At Wt. of enriched Lithium	(u_9) 0.0015	(u_{16}) 0.0015
R_A / R_B Ratio ^{6}Li/^{7}Li in enriched isotope	(u_{10}) 0.2	(u_{17}) 4

Uncertainty in ^{6}Li/^{7}Li isotopic ratios of the synthetic mixtures

$$R^{6}/_{7}{}_{[AB]} = \frac{\left(\frac{[C*W*A.F.^{6}]_A}{[Av.At.Wt.]_A}\right) + \left(\frac{[C*W*A.F.^{6}]_B}{[Av.At.Wt.]_B}\right)}{\left(\frac{[C*W*A.F.^{7}]_A}{[Av.At.Wt.]_A}\right) + \left(\frac{[C*W*A.F.^{7}]_B}{[Av.At.Wt.]_B}\right)}$$

From uncertainty for rest of the terms in the above equation,

Total uncertainty in ^{6}Li/^{7}Li isotopic ratios ($^{6/7}R_{[AB]}$) in synthetic mixtures was calculated to be u_{Rab} = 0.3%

References

1. ""What is Your Cosmic Connection to the Elements?", James C. Lochner, Gail Rohrbach, Kim Cochrane, National Aeornautics and Space Administration, **2003**, erc.ivv.nasa.gov/pdf/190387main_Cosmic_Elements.pdf
2. "Cosmic origin of the chemical elements rarety in nuclear astrophysics", Elisabeth Vangioni, Michel Casse, *Frontiers in Life Science*, **2018**,10-1, 84 – 97
3. "The origin of deuterium", Richard I, Epstein, James M. Lattimer, David N. Schramm, *Nature*, **1976**, 263, 198 - 202
4. "Deuterium: a precious gift from the Big Bang (iter.org)", R. Arnoux, ITER Newsline, **2011**, 167, 3
5. "Abundances of the elements: Meteoritic and solar", Edward Anders, Nicolas Grevesse, *Geochimica & Cosmochimica Acta*, **1988**, 53, 197- 214
6. "Synthesis of the elements in stars", E. Margaret Burbidge, G. R. Burbidge, William A. Fowler, F. Hoyle, *Reviews of modern physics*, **1957**, 29, 547 – 654
7. "The Evolution and explosion of massive stars. II. Explosive hydrodynamics and nucleosynthesis", Woosley S. E., Thomas A. Weaver, T., *ApJ Suppl.*, **1995**, 101, 181 - 235
8. "Astrophysics: Lithium probes the universe", David N. Schramm, *Nature*, **1985**, 317 386 – 387
9. "On the origin of the elements ($Z \leq 6$)", Hubert Reeves, *Reviews of modern physics*, **1994**, 66, 193 – 216
10. "On the origin of the light elements", Hubert Reeves, *Annu. Rev. Astrophys*. **1974**, 12, 437 – 470

11. “Evolution of Beryllium abundances in the galactic halo”, Sean G. Ryan, John E. Norris, M. S. Bessell, Constantine P. Deliyannis, *The Astrophys. J.*, **1992**, 388, 184 – 189
12. “The Evolution of galactic Boron and the production site of the light elements”, D. K. Duncan, F. Primas, L. M. Rebull, A.M. Bosegaard, Constantine P. Deliyannis, L. M. Hobbs, J. R. King, S. G. Ryan, *The Astrophys. J.*, **1997**, 488, 388 – 349
13. J. J. Thomson, Recollect. Reflect., G. Bell and Sons, London, **1936**, P. 341
14. “Mass Spectrometry and isootpes: A century of research and discussion”, H. Budzikiewicz, R. D. Grigsby, *Mass Spectrom. Rev.*, **2006**, 25, 146 – 157
15. “Inductively coupled plasma mass spectrometry (ICP-MS) and laser ablation ICP-MS for isotope analysis of long-lived radionuclides”, Becker, J. S., *Int. J. Mass Spectrom.*, **2005**, 242, 183 - 195
16. “Recent developments in isotope analysis by advanced mass spectrometric techniques, plenary lecture, Becker”, J. S., *J. Anal. At. Spectrom.*, **2005**, 20, 1173
17. “Isotope dilution mass spectrometry”, K. G. Heumann, *Int. J. Mass Spectrom.*, **1992**, 118-119, 575 - 592
18. “Recent developments in thermal ionization mass spectrometric techniques for isotope analysis. A review”, K. G. Heumann, S. Eisenhut, , S. Gallus, E. H. Hebeda, R. Nusko, A. Vengosh, T. Walczyk, *Analyst*, **1995**, 120, 1291 - 1299
19. “Progress in isotope analysis at ultra-trace level by AMS”, Kutschera, W., *Int. J. Mass Spectrom.*, **2005**, 242, 145 - 160
20. “Laser ablation inductively coupled plasma mass spectrometry for direct isotope ratio measurements on solid samples”, C. Pickhardt, H.-J. Dietze, and J. S. Beck er, *Int. J. Mass Spectrom.*, **2005**, 242, 273

21. “Modern Isotope Ratio Mass Spectrometry”, Platzner, I. T., John Wiley & Sons, Chichester **1997**, 145
22. “Recent developments in isotope ratio measurements by resonance ionization mass spectrometry”, Wendt, K. and Trautmann, N., *Int. J. Mass Spectrom.*, **2005**, 242, 161 - 168
23. “The development of multiple collector mass spectrometry for isotope ratio measurements”, Wieser, M. E. and Schwieters, J. B., *Int. J. Mass Spectrom.*, **2005**, 242, 97 - 115
24. “Mass spectrometry and isotopes: a century of research and discussion”, Budzikiewicz, H. and Grigsby, R. D., *Mass Spectrom. Rev.*, **2006**, 25, 146
25. “Determination of uranium isotopic composition and 236U content of soil samples and hot particles using inductively coupled plasma mass spectrometry”, Boulyga, S. F. and Becker, J. S., *Fresenius’ J. Anal. Chem.*, **2001**, 370, 612
26. “Isotope ratio measurements of spent reactor uranium in environmental samples by using inductively coupled plasma mass spectrometry”, Boulyga, S. F., Becker, J. S., Matusevitch, J. L. and Dietze, H. J., *Int. J. Mass Spectrom.*, **2000**, 203, 143 - 154
27. “Cosmic Lithium-Beryllium-Boron story”, Elisabeth Vangioni-Flam, Michel Casse, *Astrophysics and Space Science*, **1999**, 265, 77 – 86
28. “Cosmochemistry of Lithium”, Tomascak P., Magna T., Dohmen R., *Advances in Isotope Geochemistry*, **2015,** 19 – 46, http://dx.doi.org/10.1007/978-3-319-01430-2_3
29. “Lithium – 6: Evolution from Big Bang to present”, Elisabeth Vangioni-Flam, Michel Casse, Audoze J, *New Astron*, **1999**, 4, 245 – 254
30. “The primordial Lithium problem”, B. D. Fields, *Ann. Rev. Nucl. Part. Sci.*, **2011**, 61, 47 - 68
31. “The Cosmochemistry of Boron Isotopes”, Ming-Chang Liu, Marc Chaussidon, *Advances in Isotope Geochemistry*, **2018**, pg. 273 – 289, https://doi.org/10.1007/978-3-319-64666-4_11

32. “Coprecipitation and isotopic fractionation of boron in modern biogenic carbonates”, Vengosh A., Kolodny Y., Starinsky A., Chivas A. R., McCulloch M. T., *Geochim. Cosmochimica Acta*, **1991**, 55, 2901 – 2910
33. “Mobilization of boron in convergent margins: Implications for the boron geochemical cycle”, You C. F., Spivack A. J., Smith J. H., Gieskes, J. M., *Geology*, **1993**, 21, 207 – 210
34. “Alteration of the oceanic crust: Implications for geochemical cycles of lithium and boron”, W. E. Seyfried, D. R. Janecky, M. Mottl, *Geochim. Cosmochim. Acta*, **1984**, 48, 557 – 569
35. “Lithium concentration and isotopic composition of rocks from DSDP/ODP Hole 504B, PANGAEA”, L. H. Chan, Jeffrey C. Alt, Damon A. H. Teagle, *Earth & Planetary Science Letters*, **2002**, 201, 187 – 201
36. “Lithium, Boron and their isotopes in sediments and pore waters of ocean drilling program site 808, Nankai Trough: Implications for fluid expulsion in accretionary prisms”, C. F. You, L. H. Chan, A. J. Spivack, J. M. Gieskes, *Geology*, **1995**, 23(1), 37 – 40
37. “In-situ lithium and boron isotope determinations in mica, pyroxene and serpentine by LA-MC-ICP-MS”, Celine Martin, Emmanuel Ponzevera, George Harlow, Chemical *Geology*, **2015**, 412, 107 -116
38. “Precise and accurate boron and lithium isotopic determinations for small sample-size geological materials by MC-ICP-MS”, Yung Hsin Liu, Kuo Fang Huang, Der Chuen Lee, *J. Anal. At. Spectrom.*, **2018**, 33, 846 – 855
39. “Tracer Hydrology”, Leibundgut C., Seibert J., Tracer Hydrology In. Peter Wilderer (ed.) *Treatise on Water Science*, **2011**, 2, 215 – 236
40. “Boron isotope application for tracing sources of contamination in groundwater”, A. Vengosh, K. G. Heumann, S. Juraske, R. Kasher, *Environ. Sci. Technol.*, **1994**, 28, 1968 – 1974

41. “Determination of boron isotopic variations in aquatic systems with negative thermal ionization mass spectrometry as a tracer for anthropogenic influences”, S. Eisenhunt, K. G. Heumann, A. Vengosh, Fresensius, *J. Anal. Chem.*, **1996**, 354, 903 – 909
42. “Bor in Trinkwassern der Bundesrepublik Deutschland”, Wiecken S., Wubbold Weber S., *SOFW-Journal*, **1995**, 121, 428 – 436
43. “Review of Lithium in aquatic environment: Distribution in the United States, Toxicity and case example of groundwater contamination”, Lynn Adams Kszos, Arthur J. Stewart, *Ecotoxicology*, **2003**, 12, 439 – 447
44. “Seawater residence times of some elements of geochemical interest and the salinity of the oceans”, Christophe Lecuyer, *Bull. Soc. Geol. France*, **2016**, 187(6), 245 – 260
45. “Oceanography: An invitation to marine Science”, Tom S. Garrison, Robert Ellis, **2015**, Pg. 206
46. “Scrutinizing the carbon cycle and CO_2 residence time in the atmosphere”, Hermann Harde, *Global & Planetary Change*, **2017**, 152, 19 – 26
47. “Lithium isotopes in foraminifera shells as a novel proxy for the ocean dissolved inorganic carbon (DIC)”, Nathalie Vigier, Claire Rollion Bard, Yael Levenson, Jonathan Erez, C. R., *Geoscience*, **2015**, 347, 43 - 51
48. “Boron isotopic composition and concentration in modern marine carbonates”, Hemming N. G., Hanson G. N., *Geochim. Cosmochim. Acta*, **1992**, 56, 537 – 543
49. “Seawater pH, pCO_2 and $[CO_3^{2-}]$ variations in the Caribbean Sea over the last 130 kyr: A boron isotope and B/Ca study of planktic foraminifera”, Foster G., *Earth Planet. Sci. Lett.*, **2008**, 271 (1-4), 254 – 266

50. “Li partitioning in the benthic foraminifera Amphistegina lessonii”, G. Langer, A. Sadekov, S. Thoms, A. Mewes, G. Nehrke, M. Greaves, S. Misra, J. Bijma, H. Elderfield, *Geochem. Geophys. Geosyst.*, **2015**, 16, 1 - 5
51. “Boron isotopes and B/Ca in benthic foraminifera: Proxy for deep ocean carbonate system”, Rae J. W. B., Foster G. L., Schmidt D. N., Elliott T., *Earth Planet. Sci. Lett.*, **2011**, 302, 403 – 413
52. https://www.world-nuclear.org/information-library/current-and-future-generation/lithium.aspx , **2017**
53. “Lithium Isotope enrichment: Feasible domestic enrichment alternatives”, Tim Ault, Krzysztof Brozek, Lingchen Fan, Micah Folsom, Joshua Kim, Joshua Zeismer, Report UCBTH – 12 – 005, Dept. Nucl. Eng., Univ. California, Berkeley, **2012**
54. “Synthesis and fabrication of lithium titanate pebbles for ITER breeding blanket by solid state reaction and spherodization”, D. Mandal, M. R. K. Shenoi, S. K. Ghosh, Fusion Eng. Design, **2010**, 85, 819 – 823
55. K. Suri, C. Subramanian, J. K. Sonber and T. S. R. Ch. Murthy, Synthesis and consolidation of boron carbide: A Review, *(Full critical review) International Materials Review*, 2010, **55**, 4
56. Subramanian, T. S. R. Ch. Murthy, A. K. Suri, Synthesis and consolidation of titanium diboride, *Int. J. Refract. Met. Hard Mater*, 2007, **25**, 345
57. J. K. Sonber K. Sairam, T. S. R. Ch. Murthy, A. Nagraj, C. Subramanian and R.C. Hubli, Synthesis, densification and oxidation study of lanthanum hexaboride, *J European Ceramic Society*, 2014, **34**, 1155

58. T.S.R.Ch. Murthy, J.K. Sonber, C. Subramanian, R.C.Hubli N. Krishnamurthy and A.K. Suri, Densification, characterization and oxidation studies of (Ti,Cr) B2+20%MoSi2, *Int. J. Refract. Met. Hard Mater,* 2013, **37**, 12
59. J.K. Sonber, T. S. R. Ch. Murthy, C.Subramanian, R. C. Hubli and A. K. Suri, Synthesis, densification and characterization of EuB6, *Int. J. Refract. Met. Hard Mater,* 2013, **38**, 67
60. J. K. Sonber, T. S. R. Ch. Murthy, C. Subramanian, Sunil Kumar, R. K. Fotedar and A.K. Suri, Investigations on synthesis of ZrB2 and development of new composites with HfB2 and TiSi2, *Int. J. Refract. Met. Hard Mater,* 2011, 29, 21
61. "Introdcution: Mass Spectrometry", 2nd edition, J. H. Gross, **2004**, Pg.6, https://doi.org/10.1007/3-540-36756-X_1
62. "Accurate and high-precision measurement of lithium isotopes in two reference materials by MC-ICPMS", R. Millot, C. Guerrot, N. Vigier, *Geostand. Geoanal. Research*, **2004**, 28, 153 – 159
63. "Handbook of Radioactivity Analysis", 2nd edition, G. Huber, G. Passler, K. Wendt, J. V. Kratzand, N. Trautmann, **2003**, 799 – 843
64. "Isotopic analysis of lithium as thermal dilithium fluoride ions", L. W. Green, J.J. Leppinen, N. L.Elliot, *Anal. Chem.,* **1988**, 60, 34 - 37
65. "Precise determination of lithium isotopic composition in low concentration natural samples", You Chen-feng, Chan Lui-heung, *Geochimica et Cosmochimica Acta*, **1996**, 60, 909 - 915
66. "High Precision isotopic measurement of lithium by thermal ionization mass spectrometry", Y. K. Xiao, E.S. Beary, *Int. J. Mass Spectrom. Ion Processes,* **1989**, 94**,** 107 - 114

67. “Precise lithium isotopic analysis by Thermal Ionization Mass Spectrometry using lithium phosphate as ion source material”, T. Moriguti, E. Nakamura, *Proc. Japan Acad. Ser.B,* **1993**, 69, 123 - 128
68. “A procedure for the isotopic analysis of boron by negative thermal ionization mass spectrometry”, N.G. Hemming, G.N. Hanson, *Chem. Geol.*, **1994**, 114, 147 - 156
69. “Determination of boron isotopic variations in aquatic systems with negative thermal ionization mass spectrometry as a tracer for anthropogenic influences”, S. Eisenhut, K.G. Heumann, A. Vengosh, *Fres. J. Anal. Chem.*, **1996**, 354, 903
70. “Boron isotope ratio measurement by negative thermal ionization mass spectrometry method using boron-free seawater”, A. Sonoda, Y. Makita, K. Ooi, T. Hirotsu, *J. Nucl. Sci. Technol.*, **2002**, 39, 295
71. “A 10-fold improvement in the precision of boron isotopic analysis by negative thermal ionization mass spectrometry”, J. J. Shen, C. F. You, *Anal. Chem.*, **2003**, 75, 1972-1977
72. “Accurate and precise isotopic measurement of sub-nanogram sized samples of foraminiferal hosted boron by total evaporation N-TIMS”, G.L. Foster, Y. Ni, B. Haley, T. Elliott, *Chem. Geol.*, **2006**, 230, 161
73. E.J. Catanzaro, C.E. Champion, E.L. Garner, G.Marinenko, K.M. Sappenfield, W.R. Shields, *Natl. Bur. Stand. (US) Spec. Publ.*, **1970**, 17, 260
74. “Application of dicesium metaborate ion for the determination of boron by thermal ionization mass spectrometry”, K.L. Ramakumar, P.S. Khodade, A.R. Parab, S.A. Chitambar, H.C. Jain, *J. Radioanal. Nucl. Chem.*, **1985**, 107, 215
75. “Boron isotopic composition of marine and nonmarine evaporite borates”, G.H. Swihart, P.B. Moore, E.L. Callis, *Geochim. Cosmochim. Acta,* **1986**, 50, 1297 - 1301

76. “Determination of boron isotope ratios by thermal ionization mass spectrometry of the dicesium metaborate cation”, A.J. Spivack, J.M. Edmond, *Anal. Chem.,* **1986**, 58, 31.

77. “An improved method for high precision isotopic measurement of boron by thermal ionization mass spectrometry”, Y.K. Xiao, R.S. Beary, J.D. Fassett, *Int. J. Mass Spectrom. Ion Proc.*, **1988**, 85, 203 - 213.

78. “Precise boron isotopic analysis of aqueous samples: Ion exchange extraction and mass spectrometry”, W.P. Leeman, R.D. Vocke Jr, E.S. Beary, P.J. Paulsen, *Geochim. Cosmochim. Acta,* **1991**, 55, 3901

79. “Boron isotope geochemistry of metasedimentary rocks and tourmalines in a subduction zone metamorphic suite”, T. Nakano, E. Nakamura, *Phy. Ear. Planet. Inetriors.,* **2001**, 127, 233 - 252

80. “Improvements of boron isotope analysis by positive thermal ionization mass spectrometry using static multicollection of $Cs_2BO_2^+$ ions”, A. Deyhle, *Int. J. Mass Spectrom. Ion Proc.*, **2001**, 206, 79 - 89

81. “An optimized procedure for boron separation and mass spectrometry analysis for river samples” D. Lemarchand, J. Gaillardet, C. Gopel, G. Manhes, *Chem. Geol.*, **2002**, 182, 323 - 334

82. “Studies on the isotopic analysis of boron by thermal ionization mass spectrometry using NaCl for the formation of $Na_2BO_2^+$ species”, R.M. Rao, A.R. Parab, K. Sasi Bhushan, S.K. Aggarwal, *Int. J. Mass Spectrom.,*2008, 273**,** 105

83. “High Precision isotope ratio measurements of boron by thermal ionization mass spectrometry using $Rb_2BO_2^+$ ion”,Radhika M. Rao, Ankush R. Parab, K. Sasi Bhushan, Suresh Kumar Aggarwal, *Anal. Methods,* **2011**, 3, 322 – 327

84. “Thermal ionization mass spectrometry of $Li_2BO_2^+$ ions: determination of the isotopic abundance ratio of lithium”, B.P. Datta, P.S. Khodade, A.R. Parab, A.H. Goyal, S.A. Chitambar, H.C. Jain, *Int. J. Mass Spectrom. Ion Processes,* **1992**, 116, 87 - 114

85. “Molecular ion beam method of isotopic analysis: Effect of error propagation, a case study with $Li_2BO_2^+$”,B.P. Datta, P.S. Khodade, A.R. Parab, A.H. Goyal, S.A. Chitambar, H.C. Jain, *Rapid Commun. Mass Spectrom.*, **1993**, 7, 581

86. “Isotopic analysis of a ^6Li enriched lithium sample employing the $Li_2BO_2^+$ ion beam method: verification of the theoretical accuracy”, B. P. Datta, A.R. Parab, P.S. Khodade, S.A. Chitambar, H.C. Jain, *Int J. Mass Spectrom. Ion Processes,* **1995**, 142, 69 - 81

87. “Polynomial method of molecular isotopic abundance calculations: a computational note”, B. P. Datta, *Rapid Commun. Mass Spectrom.*, **1997**, 11, 1767 - 1774

88. “Error systematics of determining elemental isotopic abundance ratios by molecular ion beam method: a cast study for the simultaneous isotopic analysis of lithium and boron as $Li_2BO_2^+$”, B. P. Datta, *Rapid Commun. MassSpectrom.*, **2000**, 14, 696 - 705

89. “Error systematics of determining simultaneously the isotopic abundance ratios of natural lithium and natural boron as $Li_2BO_2^+$”, B. P. Datta, *RapidCommun. Mass Spectrom.*, **2000**, 14, 706.

90. “The thermal emission ion source in solid source mass spectrometry”, Palmer G.H., *J. Nucl. Energy,* **1958**, 7, 1 – 12

91. “A robust methodology for high precision isotopic analysis of boron by thermal ionization mass spectrometry using $Na_2BO_2^+$ ion”, Radhika M. Rao, Ankush R. Parab, K. Sasi Bhushan, Suresh K. Aggarwal, *Int. J. Mass Spectr., **2009**,* 285, 120 – 125

92. “The lithium isotope composition of international rock standards”, Rachael H. James, Martin R. Palmer, *Chem. Geology*, **2000**, 166, 319 – 26

93. “Lithium and its isotopes in major world rivers: implications for weathering and the oceanic budget”, Youngsook Huh, Lui-Heung Chan, LiboZhang, John M. Edmond, *Geochim. Cosmochim.* Acta, **1998**, 62, 2039 – 2051

94. “A lithium isotope study of hot springs and metabasalts from Mid-Ocean Ridge hydrothermal systems”, Lui-Heung Chan, John M. Edmond, Geoffrey Thompson, *J. Geophy. Research*, **1993**, 98, 9653 – 9659

95. “High yield lithium separation and the precise isotopic analysis for natural rock and aqueous samples”, Takuya Moriguti, Eizo Nakamura, *Chem. Geology*, **1998**, 145, 91 – 104

96. “The absence of lithium isotope fractionation during basalt differentiation: new measurements by multicollector sector ICP-MS”, Paul B. Tomascak, Fouad Tera, Rosalind T. Helz, Richard J. Walker, *Geochim. Cosmochim. Acta*, **1999**, 63, 907 - 910

97. “Lithium isotopic systematics of hydrothermal vent fluids at the main endeavour field, Northern Juan de Fuca Ridge”, D. I. Foustoukos, R. H. James, M. E. Berndt, W. E. Seyfried Jr., *Chem. Geology*, **2004**, 212, 17 – 26

98. “Behaviour of lithium isotopes during continental weathering: the Bidar laterite profile, India”, Basask Kisakurek, Mike Widdowson, Rachael H. James, *Chem. Geology*, **2004**, 212, 27 - 44

99. “Across-arc variation of lithium isotopes in lavas and implications for crust / mantle recycling at subduction zones”, Takuya Moriguti, Eizo Nakamura, *Earth Planet. Sci. Lett.*, **1998**, 163, 167 – 174

100. "Lithium isotope evidence for light element decoupling in the Panama subarc mante", Paul B. Tomascak, Jeffrey G. Ryan, Marc J. Defant, *Geology*, **2000**, 28, 507 – 510

101. "Lithium isotope geochemistry of the Hawaiian plume: results from the Hawaii scientific drilling project and Koolau volcano", Lui-Heung Chan, Frederick A. Frey, *Geochem. Geophy. Geosys.*, **2003**, 3, doi:10.1029/2002GC000365

102. "Lithium and lithium isotope profiles through the upper oceanic crust: a study of seawater – basalt exchange at ODP sites 504B and 896A", Lui-Heung Chan, Jeffrey C. Alt, Damon A. H. Teagle, *Earth Planet. Sci. Lett.*, **2002**, 201, 187 – 201

103. "Lithium isotope geochemistry of sediments and hydrothermal fluids of the Guaymas Basin, Gulf of California", Lui-Heung Chan, Joris M. Gieskes, Chen-Feng You, John M. Edmond, *Geochim. Cosmochim. Acta, **1994***, 58, 4443 – 4454

104. "Lihtium isotope geochemistry of pore waters from ocean drilling program sites 918 and 919, Irminger Basin", Libo Zhang, Lui-Heung Chan, Joris M. Gieskes, *Geochim. Cosmochim. Acta, **1998***, 62, 2437 – 2450

105. "The alkali element and boron geochemistry of the Escanaba trough sediment-hosted hydrothermal system", Rachael H. James, Mark D. Rudnicki, Martin R. Palmer, *Earth Planet. Sci. Lett.*, **1999**, 171, 157 – 169

106. "Lithium inputs to subduction zones", Claudia Bouman, Tim Elliott, Pieter Z. Vroon, *Chem. Geology*, **2004**, 212, 59 - 79

107. "Lithium isotopic composition and concentration of the upper continental crust", F. Z. Teng, W F. McDonough, R. L. Rudinick, C. Dalpe, P. B. Tomascak, B. W. Chappell, S. Gao, *Geochim. Cosmochim. Acta, **2004***, 68, 4167 – 4178

108. "The boron isotope systematics of Icelandic geothermal water: 1. Meteoric water charges systems", J. K. Aggarwal. M. R. Palmer, T. D. Bullen, S. Arnorsson, K. V. Ragnarsdottir, *Geochim. Cosmochim. Acta, **2000**,* 64, 579 – 585

109. "Boron isotope variations in nature: a synthesis", S. Barth, *Geol. Rundsh*, **1993**, 82, 640 – 651

110. "Stable isotope geochemistry of sediment-hosted groundwater from a Late Paleozic - Early Mesozoic section in central Europe", S. Barth, *J. Hydrology*, **2000**, 235, 72 – 87

111. "Secular boron isotope variations in the continental crust: an ion microprobe study", Marc Chaussidon, Francis Albarede, *Earth Planet. Sci. Lett.,* **1992**, 108, 229 - 241

112. B. Chetelat, C. Q. Liu, J. Gaillardet, Q. L. Wang, Z. Q. Zhao, C. S. Liang, Y. K. Xiao, *Geochim. Cosmochim. Acta,* **2009**, 73, 6084 – 6097

113. "Identification of groundwater contaminations by landfills using precise boron isotope ratio measurements with negative thermal ionization mass spectrometry", S. Eisenhut, K. G. Heumann, *Frensius J. Anal. Chem.,* **1997**, 359, 375 – 377

114. "Boron and magnesium isotopic composition of seawater", G. L. Foster, P. A. E. Pogge von Strandmann, J. W. B. Rae, *Geochem. Geophy. Geosys.*, **2010**, 11, doi:10.1029/2010GC003201

115. "Boron isotope ratio measurements with a double focusing magnetic sector ICP mass spectrometer for tracing anthropogenic input into surface and groundwater", Hans-Eike Gabler, Andreas Bahr, *Chem. Geology* **1999**, 156, 323 – 330

116. "Boron isotopic compositions of corals: Seawater or diagenesis record?", Jerome Gaillardet, Claude Jean Allegre, *Earth Planet. Sci. Lett.,* **1995**, 136, 665 – 676

117. "Boron isotope composition of tourmalinite and vein tourmalines associated with gold mineralization, Serra do Itaberaba Group, central Ribeira Belt, SE Brazil", G. M. Garda, R. B. Trumbull, P. Beljavskis, M. Widenbeck, *Chem. Geology,* **2009**, 264, 207 – 220

118. "Boron isotopic composition and concentration in modern marine carbonates", N. G. Hemming, G. N. Hanson, *Geochim. Cosmochim. Acta,* **1991**, 56, 537 – 543

119. "Boron and lithium isotopes as groundwater tracers: a study at the Fresh Kills Landfill, Staten Island, New York, USA", James F. Hogan, Joel D. Blum, *Applied Geochem.*, **2003**, 18, 615 – 627

120. Gehrcke E., Reichenheim O., Ber. Bunsenges., *Phys. Chem.*, **1906**, 8, 559

121. "A new method of positive ray analysis", Dempster A. J., *Phys. Rev.*, **1918**, 11, 316

122. "Thermionic effects caused by vapours of alkali metals", Langmuir I., Kingdom K. H., *Proc. Roy. Soc. A.*, **1925**, 107, 61, https://doi.org/10.1098/rspa.1925.0005

123. "Surface ionization source using multiple filaments", Inghram M. G., Chupka W. A., *Rev. Sci. Instrum.*, **1953**, 24, 518, https://doi.org/10.1063/1.1770774

124. "Mass spectrometry of nanogram-size samples of lead", Cameron A. E., Smith D. H., Walker R. L., *Anal. Chem.*, **1969**, 41, 525

125. "An experimental investigation of surface ionization (iastate.edu)", Miles Joel Dresser, **1964**

126. "Inorganic Mass Spectrometry – Fundamentals and Applications", Chrisotpher M. Barshick, Douglas C. Duckworth, David H. Smith, Marcel Dekker, New York, **2000** Pg 8.

127. "Rays of positive electricity", J. J. Thomson, *Philos. Mag.*, **1910**, 20, 752

128. "Further experiments on positive rays", J. J. Thomson, *Philos. Mag.*, **1912**, 24, 209

129. "Rays of Positive Electricity and their Application to Chemical Analyses, Longman, Green and Co., London", J. J. Thomson, **1913**

130. “Historical Perspectives Part B: Notable people in Mass spectrometry”, Duckworth H. E., A. J. Dempster, et al, *The encyclopedia of mass spectrometry*, **2015**, 53 - 54

131. W. Wien, Wied. *Ann.*, **1898**, 65, 440

132. “A positive ray spectrograph”, Aston F. W., *Phil. Mag.*, **1919**, 38, 707

133. “Ionen-und elektronenoptische zylinderlinsen und Prismen I”, R. Herzog, *Z. Phys.*, **1934**, 89, 447 - 473

134. “Modern Isotope Ratio Mass Spectrometry”, I. T. Platzner, Wiley, New York, **1997**, Pg. 4, https://doi.org/10.1002/(SICI)1097-0231(19980615)12:11%3C749::AID-RCM214%3E3.0.CO;2-I

135. “Inorganic Mass Spectrometry – Principles and Applications”, J. Sabine Becker, **2007**, 10.1002/9780470517222

136. “Sector Field Mass Spectrometry for Elemental and Isotopic analysis” T. Prohaska, J. Irrgeher, A. Zitek, N. Jakubowski, **2014**, https://doi.org/10.1039/9781849735407

137. “Focusing and dispersing properties of a stigmatic crossed-field energy analyzer”, A. Galejs, C. E. Kuyatt, *J. Vac. Sci. Technol.*, **1978**, 15(3), 865 – 867

138. “Sector Mass Spectrometers”, R. Bateman, Encycl. Spectros. Spectrom. 3rd edition, **2017**, 50 – 55

139. “Analysis of the dynamic Faraday cup”, D. Kucerovsky, Z. Kucerovsky, *J. Phys. D: Appl. Phys.*, **2003**, 36, 2407 – 2416

140. “Improved faraday collector for magnetic sector mass spectrometers”, R. K. Bhatia, Varun K. Y., Yogesh K. Babu R. G., E. Ravishankar, T. K. Saha, V. Nataraju, S. K. Gupta, *Inter. J. Mass Spectrom.*, **2015**, 393, 58 – 62

141. "Improving precision and signal/noise ratios for MC-ICPMS", T. Breton, Nicholas S. Lloyd, A. Trinquier, Claudia Bouman, J. B. Schwieters, *Procedia Earth & Planet. Sci.*, **2015**, 13, 240 – 243

142. "MS Detectors", D. W. Koppenaal, C. J. Barinaga, M. B. Denton, R. P. Sperline, G. M. Hieftje, G. D. Schilling, F. J. Andrade, J. H. Barnes, *Anal. Chem.*, **2005**, 77, 21, 418A – 427A

143. "Faraday cup with nanosecond response and adjustable impedance for fast electron beam characterization", Jing Hu, Joshua L. Rovey, *Rev. Sci. Instr.*, **2011**, 82, 073504 (1-7)

144. "Ion detection in Inductively Coupled Plasma Mass Spectrometry Handbook", K. Hunter, D. Stresau, ed. S. M. Nelms, Blackwell Publishing Ltd., **2005**

145. ISOPROBE -T Instrument Guide

146. TRITON-PLUS Instrument Operational Manual

147. "Linearity tests for secondary electron multipliers used in isotope ratio mass spectrometry", S. Richter, S. A. Goldberg, P. B. Mason, A. J. Traina, J. B. Schwieters, *Inter. J. Mass Spectr.*, **2001**, 206, 105 – 127

148. "Fractionation in the thermal ionization source", K. Habfast, *Inter. J. Mass Spectr. Ion Phy.*, **1983**, 51, 165 – 189

149. "Fractionation correction and multiple collectors in thermal ionization isotope ratio mass spectrometry", K. Habfast, *Inter. J. Mass Spectr.*, **1998**, 176, 133 – 148

150. "Subcommission on geochronology: convention on the use of decay constants in geo- and cosmo-chronology", Steiger R. H., Jager E., *Earth Planet. Sci. Lett.*, **1977**, 36, 359 - 362

151. "Variations in $^{143}Nd/^{144}Nd$ and $^{87}Sr/^{86}Sr$ ratios in oceanic basalts", R. O'nions, P. Hamilton, N. Evensen, *Earth Planet. Scie. Lett.*, **1977**, 34, 13 – 22

152. "Ca isotope fractionation on the Earth and other solar system materials", W. Russell, D. Papanastassiou, T. Tombrello, *Geochim. Cosmochim. Acta*, **1978**, 42, 1075 – 1090

153. "Lithium isotope analysis by thermal ionization mass spectrometry of lithium tetraborate", Chan Lui-H, *Anal. Chem.*, **1987**, 59, 2662 - 2665

154. "Simultaneous measurement of lithium and boron isotopes as lithium tetraborate ion by thermal ionization mass spectrometry", S. K. Sahoo, A.Masuda, *Analyst*, **1995**, 120, 335-339

155. "Measurement of the isotopic ratio of Boron", R. Gensho and M. Honda, *Mass Spectroscopy (Japan)*, **1971**, 19, 134 – 143

156. "Lithium isotopic composition of submarine basalts", Chan L.H.; Edmond J.M.; Thompson G.; Gillis K., *Earth and Planetary science letters*., **1992**, 108, 151-160

157. "Gaseous metaborates - I. Mass Spectrometric study of the vaporization of lithium and sodium metaborates", A. Büchler and J.B. Berkowitz-Mattuck, Gaseous Metaborates. I. *J. of Chem. Phys*., **1963**, 39, 286 – 291, https://doi.org/10.1063/1.1734243

158. "Thermodyanamic quantities for reactions of alkali metaborate monomer and dimer vapours", M. Asano and Y. Kato, T. Harada, Y. Mizutani, *Mass Spectroscopy*, **1992**, 40, 9-15

159. "Effect of lithium enrichment on the tritium breeding characteristics of various breeders in a fusion driven hybrid reactor", Mustaga Ubeyli. *J. Fusion Energ.* **2009**, 28, 300

160. "Surface ionization mechanism of alkali halides", H. Iwabuchi, M. Nomura, K.Lio, Y. Fuji, T. Suzuki *Vacuum*, **1996**, 47, 501 – 504

161. "Role of graphite in isotopic analysis of boron in metal boron alloys by Positive-Thermal Ionization Mass Spectrometry", R. M. Rao, S. Jagadish Kumar, K. Sasi Bhushan, Ankush R. Parab, D. Alamelu, S. K. Aggarwal, *Int. J. of Mass Spectrom*., **2014**, 364, 21–24

162. "A secondary isotopic standard for $^{6}Li/^{7}Li$ determinations", Flesch G. D., Anderson A R., Svec H. J. *Inter. J. Mass Spectrom. Ion Pysics,* **1973**, 12, 265 – 272

163. "High precision isotopic measurement of lithium by thermal ionization mass spectrometry", S. K. Sahoo, A.Masuda, *Int. J. of Mass Spectrom.and Ion Processes,* **1995**, 151, 189 -196

164. "Re-evaluation of the certified isotope amount ratio of IRMM-016 and re-certification of the isotope amount ratio of IRMM-15", S. Duta, M. Berglund, P. Taylor, *IRMM Report No EUR 21655 EN* **2005**

165. "Simultaneous determination of non-natural isotopic composition of Li and B employing $Li_2BO_2^+$ by Thermal Ionization Mass Spectrometry", K. Sasi Bhushan, R. M. Rao, D. Alamelu, S. Jagadish Kumar, Raju V. Shah, A. R. Parab, *Int. J. Mass Spectr.*, **2016**, 406, 20 – 28

166. "Precise and rapid isotopic analysis of lithium in refractory materials using $NaLiBO_2^+$ by thermal ionization mass spectrometry (TIMS)", Radhika M. Rao, K. Sasi Bhushan, S. Jagadish Kumar, Raju Shah, *Int. J. Mass Spectr.*, **2020**, 451, 116292

167. "Report on preliminary experience with total evaporation measurements in thermal ionization mass spectrometry", R. Fiedler, D. Donohue, G. Grabmueller, A. Kurosawa, *Inter. J. Mass Spectr. Ion Proc.,* **1994**, 132, 207 - 215

168. "Total evaporation method for uranium isotope-amount ratio measurements", K. J. Mathew, G. O'Connor, A. Hasozbek and M. Kraiem, *J. Anal. At. Spectrom.,* **2013**, 28, 866-876

169. "Assessment of international reference materials for isotope-ratio analysis (IUPAC Technical Report)", Willi A. Brand, Tyler B. Coplen, JochenVogl, Martin Rosner and Thomas Prohaska, *Pure Appl. Chem.*, **2014**, 86(3), 425–467

170. "Improved techniques for high accuracy isotope ratio measurements of nuclear materials using thermal ionization mass spectrometry", S. Richter, S.A. Goldberg, *Inter. J. Mass Spectr.*, ***2003***, 229, 181–197

171. "Mass spectrometric analysis for nuclear safeguards", Sergei Boulyga , Stefanie Konegger-Kappel, Stephan Richterb and Laure Sangely, *J. Anal. At. Spectrom.*, **2015**, 30, 1469-1489

172. "Study on effect of sodium-based buffers on the isotopic measurement of boron using $Na_2BO_2^+$ by thermal ionization mass spectrometry", K. Sasi Bhushan, Radhika M. Rao, Preeti G. Goswami and S. Kannan, *J. Radioanal. Nucl. Chem.*, **2019**, 323, 1367

173. "The preparation of precisely defined lithium isotope mixtures", J. Pauwels, K. F. Lauer, Y. L. Duigou, P. D. Bievre and G. H. Debus, *Anal. Chim. Acta*, **1968**, 43, 211

174. "Preparation and characterisation of synthetic mixtures of lithium isotopes", H. P. Qi, M. Berglund, P. D. P. Taylor, F. Hendrickx, , A. Verbruggen, P. De Bièvre, *Fresenius J Anal Chem.*, **1998**, 361, 767 – 773

175. "The preparation and use of synthetic isotope mixtures for testing mass spectrometers", K. J. R. Rosman, W. Lycke, R. Damen, R.Werz, F. Hendrickx, L. Traas and P. D. Bievre, *Int. J. of Mass Spectrom. and Ion Proc.*, **1987**, 79, 61.

176. "The preparation and use of synthetic isotope mixtures for testing the accuracy of the PTIMS method for $^{10}B/^{11}B$ isotope ratio determination using boron mannitol complex and NaCl for the formation of $Na_2BO_2^+$", Radhika M. Rao, Ankush R. Parab and Suresh Kumar Aggarwal, *Anal. Methods*, **2012**, 4, 3593 - 3599

177. "Mass Discrimination During MC-ICPMS Isotopic Ratio Measurements: Investigation by Means of Synthetic Isotopic Mixtures (IRMM-007 Series) and Application to the Calibration of Natural-Like Zinc Materials (Including IRMM-3702 and IRMM-651)", E. Ponzevera, C.

R. Quétel, M. Berglund, P. D. P. Taylor, P. Evans, R. D. Loss and G. Fortunato, *J. Am. Soc. Mass Spectrom.*, **2006**, 17, 1412.

178. "Validation of the analytical linearity and mass discrimination correction model exhibited by a multiple collector inductively coupled plasma mass spectrometer by means of a set of synthetic uranium isotope mixtures"**,** P. D. Taylor, P D. Bievre, A. J. Walder and A. Entwistle, *J of Anal. At. Spectrom.*, **1995**, 10, 395.

179. "A Re-deterrnination of the Relative Abundances of the Isotopes of Carbon, Nitrogen, Oxygen, Argon, and Potassium", Alfred O. Nier, *Physical Review*, **1950**, 77, 789 - 793

180. "Absolute isotopic composition and the atomic weight of a natural sample of lithium", E. Michiels and P. D. Bievre, *Int. J. of Mass Spectrom. and Ion Phy.*, **1983**, 49, 265.

181. "An enriched ^{6}Li isotope reference material", A. Lamberty and P. D. Bievre, *Int. J. of Mass Spectrom. and Ion Proc.*, **1988**, 83, 135.

182. "Isotope reference materials for present and future isotope research", J. Vogl and W. Pritzkow, *J. Anal. At. Spectrom.*, **2010**, 25, 923 – 932.

183. "Isotope dilution thermal ionization mass spectrometry (ID-TIMS) for determination of concentration of enriched lithium using $NaLiBO_2^+$ ions", K. Sasi Bhushan, Preeti G. Goswami and Radhika M. Rao, *J. of Radioanalytical and Nuclear Chem.*, **2020**, 326, 1009 – 1017; https://doi.org/10.1007/s10967-020-07409-w

184. "Non-destructive quantification of total boron and its isotopic composition in boron based refractory materials by PIGE and inter-comparison study using TIMS and titrimetry", R. Acharya, S. K. Wasim Raja, Sumit Chhilar, J. Gupta, J. K. Sonber, T. S. R. Murty, K. Sasi Bhushan, Radhika M. Rao, S. Majumdar and P. K. Pujari, *J. Atom. Absorp. Spectrom*, **2018**, 33, 784

185. "Oxidative pyrolysis combined with the microwave assisted extraction method for the multi-elemental analysis of boron carbide powders by inductively coupled plasma optical emission spectrometry (ICP-OES)", M. V. Balarama Krishna, G. Venkateswarlu, S. Thangavel and D. Karunasagar, *Anal. Methods*, **2013**, 5, 1515

186. "Determination of boron concentration in borosilicate glass, boron carbide and graphite samples by conventional wet-chemical and nuclear analytical methods", K. Venkatesh, Sumit Chhillar, Granthali S. Kamble, Shailaja P. Pandey, Manisha Venkatesh, Sanjukta A. Kumar, Sanjiv Kumar, R. Acharya, P. K. Pujari and A. V. R. Reddy, *J. Radioanal. Chem.*, **2014**, 302, 1425

187. "Fusion method for sample preparation for isotopic composition determination of boron in refractory materials by thermal ionization mass spectrometry with validation using dissolved and purified samples", K. Sai Bhushan, Preeti G. Goswami, K. Venaktesh, Sanjukta A. Kumar, Radhika M. Rao, *Int. J. Mass Spectr.*, **2021**, 467, 116624

188. "Precise determination of $^{6}Li/^{7}Li$ isotopic ratio with $NaLiBO_2^+$ ion using total evaporation and ion integration by Thermal Ionization Mass Spectrometry (TIMS)", K. Sasi Bhushan, Preeti G. Goswami, R. M. Rao, *Int. J. Mass Spectr.*, **2021**, https://doi.org/10.1016/j.ijms.2021.116683

189. "Determination of isotopic composition of Lithium in synthetic ground water samples as $NaLiBO_2^+$ using Thermal Ionization Mass Spectrometry", K. Sasi Bhushan, Vivek G. Mishra, Dipti J. Shah, Preeti G. Goswami and R. M. Rao, (NUCAR-2019), January 15-19, **2019**

190. "Lithium analysis by Thermal Ionisation Mass Spectrometry in Methyl Sulphonic Acid, a medium of chromatographic separation", K. Sasi Bhushan, Preeti G. Goswami and R. M. Rao, 32nd ISMAS-**2019**, MPH, TSH, Mumbai CP-43 Pg. 204